Department of Mechanical Engineering

Texas A&M University
College Station, Texas

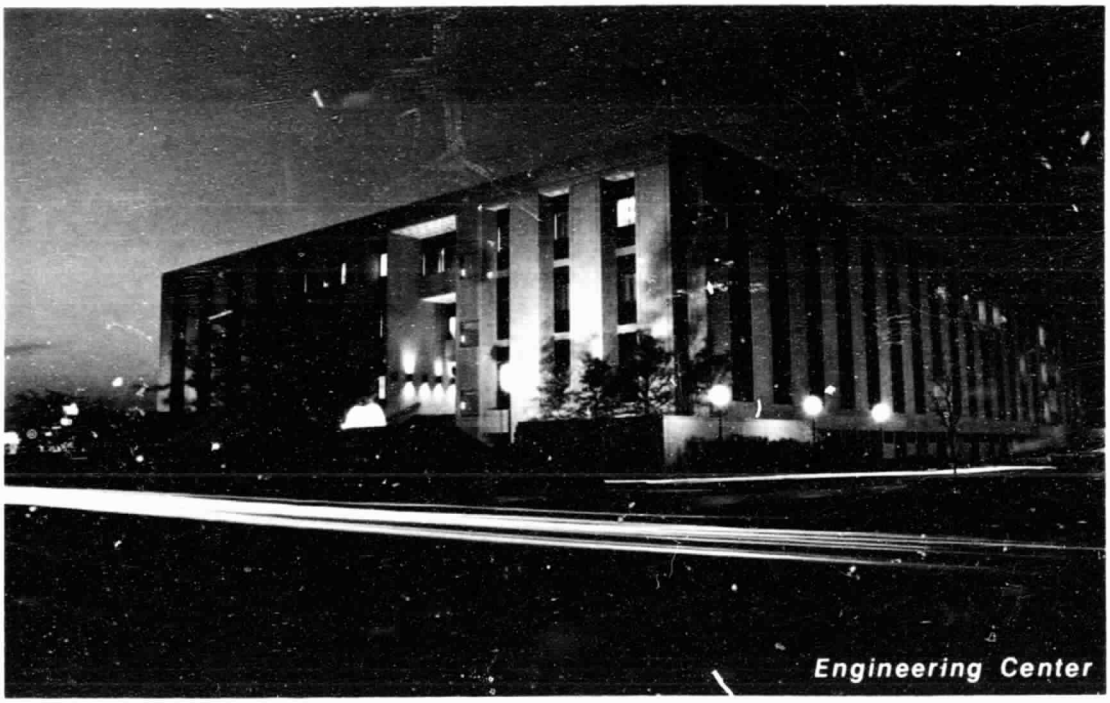

EDUCATION
for tomorrow's
LEADERS

Texas A&M University

Mechanical Engineering Department

College Station, Texas 77843

"The Role of Coherent Structures in the Generation of Noise for Subsonic Jets"

For the Period

November 1, 1980

to

October 31, 1981

April 5, 1982

Yearly Progress Report

Grant NAG 1-112

Gerald L. Morrison

Prepared for

NASA Langley Research Center

Hampton, Virginia 23665

MACH NUMBER DEPENDENCE OF THE COHERENT STRUCTURE IN HIGH SPEED SUBSONIC JETS

A Thesis

by

KEVIN WILLIAM WHITAKER

Submitted to the Graduate College of
Texas A&M University
in partial fulfillment of the requirement for the degree of

MASTER OF SCIENCE

May 1982

Major Subject: Mechanical Engineering

ABSTRACT

Mach Number Dependence of the Coherent Structure in High Speed Subsonic Jets. (May 1982)

Kevin William Whitaker, B.M.E., General Motors Institute

Chairman of Advisory Committee: Dr. Gerald L. Morrison

The coherent structure in high Reynolds number (184,000 to 262,000), Mach number 0.6 to 0.8 axisymmetric cold air jets exhausting at atmospheric pressure has been studied. The mean flow and the statistical time averaged turbulence properties have been measured. Spectra showed a very broad frequency content which shifted towards the lower frequencies as the flow progressed downstream. The coherent structure in the jets was measured using two hot-wire probes and cross correlations as well as artificial excitation. It was shown through hot-wire measurements that artificial excitation did not alter the frequency content of the jet. Hot-wire decomposition was performed according to the method of Horstman and Rose. The coherent structure was represented in a wave format. The axial wave number was measured for several frequencies ($0.12 < St < 1.27$) and was compared to results obtained by other investigators for various Mach and Reynolds numbers.

The results indicate that the axial wave number-frequency relationship was the same for a wide range of Mach (0.3 to 2.5) and Reynolds (3,700 to over 200,000) numbers. Measurements of the azimuthal mode numbers show that several modes from n = -3 to +3 exist simultaneously in various quantities at the different frequencies studied.

Acoustic measurements were made in the near ($r/D < 60$, $x/D < 60$) field of the Mach number 0.6 jet. Sound pressure level contours showed that noise appeared to be radiated from a location near the end of the potential core. Directivity plots revealed a dependence of the radiated noise frequency content upon the angle from the jet axis. The spectra of this noise shifted towards higher frequencies as the angle from the jet axis increased. It was also found that mid-band excitation frequencies ($0.474 < St < 0.632$) produced an increase in full spectrum noise.

ACKNOWLEDGEMENTS

The author would like to recognize the National Science Foundation (Grant No. ENG 79-08002) and the National Aeronautics and Space Administration (Grant No. NAG 1-112) whose financial support made this study possible.

The author also wishes to express his deepest appreciation to his committe chairman, Dr. G.L. Morrison, and to his other committe members, Dr. J.C. Dutton and Dr. G.B. Tatterson, for their invaluable guidance during this study.

TABLE OF CONTENTS

LIST OF TABLES

LIST OF FIGURES

NOMENCLATURE

Symbol	Description
Au	velocity fluctuation sensitivity coefficient
A_ρ	density fluctuation sensitivity coefficient
At	stagnation temperature fluctuation sensitivity coefficient
Am	mass velocity fluctuation sensitivity coefficient
C_{ph}	phase velocity of disturbance
D	diameter of the jet
d	local shear layer thickness
e'	fluctuating hot-wire voltage
$\bar{E}$	mean hot-wire voltage
f	frequency (Hz)
k	complex wave number
k_i	imaginary portion of k
k_r	real portion of k
M	Mach number
$\tilde{m}$	mass velocity fluctuation $((\rho u)')$ nondimensionalized by the local mean value of mass velocity $(\overline{\rho u})$
$\tilde{m}_e$	mass velocity fluctuation $((\rho u)')$ nondimensionalized by the mean value of the mass velocity $(\overline{\rho U}_o)$ at the jet exit
n	azimuthal mode number
q	flow disturbance
Q(r)	radial dependence of the wave amplitude
Re	Reynolds number $(\rho U_o D/\mu)$

Symbol	Description
r	radial distance from the jet centerline
r(b)	radial distance from the jet centerline where u = bU
Rw	hot-wire resistance
Rr	hot-wire cold resistance
St	Strouhal number (fD/U_o)
S_{aw}	hot-wire overheat ratio ((Rw - Rr)/Rr)
T_o	stagnation temperature
Tw	hot-wire temperature
t	time
u	local velocity
U	centerline velocity of the jet at a given x location
U_o	centerline velocity at the exit of the jet
w	frequency (rad/sec)
x	downstream distance from the nozzle exit
xc	length of the potential core
η	(r-r(0.5))/d
λ	axial wavelength
θ	azimuthal angle
ϕ	relative phase
Φ	angle from jet axis
ρ	density
μ	viscosity
( )rms	root mean square of fluctuating quantity
( )	time averaged quantity

I. INTRODUCTION

The role of large scale coherent structures in the noise generation process of jets has been analytically and experimentally investigated for many years. Many of the theories[1-11] predict that the organized structure in the jet is of prime importance in the noise production mechanism.

For low Reynolds number, transonic and supersonic jets[12-17], large scale organized structures which cause a major portion of the radiated noise have been experimentally confirmed. In subsonic jets, many experiments have been performed in order to determine the noise production mechanism. Mollo-Christensen[18] first observed the coherent structure in subsonic jets ($0.15 < M < 0.9$) by using space-time correlations in the near pressure field. He also measured far field noise spectra and directivity patterns. It was believed that the organized structure radiated acoustic energy more effectively than a random structure.

Crow and Champangne[19] examined the organized structure in very low speed jets of air ($M < 0.1$) by using a speaker to artificially excite the jets in the axisymmetric mode ($n=0$). They used both hot-wire anemometry and flow

---

The citations on the following pages follow the style of the AIAA Journal.

visualization to identify the flow field. It was concluded that there was an orderly structure in the jets and this structure could be approximately characterized by a linear stability theory. They observed an instability wave in the shear layer at the nozzle exit. Further downstream there was a puff formation involving the whole jet column which was scaled on the jet diameter.

Moore[20] continued the work and investigated the axisymmetric instability of subsonic jets over a wider range of Mach numbers (M = 0.3, 0.5, and 0.83). He showed that the jets had a definite large scale coherent structure. This structure started as an instability wave on the shear layer, was amplified and finally rolled up into vortices which moved along the shear layer and provided large scale mixing. He also pointed out that by using excessive excitation levels in the experiment, the jet flow field could be significantly altered. At the higher levels of excitation, the instability wave on the shear layer became nonlinear and unrelated to the input. Using low level excitation, it was possible to identify and characterize the coherent structure as an instability wave.

Michalke and Fuchs[21] determined that a strictly axisymmetric model was inappropriate for an unexcited jet (M = 0.18). They measured the azimuthal distribution of the pressure fluctuation space correlation using two microphones fitted with nose cones. By Fourier analysis,

they found that the first four modes (n = 0, 1, 2, and 3) dominated the pressure fluctuation field. However, when hot-wire anemometry was used to measure the velocity fluctuations, it was determined that more modes (n = 0 to 8) were important in the jet.

Chan[4-6] has studied the first three modes (n = 0, 1, 2) of a subsonic jet (M = 0.22). He was able to excite any of the three modes by varying the phase distribution of six acoustic drivers located at 60 degree intervals around the azimuth of the jet. He found that the disturbance (instability wave) grew rapidly as it progressed downstream. For all three modes, the disturbances were well modeled by a wave theory in which the local properties of the wave propagation were described by a linear stability solution of a divergent shear flow. He also measured wavelength and pressure fluctuation amplitudes for the different modes.

Lau et. al.[22,23] performed measurements in the flow fields of Mach number 0.09 to 0.3 jets. They postulated that the flow structure was an axial array of fairly evenly spaced vorticies moving downstream in the mixing region of the jet. Brunn[24] continued this idea in a Mach number 0.13 jet by using a conditional sampling technique and determining that there was vortex pairing occurring at this low Mach number.

Kalghati[25] used an optical method (laser beam

deflection) to study coherent structures in the first six diameters of flow for five different axisymmetric jets with varying densities and Mach numbers (M = 0.195 to 0.78). He showed that the length scales of the coherent structures in the five different jets increased as the flow progressed downstream. The convection velocities of the coherent structures initially increased as the flow progressed downstream and reached a maximum at four diameters from the exit.

Maestrello and Fung[26] used microphones in the near acoustic field of a turbulent Mach number 0.669 jet in order to study the large scale structure. They found that the large scale structure originated near the jet exit which appeared first as a roll up on the mixing layer of the flow within one diameter from the jet exit, became fully developed at approximately three diameters and disappeared beyond the end of the potential core. The Strouhal number based on the most probable frequency for the fully developed structure was in the range of 0.3 to 0.4. The convection velocity was relatively low at the exit of the nozzle, reached a maximum at the end of the potential core, and decreased as the flow progressed further downstream.

Kibens[27,28] has shown that for incompressible flows (M < 0.3) with a laminar shear layer at the exit of the jet, an instability whose wavelength scaled upon the thickness

of the shear layer was generated. As the flow progressed downstream, the shear layer became thicker and the frequency of the coherent structure halved according to a vortex pairing phenomenon where the wavelength of the new spectral component was again scaled upon the thickness of the shear layer. Eventually, after several pairings during the first few diameters of the flow, a coherent structure whose wavelength scaled on the diameter of the jet was obtained and the vortex pairing ceased. The resulting Strouhal number was around 0.4.

Kibens also observed that if the shear layer was initially turbulent instead of laminar, the pairing process did not appear to occur. The jet initially developed a coherent structure whose wavelength scaled on the jet diameter with the same Strouhal number as was eventually reached in the case of an initially laminar shear layer.

The behavior of the subsonic jet studied by Kibens, which initially had a laminar shear layer, was very different from the compressible ($M > 1.4$) jets studied by Morrison and McLaughlin[15]. The supersonic jets studied possessed laminar shear layers at the exit of the nozzle just as the incompressible jets of Kibens. However, the initial instability observed in the compressible jets had wavelengths which scaled upon the diameter of the jet in the same manner as the incompressible jets with turbulent shear layers. In addition, there was no subharmonic

production in the supersonic jets and hence, no direct evidence of vortex pairing.

The investigations of Kibens, and Morrison and McLaughlin indicate that there is an apparent change in the fundamental nature of the coherent structures depending upon the compressibility of the flow. In addition, Kibens found that the initial development of the coherent structure depended upon the condition of the shear layer (laminar or turbulent) at the exit of the jet.

The research presented here was conducted to investigate the aforementioned differences. This was done by comparing the work of several investigators with some new measurements made at Texas A&M University in an effort to determine some of the dependence of the coherent structure upon Mach number, Reynolds number, and initial shear layer conditions.

II. EXPERMENTAL APPARATUS

Facility

The experiments were performed in the free jet test facility shown schematically in Figure 1. Round axisymmetric air jets 1.25 cm in diameter were exhausted at atmospheric pressure into an anechoic chamber. An anechoic chamber was used so that noise radiated by the jet did not reflect from nearby surfaces and possibly alter the jet. Compressed air was supplied by a reciprocating compressor to a 30 cm diameter stilling chamber by way of a storage tank, water aftercooler, water separator/filters, and an electronic pressure regulator. The stilling chamber consisted of sections of foam rubber, perforated plates, honeycomb, and several fine screens. The nozzle used had a contour described by a third order polynomial and the contraction ratio from the stilling chamber to the nozzle exit was over 200:1. The jets had a stagnation temperature of 293^{o}K. This flow system resulted in a jet with uniform parallel flow at the exit and a low level of turbulence.

The anechoic chamber was equipped with a three degree of freedom (vertical, horizontal, and axial) probe drive system. Hot-wires, Pitot-static pressure probes, or microphones could be readily mounted on this basic probe drive system. Precision 10-turn potentiometers mounted on the probe drive system provided DC voltages proportional to

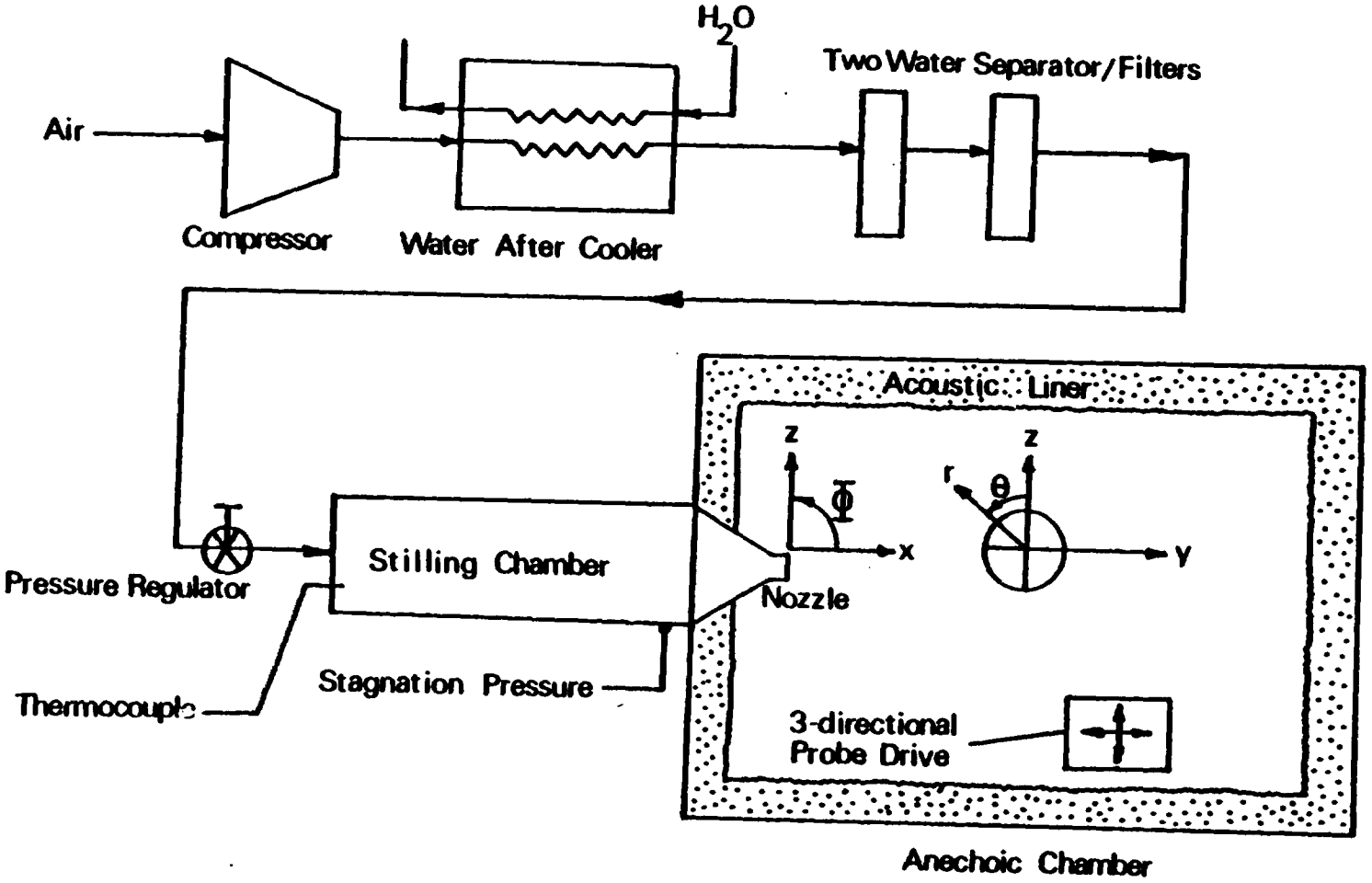

Figure 1. Schematic diagram of jet test facility

probe location. This system allowed accurate and repeatable probe positioning when care was taken to eliminate mechanical backlash. A hand operated portable probe drive system was also placed in the test chamber when two probe measurements were required.

Instrumentation

A Pitot-static pressure probe was used to measure the mean flow field. This probe was a conventional, round-nosed tube with an outside diameter of 1.5 mm. Pressures were measured using water and mercury manometers.

Hot-wire probes operated by a dual channel TSI 1050 anemometer were used to measure the flow fluctuations. The hot-wire probes were custom made and consisted of 5 μm platinum plated wires that were 1.0 mm to 1.5 mm long. By square wave calibration, this probe-anemometer combination possessed a frequency response in excess of 40 KHz. Since the maximum frequency of interest was 20 KHz, this response was more than adequate. Signal conditioning (band pass filtering and amplification) was possible utilizing TSI 1057 signal conditioners.

Spectra, cross spectra, and cross correlations of fluctuating quantities were performed using either a Nicolet 660A Dual Channel Spectrum Analyzer or a Saicor SAI 42 Correlation and Probability Analyzer. Hot-wire voltage

fluctuation and mean voltage profiles were recorded by a Mosely Autograf Model 2FR-A X-Y plotter. The signal output from the hot-wire anemometer was measured using a Fluke 8020A Multimeter and a Hewlett Packard 3400A True RMS Voltmeter. Two General Radio 1564A Sound and Vibration Analyzers were used to bandpass filter at either 1/3 or 1/10 octave.

Acoustic measurements were made using Bruel and Kjaer condenser microphones. Depending on the frequency being studied, either a 1/4 or 1/8 inch microphone was used. All microphones were calibrated with a Bruel and Kjaer model 4220 piston phone.

The artificial excitation device used to stabilize the jet modes into one plane of oscillation was custom built at Texas A&M University. A schematic of the electronics can be seen in Figure 2. A Wavetek Model 186 function generator was used to provide the required square wave input. The 20-60 VDC was provided by a Power Mate Corporation Model BPM-60D power supply and the 15 VDC was built internal to the device. The device operated by generating sufficient voltage to create a spark across a 1.5 mm gap between two electrodes. This spark effectively put a small controlled disturbance in the jet. Electrodes for the excitation device consisted of 1/16 inch diameter, two percent thoriated tungsten rods. In order to stabilize the spark at one location, the tips of the electrodes were

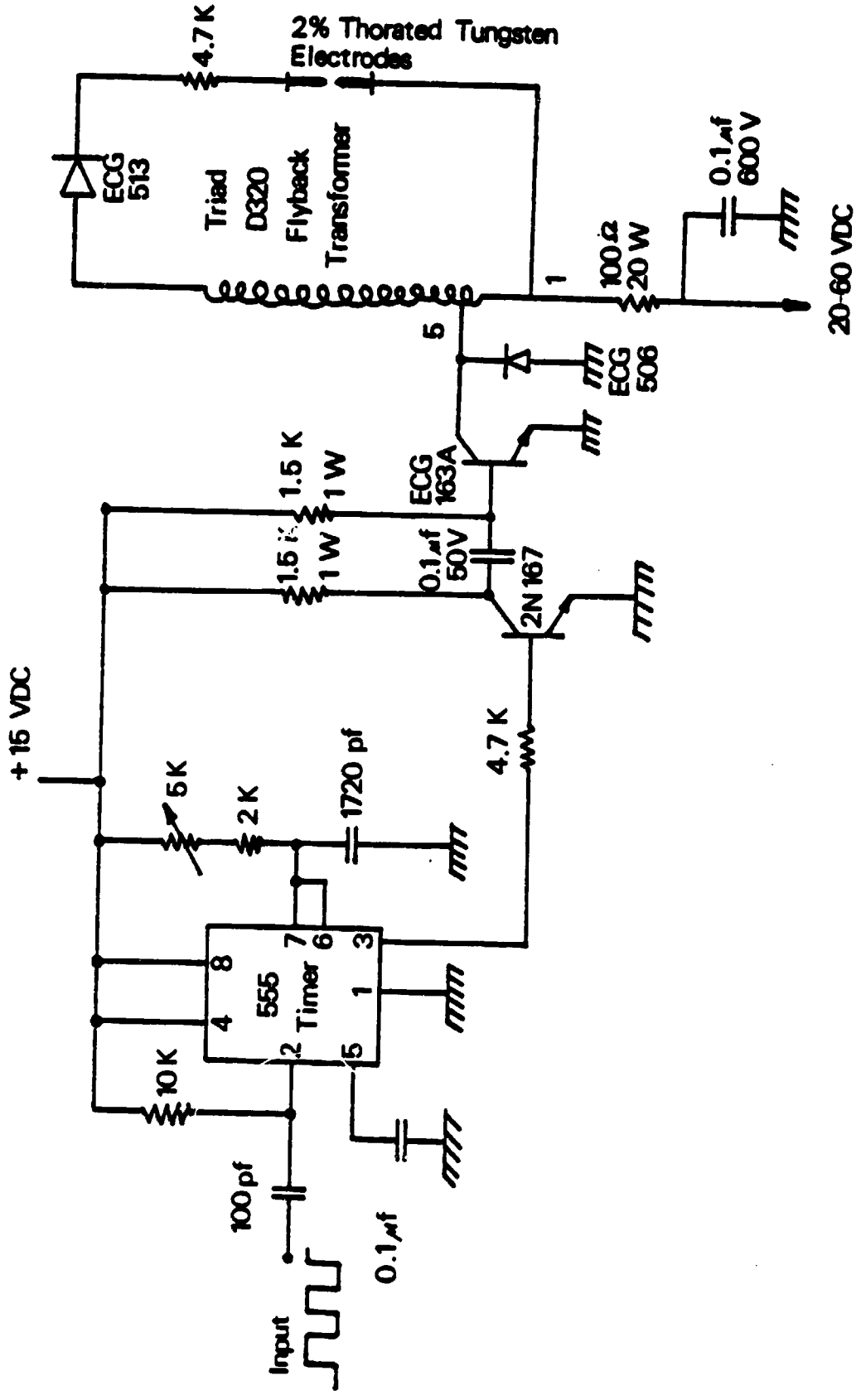

Figure 2. Circuit diagram of artificial exciter

ground into sharp points. These electrodes were mounted on the bottom of the jet nozzle ($\Phi = 180^{\circ}$) placing them right at the exit of the jet (x/D=0). The electrode points were put into the shear layer with one electrode further into the jet than the other so that the spark would jump across the shear layer.

III. PROCEDURE

Jet Operating Conditions

The majority of the identification and characterization of large scale coherent structures involving the direct measurement of the flow structures in jets has been done for either low subsonic (M < 0.4) or supersonic jets. For high speed subsonic jets, most measurements have been acoustic in nature. The problem with this transonic region is that there is small scale turbulence which can mask the coherent structure and the basic difficulty in interpreting the flow sensors' output. The research conducted at Texas A&M University was undertaken to investigate this transonic region and experimentally identify the large scale coherent structure in the flow field of Mach number 0.6 to 0.8 jets. Table I shows the Mach numbers investigated with their corresponding Reynolds number and value of D/U_o(used to non-dimensionalize frequency)

Table I

Jet Operating Conditions

M	Re	D/U_o(sec)
0.6	184,000	.0000632
0.7	221,000	.0000548
0.8	262,000	.0000486

Characterization of the Coherent Structure

To characterize the large scale coherent structure, it must be represented by some model. In this study, the coherent structure was described using a wave type description of the same form used in linear stability analyses. The reason for this selection was that some analytical noise prediction techniques[1-10] use this model and that it has been shown to be an adequate model for low Reynolds number transonic and supersonic jets[12-17]. The model used was of the form:

$$q(x,r,\theta,t) = Q(r)\ \text{real}(\exp i(kx-wt-n\theta))$$

where $q(x,r,\theta,t)$ = flow disturbance in cylindrical coordinates

$Q(r)$ = radial dependence of the wave amplitude

w = frequency

k = complex wave number equal to k_r+ik_i

k_r = wave number in the downstream direction

$-k_i$ = amplification factor for exponential growth in the downstream direction

n = wave dependence on the azimuthal angle (mode number)

In order to characterize the coherent structure using wave theory, its wave properties (frequency, wavelength, wave orientation, wave speed, and amplitude) must be known.

The frequencies present in the jet were determined by using a spectrum analyzer to measure spectra of the flow fluctuations. This was done at different axial, radial,

and azimuthal locations in order to determine the development of the spectral content.

To measure wavelength and azimuthal mode number, two methods were available. The first method consisted of using two hot-wire probes. One probe was held stationary while the other probe was moved axially (for axial wavelength) or around the azimuth of the jet (for azimuthal mode number). The stationary probe was always placed at an azimuthal position of $\Theta = 90^{\circ}$ (where the top of the nozzle is $\Theta = 0^{\circ}$). At each new location of the movable probe, the relative phase difference between the two probe signals was determined at the frequency of interest by the use of cross correlations. The axial wavelength could then be determined from plots of relative phase as a function of axial displacement. Similarly, azimuthal mode numbers could be determined from plots of relative phase as a function of azimuthal position. Thus, knowing mode number(n), wavelength(λ), and frequency(f), the wave speed($\lambda * f$) and axial wave number($k_r = 2\pi/\lambda$) could be determined. The second method available was very similar to the first method except the stationary probe was replaced by an artificial excitation device. The relative phase difference was then determined by cross correlating the exciter input signal and the movable hot-wire probe.

In order to determine the growth rates of the fluctuating flow quantities it was necessary to decompose

the hot-wire voltage fluctuations. This was done according to a technique developed by Horstman and Rose[29]. Details of this data reduction technique can be found in the appendix. Axial and radial distributions of the flow fluctuation amplitudes in both natural and excited jets were measured. These measurements were made for both the full spectrum and individual spectral components. From the axial distributions the growth rate ($-k_i$) could be determined. The radial distributions determined the radial dependence of the wave amplitude(Q(r)).

Hot-wire Procedure

Hot-wire anemometry was used to measure axial and radial distributions of the mean flow as well as the axial flow fluctuations. All hot-wire measurements were made with the hot-wire perpendicular to the flow. With the exception of the azimuthal phase measurements, the hot-wire was also tangent to the shear annulus. To minimize probe interference, the measurements were generally made in the side shear layer ($\Theta = 270^{\circ}$). Exceptions to this procedure were made for azimuthal phase measurements and flow field profiles. For this study the output from the hot-wire probes was bandpass filtered from 1 KHz to 20 KHz.

Microphone Procedure

Sound pressure level (SPL) measurements and microphone

spectra were made with the microphone in the vertical plane of the jet centerline. This assumed that the acoustic field was axisymmetric. The output from the microphone was bandpass filtered from 1 KHz to 20 KHz to be consistant with the hot-wire filtering used. The directionality of the microphone was taken into account by sectioning the flow field into two sections. In one section ($\Phi > 60^{\circ}$) the microphone was positioned vertical and in the other section ($20^{\circ} < \Phi < 60^{\circ}$) it was placed at a 45° angle. The microphone was never positioned closer than $\Phi=20^{\circ}$ from the jet centerline to avoid placing the microphone cartridge directly in the flow of the jet.

IV. RESULTS OF FLOWFIELD MEASUREMENTS

Mean Flow

Radial and axial distributions of pitot and static pressures were made. From these measurements, Mach number distributions were determined. The axial Mach number distribution along the centerline for the three jets studied can be seen in Figure 3. By measuring the resistance of a hot-wire probe, the local stagnation temperature in the jet was found. Utilizing these pressure and temperature measurements, the local velocity was calculated.

Kibens[28] observed that the initial thickness of the shear layer and whether it was turbulent or laminar played an important role in the development of the coherent structure. To investigate the shear layer development of the jets studied in this investigation, the mean flow was represented in the format used by several other investigators[10,11,30]. It has the form of a half-Gaussian:

$$u/U = \exp(-2.773(\eta + 0.5)^{**}2) \qquad \eta > -0.5$$

$$= 1 \qquad \eta < -0.5$$

where $\eta = (r - r(0.5))/d$. This two parameter curve fit produces plots of the shear layer thickness and the jet half width as a function of downstream distance. It should be pointed out that past the end of tne potential core $d/2 = r(0.5)$ and $\eta = (r/d) - 0.5$ where d is now 1/2 the local jet

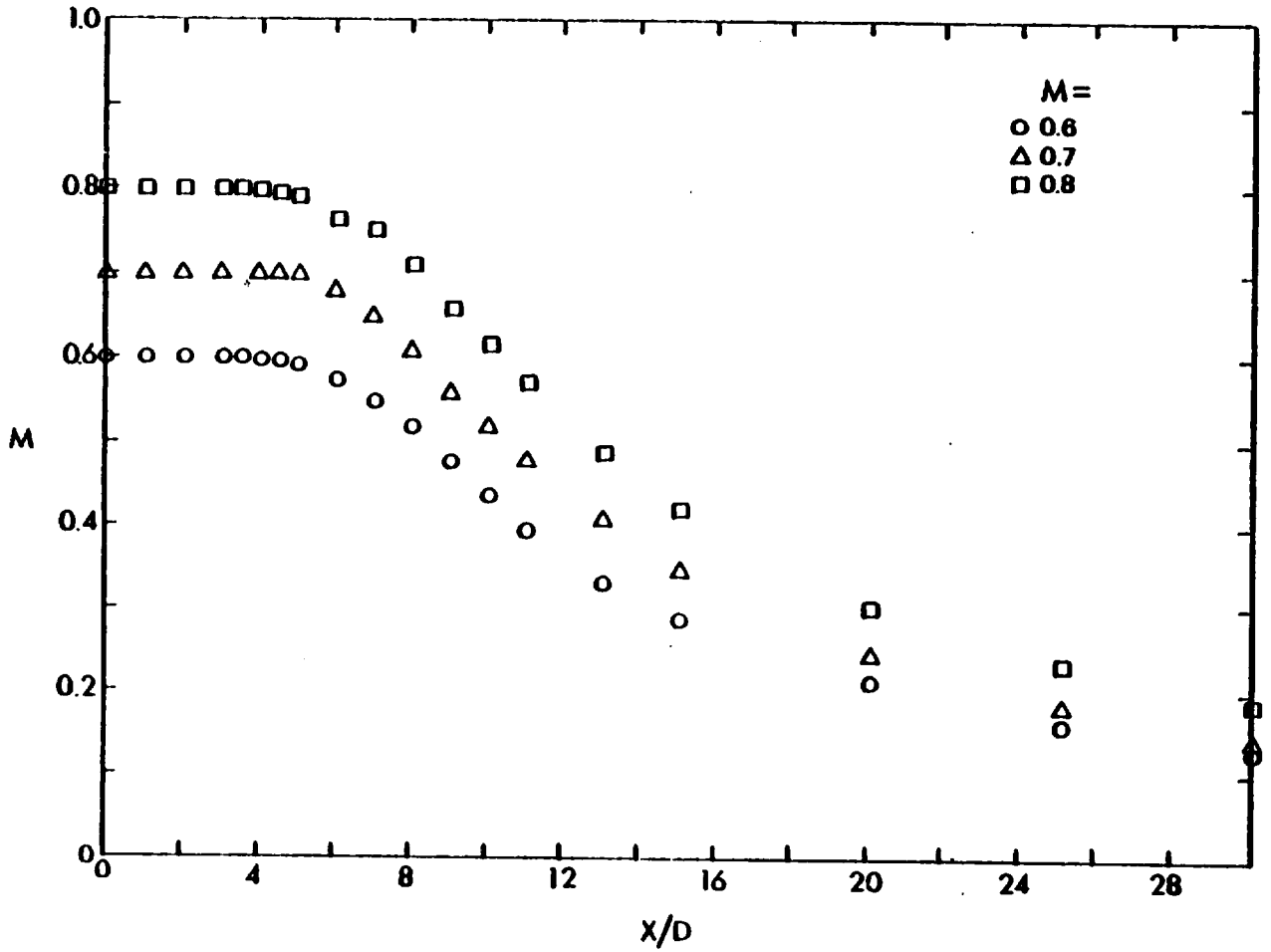

Figure 3. Axial distribution of the centerline Mach number

diameter. (The jet diameter is taken to be the diameter of the locus of points where the mean velocity is 0.01 times the local centerline velocity.) Figure 4(a) shows these curves for the three jets presently studied. In addition, curves for other high speed jets both subsonic and supersonic at various Reynolds numbers are shown in Figures 4(b) and 4(c). Table II summarizes the data from the mean flow Figure by tabulating the values of the shear layer thickness, the length of the potential core (where d/2 = r(0.5)), and if the shear layer is laminar or turbulent, all evaluated at x/D = 1.

TABLE II

Summary of Mean Flow Data

M	Re	d/2D	xc/D	Shear Layer
0.6	184,000	0.16	5	turbulent
0.7	221,000	0.12	5	turbulent
0.8	262,000	0.12	5	turbulent
1.4	3,700	0.17	8	laminar
2.0	5,200,000	0.08	9	turbulent
2.1	7,900	0.15	10	laminar
2.1	70,000	0.05	9	moderately turb
2.5	8,700	0.11	18	laminar

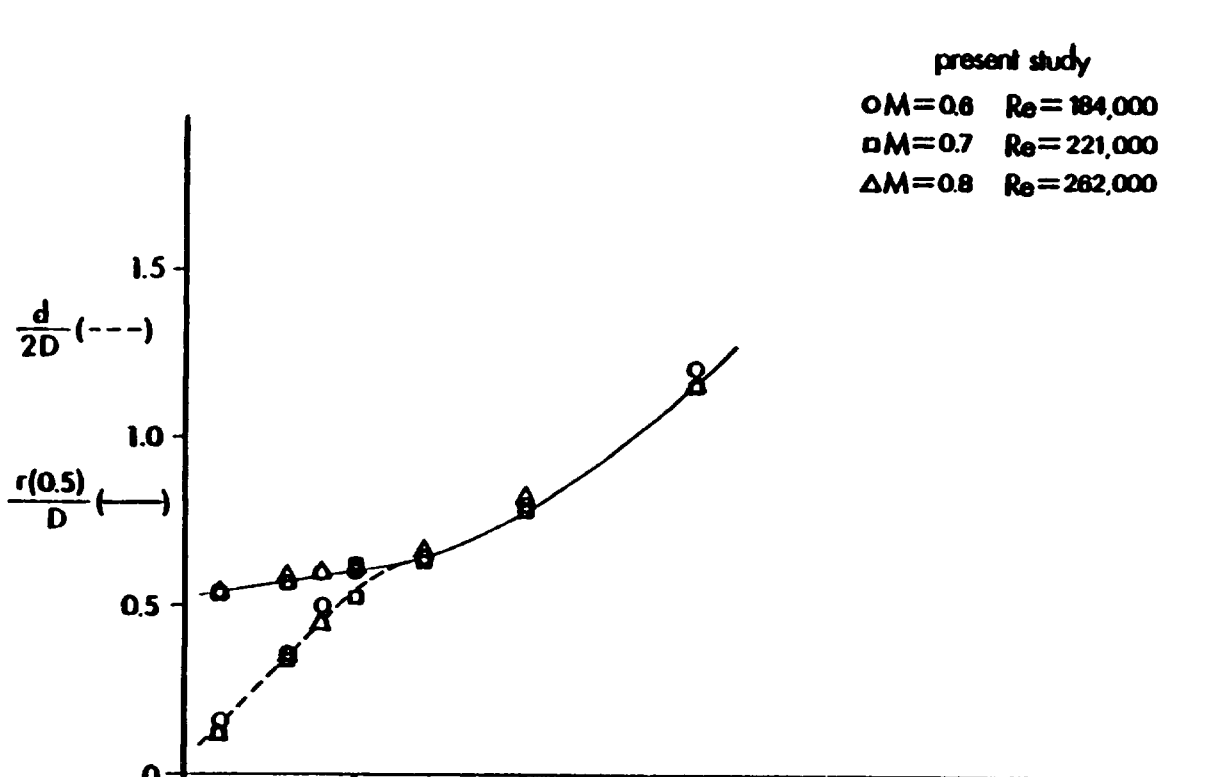

Figure 4. Variation of mean velocity profile parameters

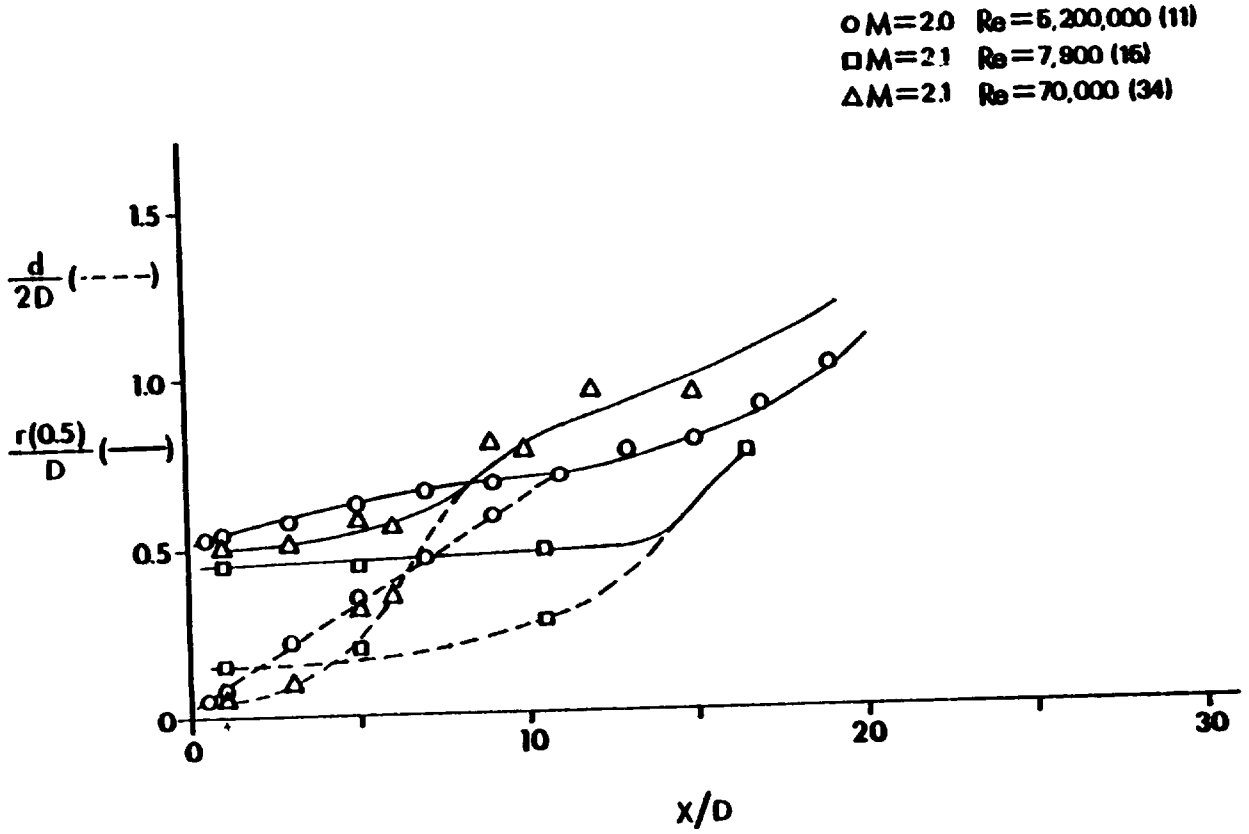

Figure 4. continued

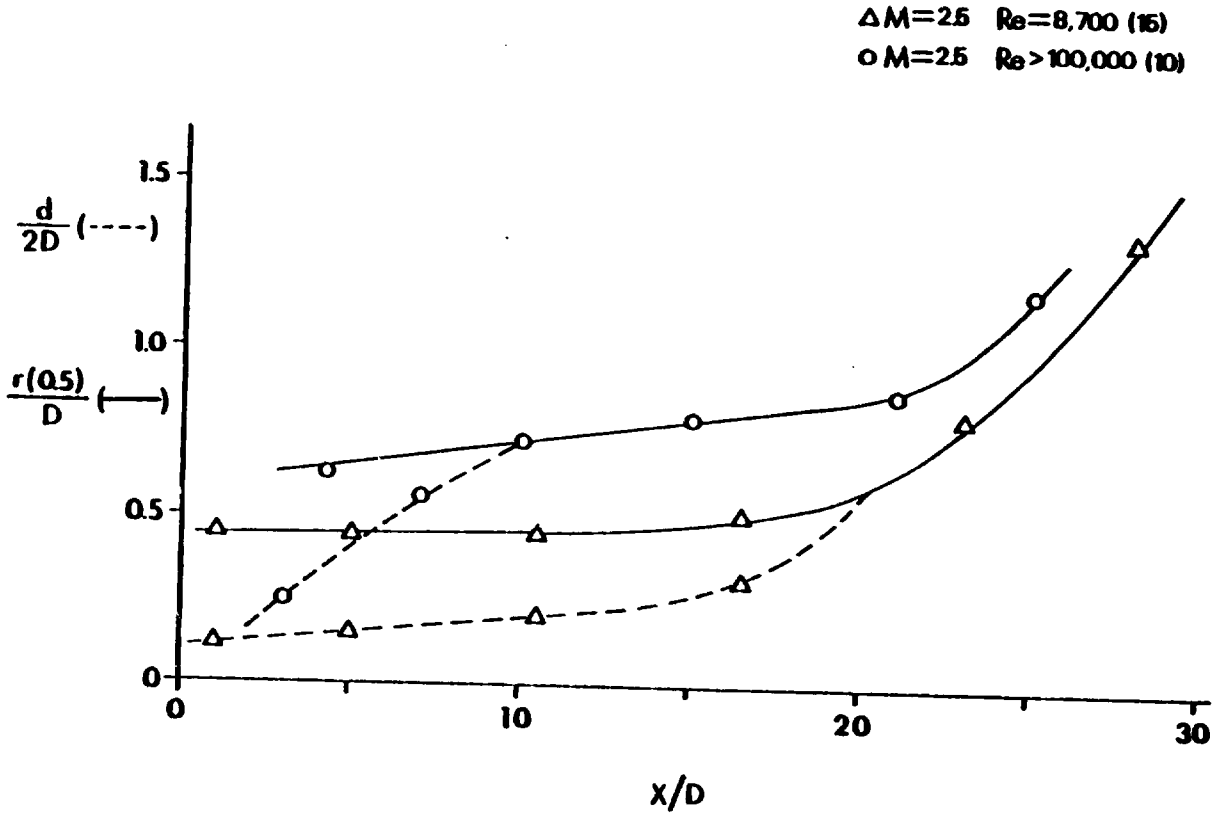

Figure 4. continued

For the range of Mach and Reynolds numbers shown, one can see how increasing the Mach number and the Reynolds number decreases initial shear layer thickness and can even shorten the length of the potential core if the shear layer is not fully turbulent at the exit of the nozzle. Figure 5 shows the dependence of the potential core length upon the Mach number for several different investigators. It can be seen that for low Mach numbers the potential core length remains fairly constant. However, for higher Mach numbers up into the supersonic range, the length of the potential core increased and hence, decreased the spread rate of the jet due to the stabilizing effect of increasing Mach number.

Spectral Content of Hot-wire Voltage Fluctuations

Spectra of the hot-wire fluctuating voltage were measured in order to determine the spectral content of the flow fluctuations at various locations in the jet. Figure 6 shows spectra recorded at several axial locations in the M = 0.7 jet. These spectra are representative of those measured in the other jets studied in this investigation. For each spectra, the hot-wire probe was located at the radial position of maximum fluctuation level. (This is approximately the center of the jet shear layer). The scale St = 0 to 1.10, represents a dimensional frequency range of 0 to 20 KHz. The linear amplitude scale was the

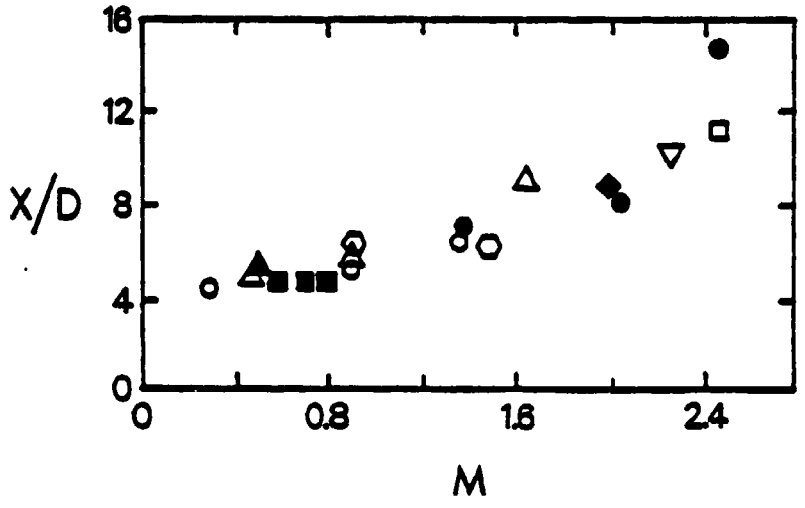

■ Present Study

○ Lau et. al. (38)

▲ Knott and Massey (39)

△ Morris (40)

● Morrison (15)

□ Potter and Jones, ▽ Eggers, ○ Warren, See (41)

◆ Troutt (34)

Figure 5. Length of potential core as a function of Mach number

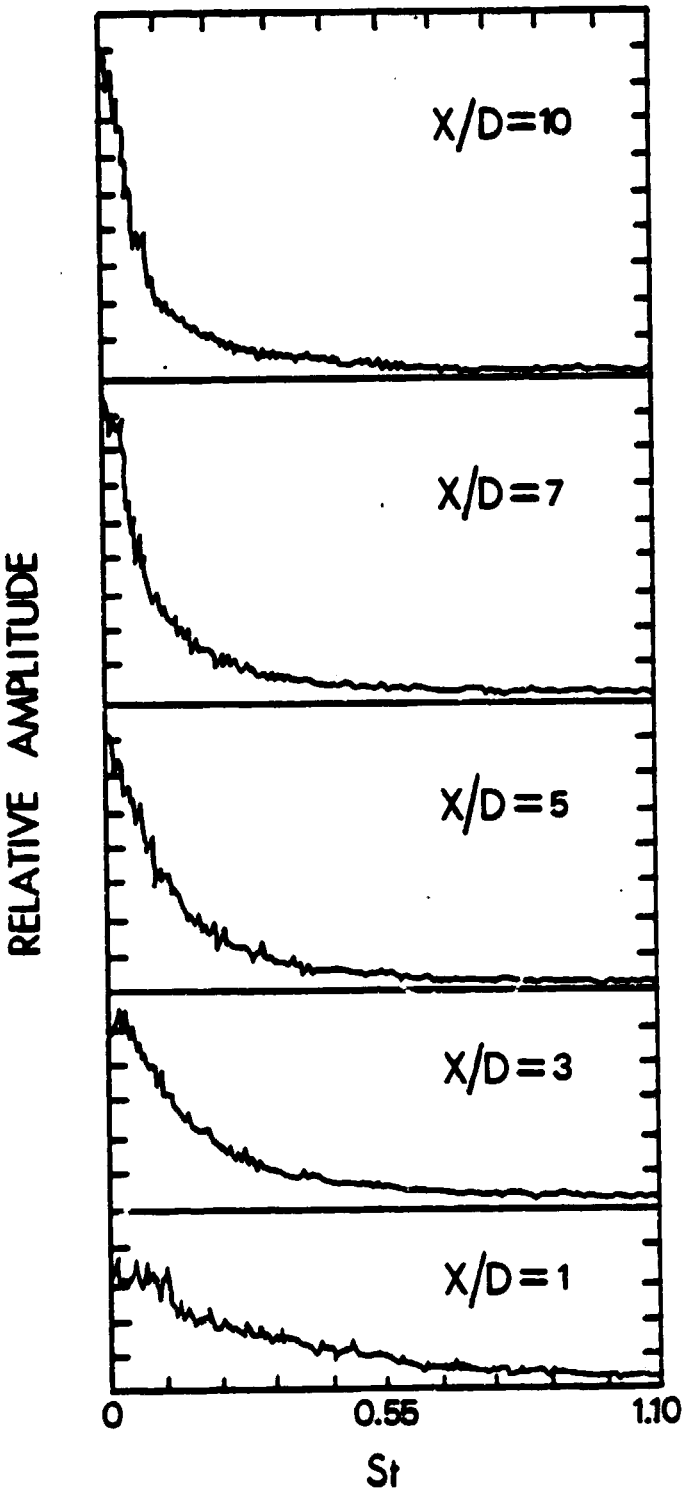

Figure 6. Hot-wire spectra, M=0.7

same for all locations.

From these recorded spectra, one can see that the frequency content of the jet was very broad with no dominant frequencies present. The frequencies shifted toward lower values as the flow progressed downstream for all three jets studied. This agrees with the near field acoustic measurements of Maestrello and Fung[26]. Since there were no obvious dominant frequencies observed in the flow, a set of frequencies was abitrarily selected to be studied. The frequencies selected for study were 2.5, 5.0, 7.5, 10.0, 15.0, and 20.0 KHz. This selection spans the frequency range observed to be important in the acoustic field by Mollo-Christensen[31].

Spectra were also taken with the M=0.6 jet artificially excited at each of the selected frequencies. This was done to determine if artificial excitation altered the frequency content of the jet. These measurements were performed with the hot-wire probe at an axial location of x/D = 1 and then repeated with the probe at x/D = 3. It was found that the artificial excitation used in this study did not alter the frequency content of the jet.

Flow Fluctuation Amplitude Distributions

The maximum amplitude of the axial mass velocity fluctuations at various axial locations was measured for all three jets of this study. This was done by placing the

hot-wire probe at a given axial location and moving it radially through the shear layer until the maximum voltage fluctuation level was found. This voltage fluctuation level was then decomposed according to the method of Horstman and Rose[29] (see appendix) into a mass velocity fluctuation level($\tilde{m}$). The resultant axial distributions of maximum axial mass velocity fluctuation amplitude can be seen in Figures 7, 8, and 9. Also included in these figures is the fluctuation level of the individual frequencies studied. For these measurements, the bandpass filter was set with a 1/10 octave window about the frequency being studied. The mass velocity fluctuation levels for the full spectrum maximized at different axial locations for each jet, but in all three cases this maximum was reached before the end of the potential core ($x/D = 5$). Beyond the end of the potential core the fluctuation levels slowly decreased. (Note that the mass velocity fluctuation level is larger than the velocity fluctuation level in the same jet due to the density variation.) On the centerline of the jets at the exit, the mass velocity fluctuation level was found to be less than 1%.

For the individual frequencies studied, the mass velocity fluctuation distributions appear to be different for each of the Mach numbers studied. In general, there was a trend for the maximum amplitude attained to increase with decreasing frequency. However, a direct comparison of

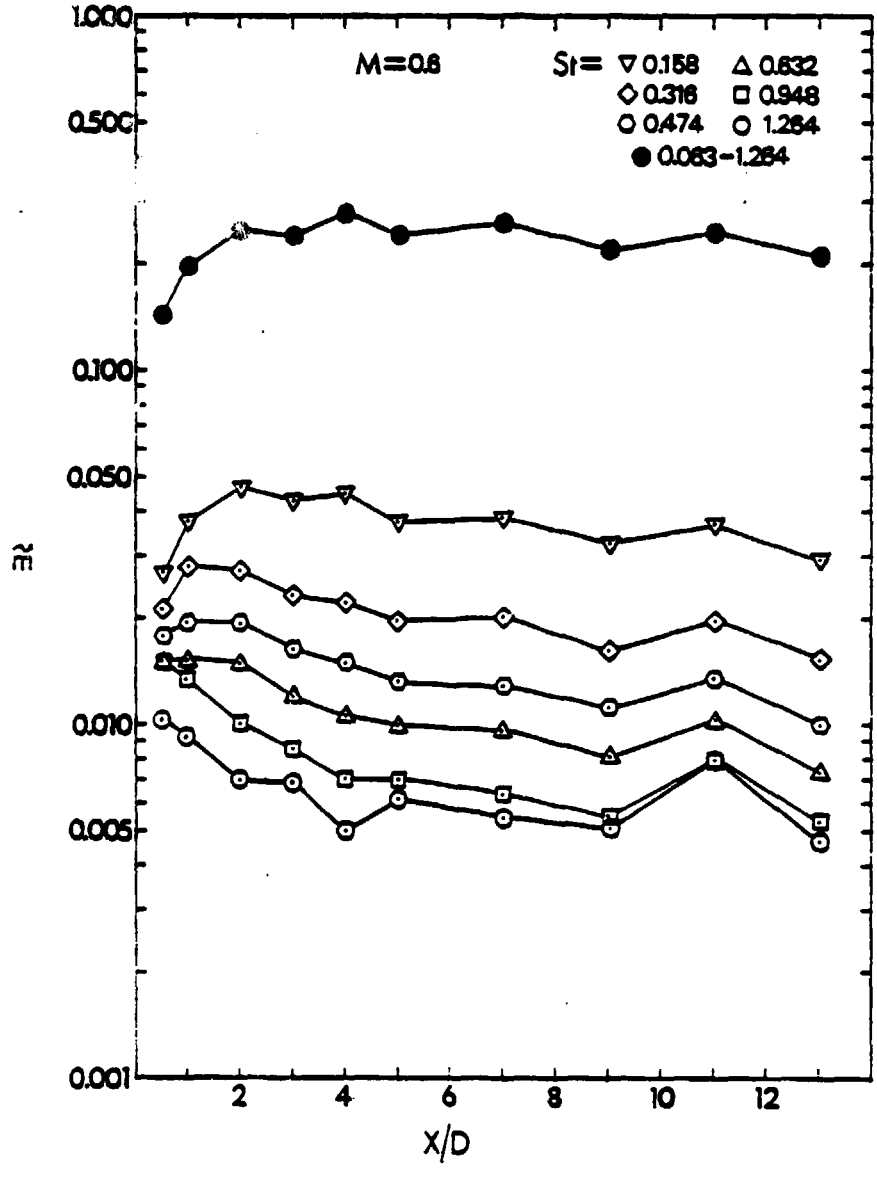

Figure 7. Axial distribution of maximum mass velocity fluctuation, M=0.6

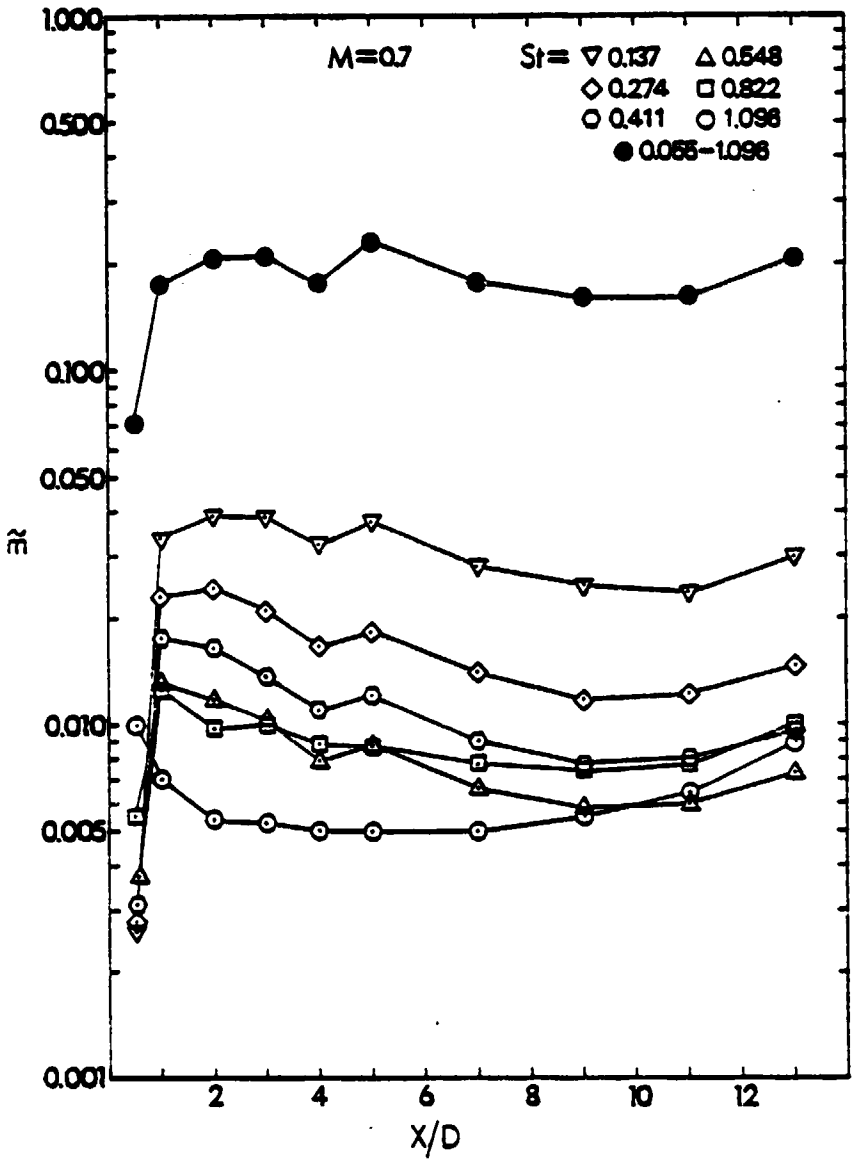

Figure 8. Axial distribution of maximum mass velocity fluctuation, M=0.7

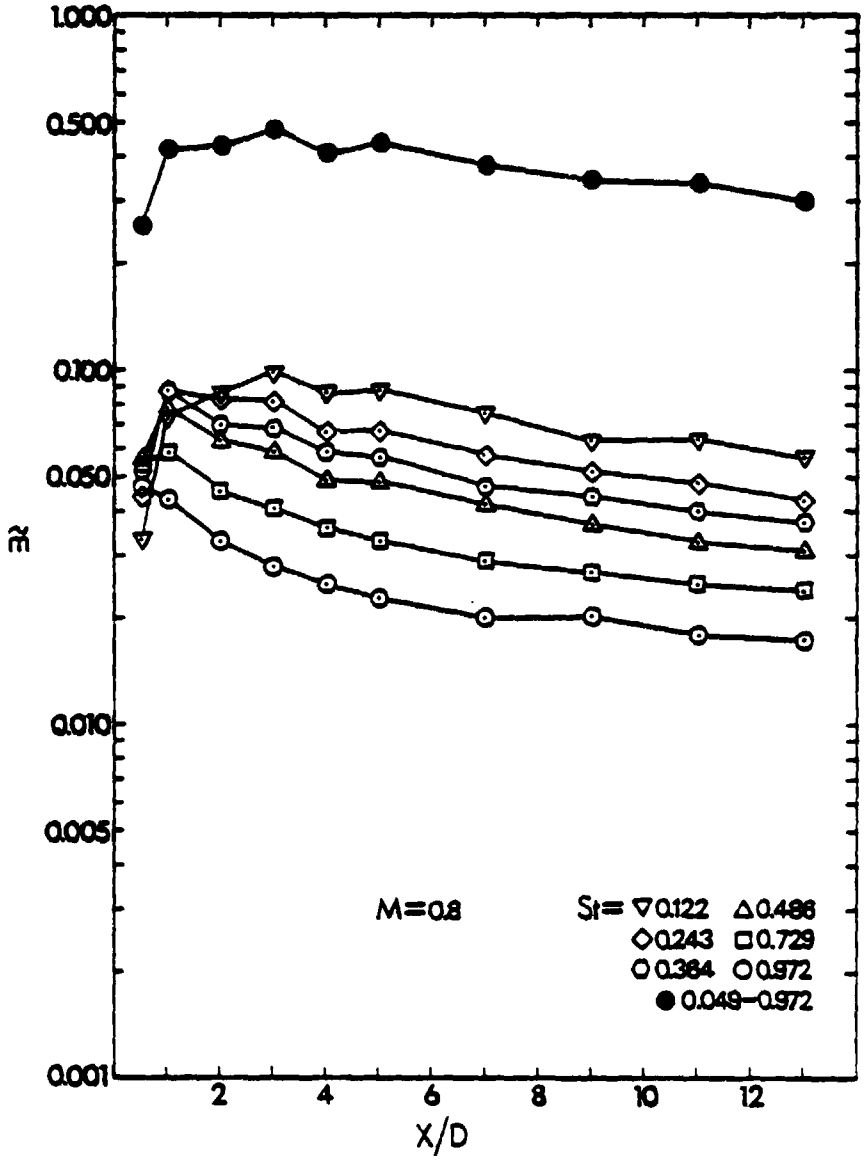

Figure 9. Axial distribution of maximum mass velocity fluctuation, M=0.8

Figures 7, 8, and 9 cannot be made because the value of mass velocity used in these figures ($\tilde{m}$) was nondimensionalized using the local mean value of the mass velocity ($\overline{\rho u}$).

Radial distributions of the mass velocity fluctuation levels were also measured at various axial locations for each of the three jets. These were obtained by moving the hot-wire probe radially through the jet in the $\Phi = 90^{\circ}$, $\Phi = 270^{\circ}$ plane. Full spectrum levels were measured for all three jets and individual frequency levels were measured for the M=0.6 jet. These distributions can be seen in Figures 10 through 18. Note that in these figures the mass velocity fluctuations ($\tilde{m}_e$) were nondimensionalized using the exit value of the mean mass velocity ($\overline{\rho U}_o$), thus allowing comparisons between Figures 10 through 18 to be made. These figures reveal that the maximum fluctuation levels occur in the shear layers before the end of the potential cores. This type of profile with fluctuation peaks on each side of the jet centerline was defined as a developing profile. As the flow progresses downstream the large amplitude fluctuations reach the jet centerline (past x/D=5) indicating the end of the potential core. Profiles with the maximum fluctuation level on the jet centerline were defined as a fully developed profile. This agrees with the axial Mach number distributions (Figure 3) which show a decrease in Mach number (indicating the end of the

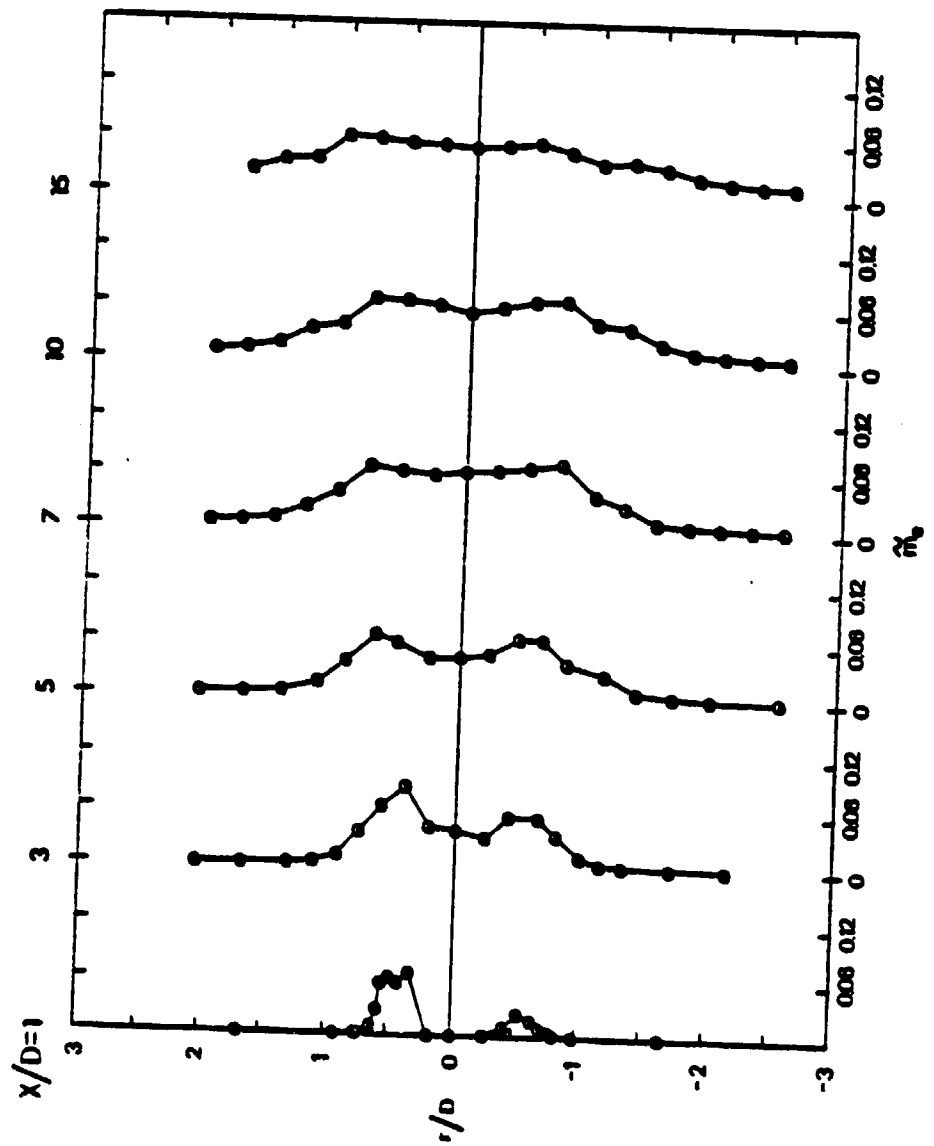

Figure 10. Radial distribution of mass velocity fluctuations, M=0.6, St = 0.063 to 1.264

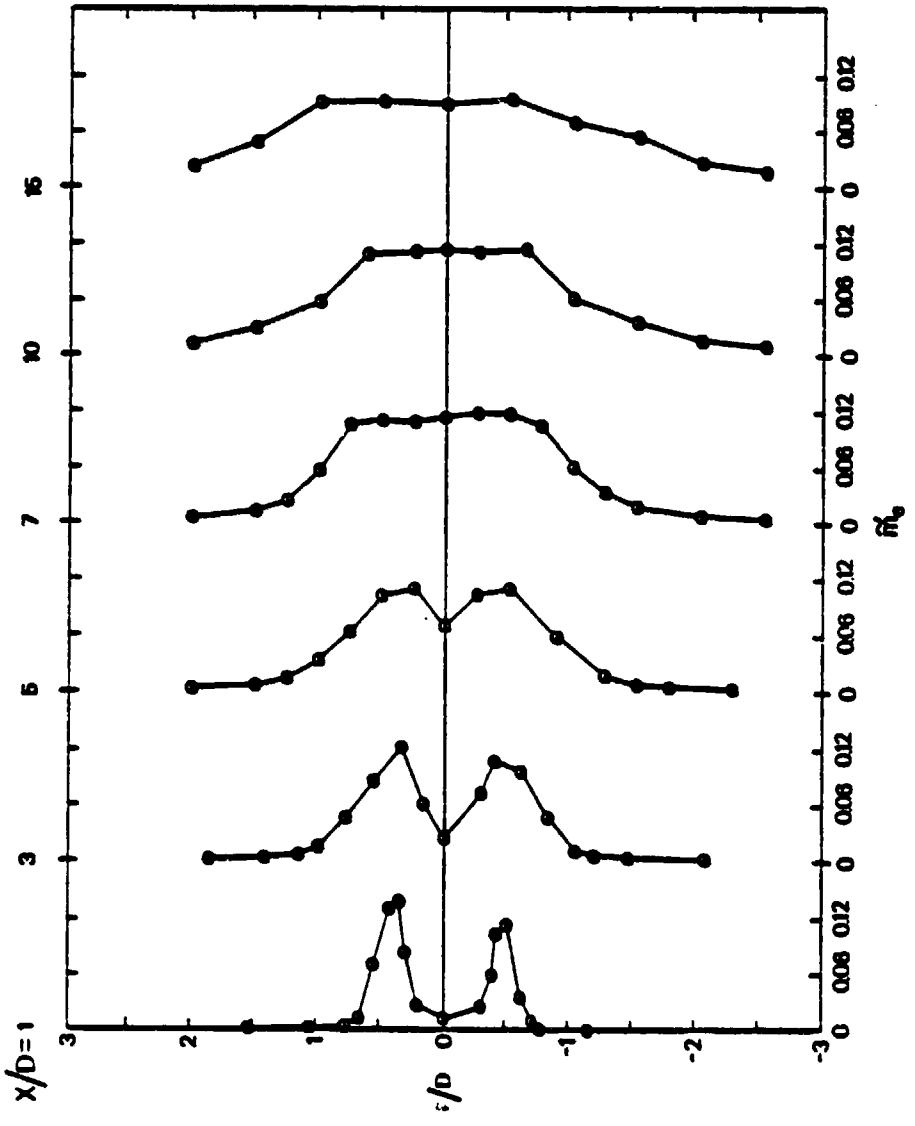

Figure 11. Radial distribution of mass velocity fluctuations, M=0.7, St = 0.055 to 1.096

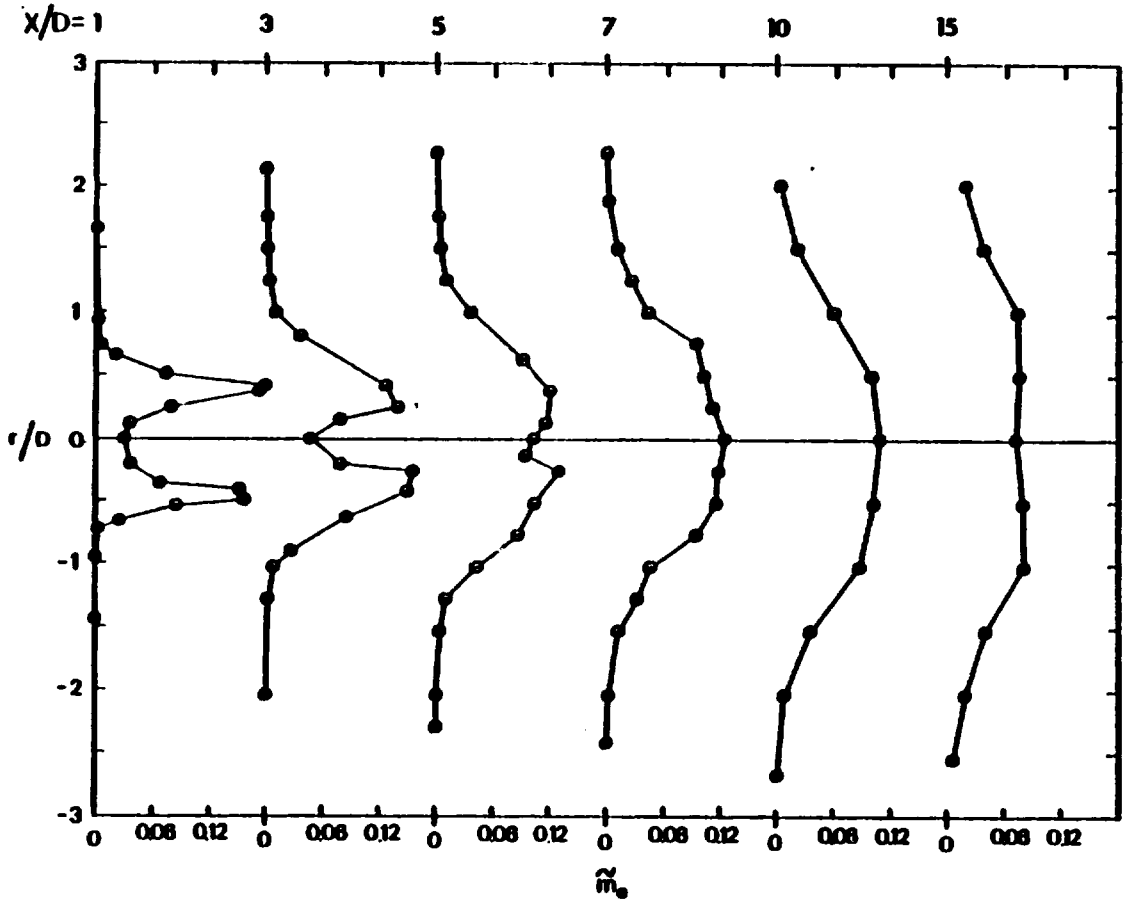

Figure 12. Radial distribution of mass velocity fluctuations, M=0.8, St = 0.049 to 0.972

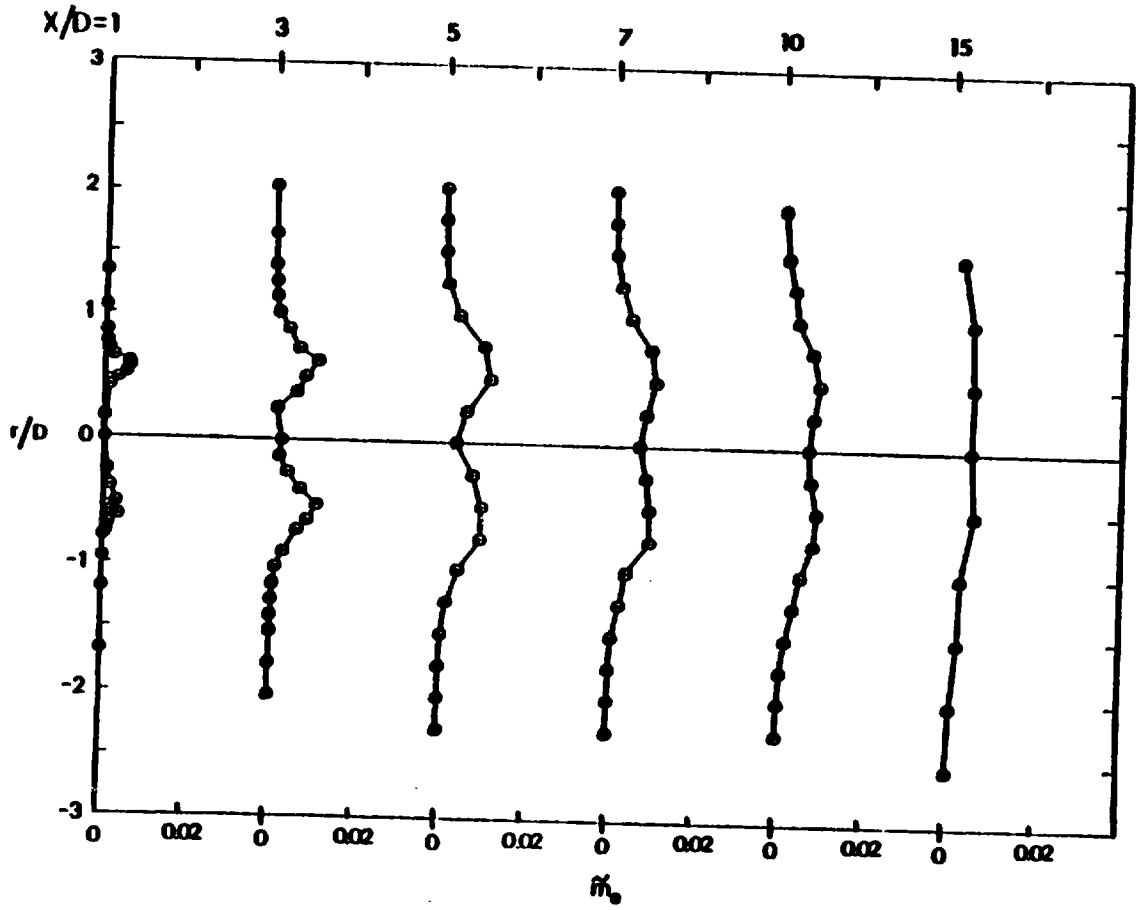

Figure 13. Radial distribution of mass velocity fluctuations, M=0.6, St = 0.158

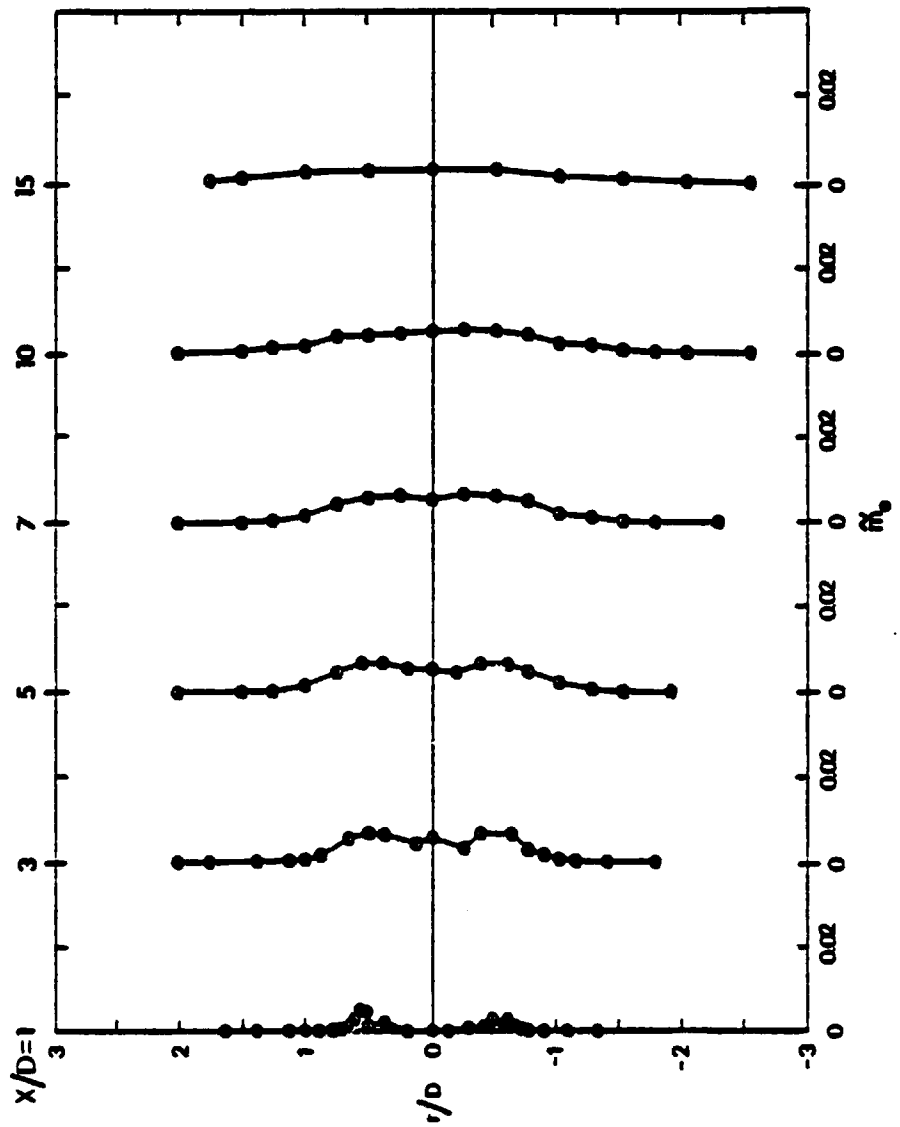

Figure 14. Radial distribution of mass velocity fluctuations, M=0.6, St = 0.316

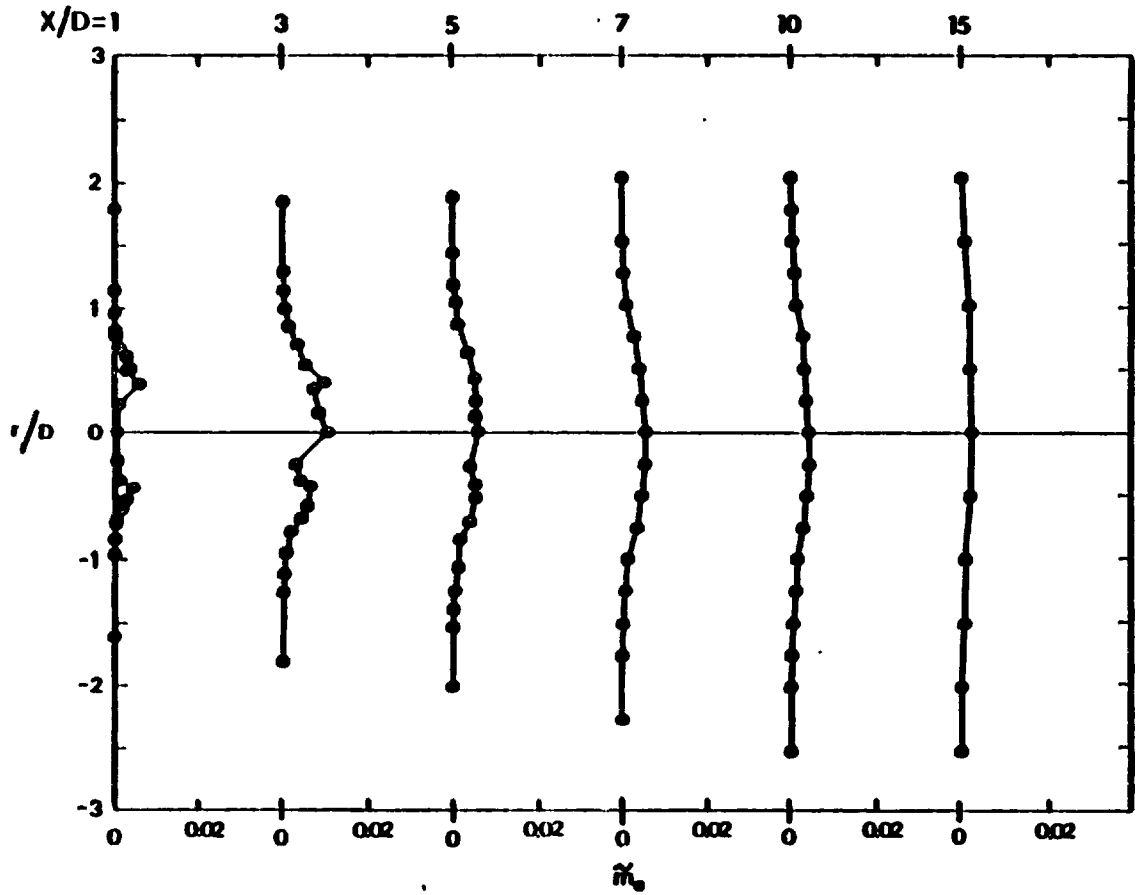

Figure 15. Radial distribution of mass velocity fluctuations, M=0.6, St = 0.474

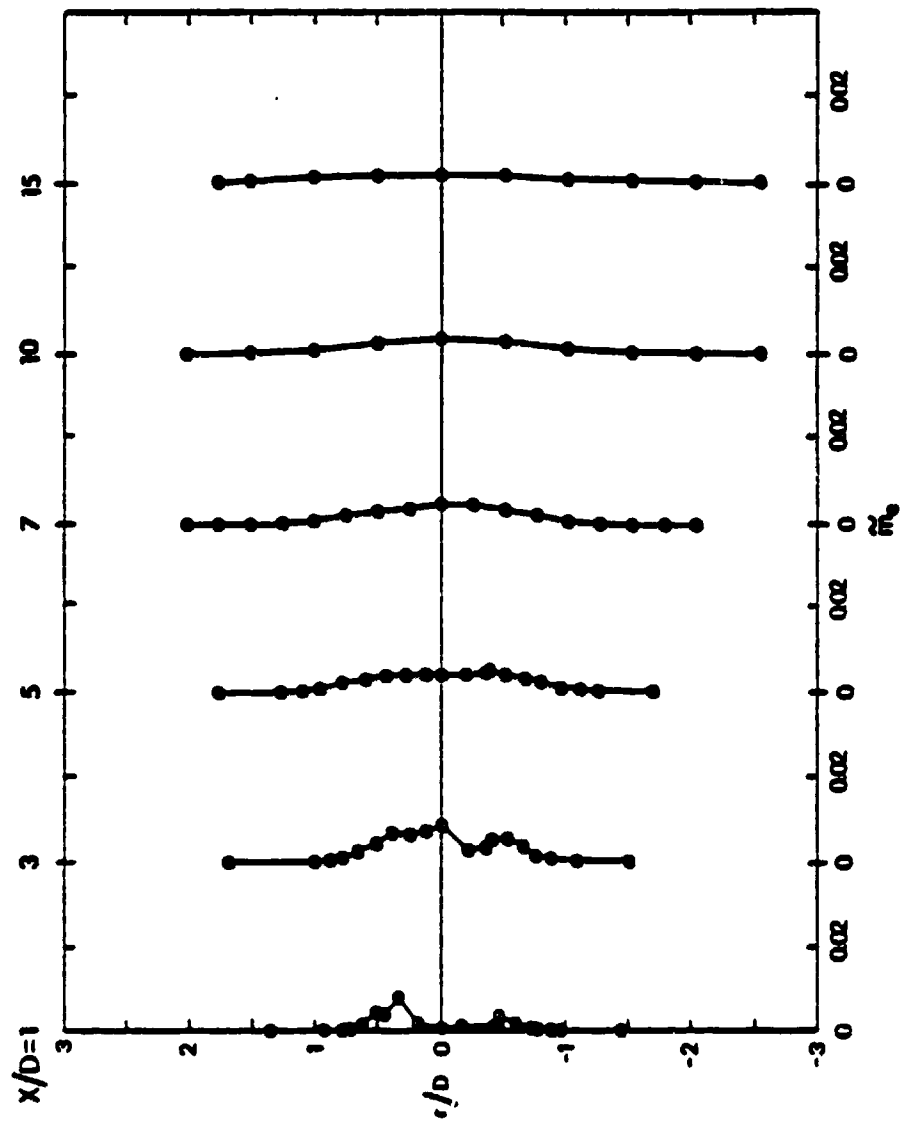

Figure 16. Radial distribution of mass velocity fluctuations, M=0.6, St = 0.632

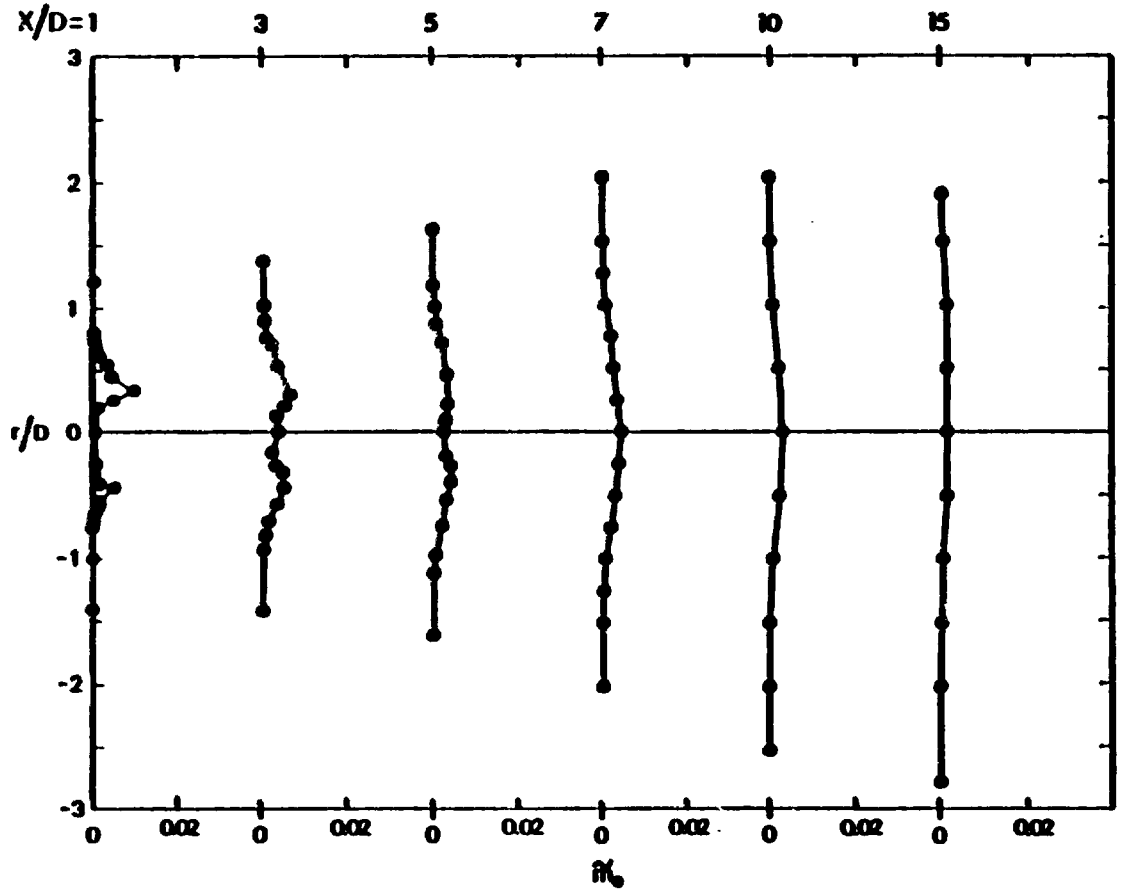

Figure 17. Radial distribution of mass velocity fluctuations, M=0.6, St = 0.948

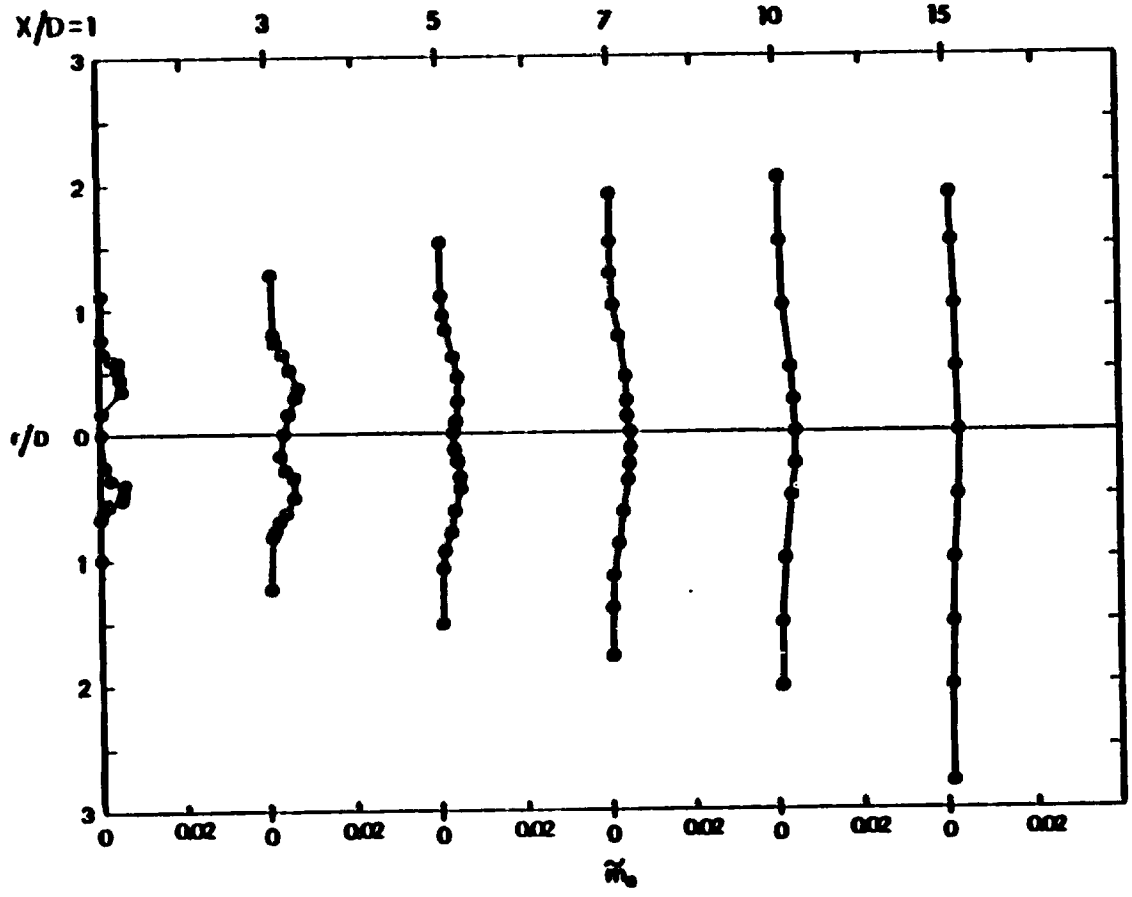

Figure 18. Radial distribution of mass velocity fluctuations, M=0.6, St = 1.264

potential core) past an axial location of x/D=5. The Mach number 0.7 and 0.8 jets yeild almost identical profiles but the fluctuation levels for the Mach number 0.6 jet are always less. Also, in Figure 10 there is obvious asymmetry in the fluctuation profile at x/D=1, which is only found in the M=0.6 jet. It is possible that since the Reynolds number is low in the M=0.6 jet (Re=184,000), the shear layer in the nozzle has not attained its maximum level of turbulence. Hence, small asymmetries in the jet nozzle could produce regions with higher turbulence levels. This effect could also be credited to probe interference. The hot-wire probe was always driven across the jet from -r/D to +r/D. Consistantly the higher fluctuation level is in the +r/D region where the probe is moving out from the potential core. The turbulence generated by the probe maybe feeding pressure fluctuations upstream into the nozzle where it causes onset of turbulence sooner and thus increases the turbulence level at the exit of the jet.

The fluctuation profiles for the individual frequencies studied exhibited two definite trends. First, the higher frequencies had fully developed profiles closer to the exit of the jet. For a frequency of 20 KHz the mass velocity profile was fully developed at x/D=7 whereas for a frequency of 2.5 KHz the profile was still developing at x/D=10. Also evident in these profiles was the difference in the radial location of maximum mass velocity before the

profiles became fully developed. The radial distance from the jet centerline decreased with increasing frequency.

Axial Wave Number Measurements

As explained in the procedure, axial wavelength and the axial wave number were measured in this study using two different techniques. The first technique consisted of using two hot-wire probes where one probe was held stationary while the other probe was moved in the axial direction to several different locations. At each location, the relative phase difference between the two probe signals was determined at the frequency of interest by the use of cross correlations. Thus, from plots of relative phase as a function of axial displacement, the axial wavelength and wave number could be determined.

This first technique was used by Armstrong[32], Morrison and Wattanachayakul[33], and the current investigation. The two later investigations used two hot-wire probes positioned at the radial location of maximum flow fluctuation level with an azimuthal separation of 180°. Armstrong however, used two microphones fitted with nosecones and placed them at r/D=0.5 with an azimuthal separation of 90°.

Figures 19, 20, and 21 show the relative phase distributions obtained by this technique for the three Mach numbers of this study for different frequencies. These

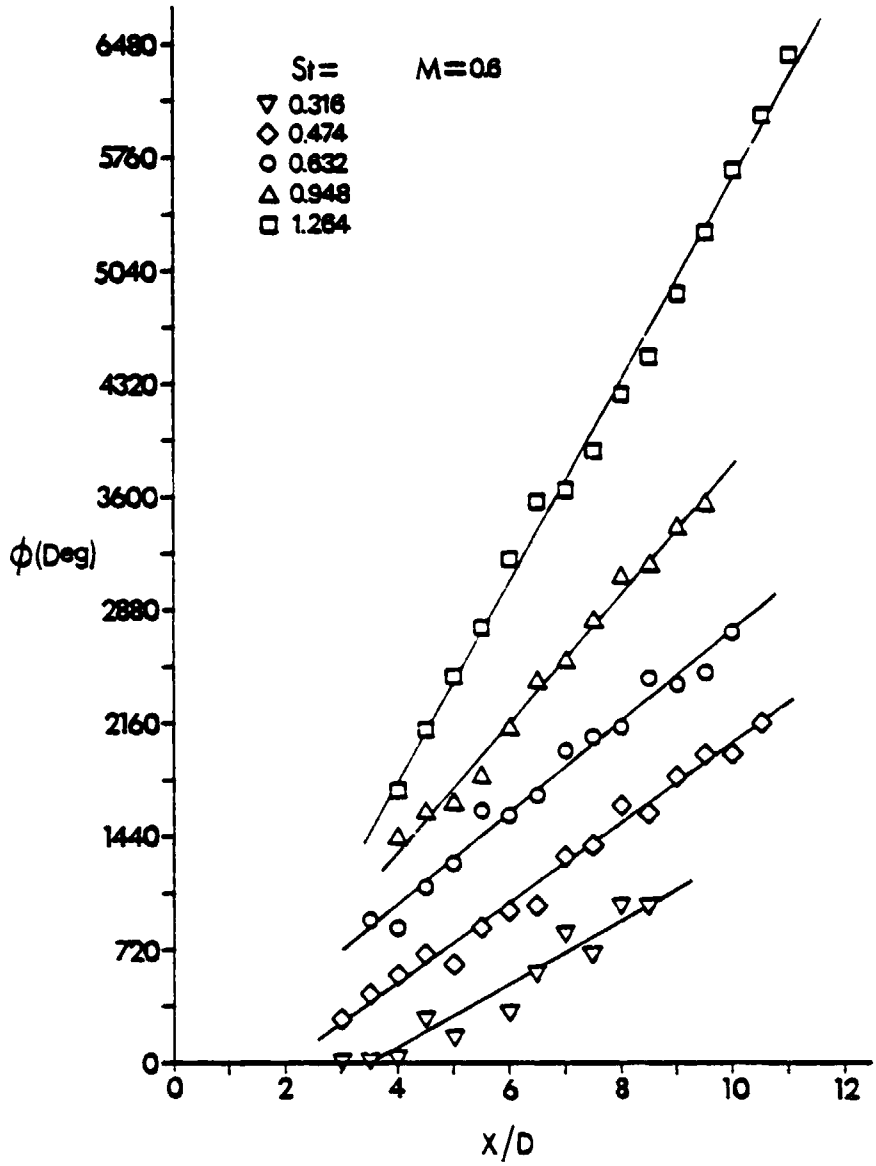

Figure 19. Axial phase distributions, M=0.6

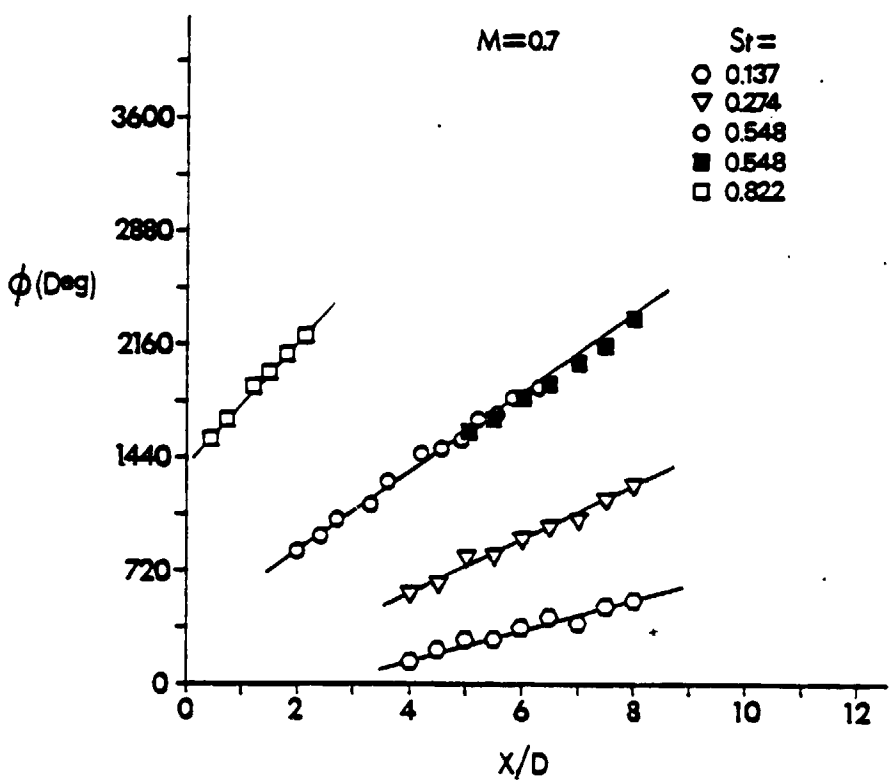

Figure 20. Axial phase distributions, M=0.7

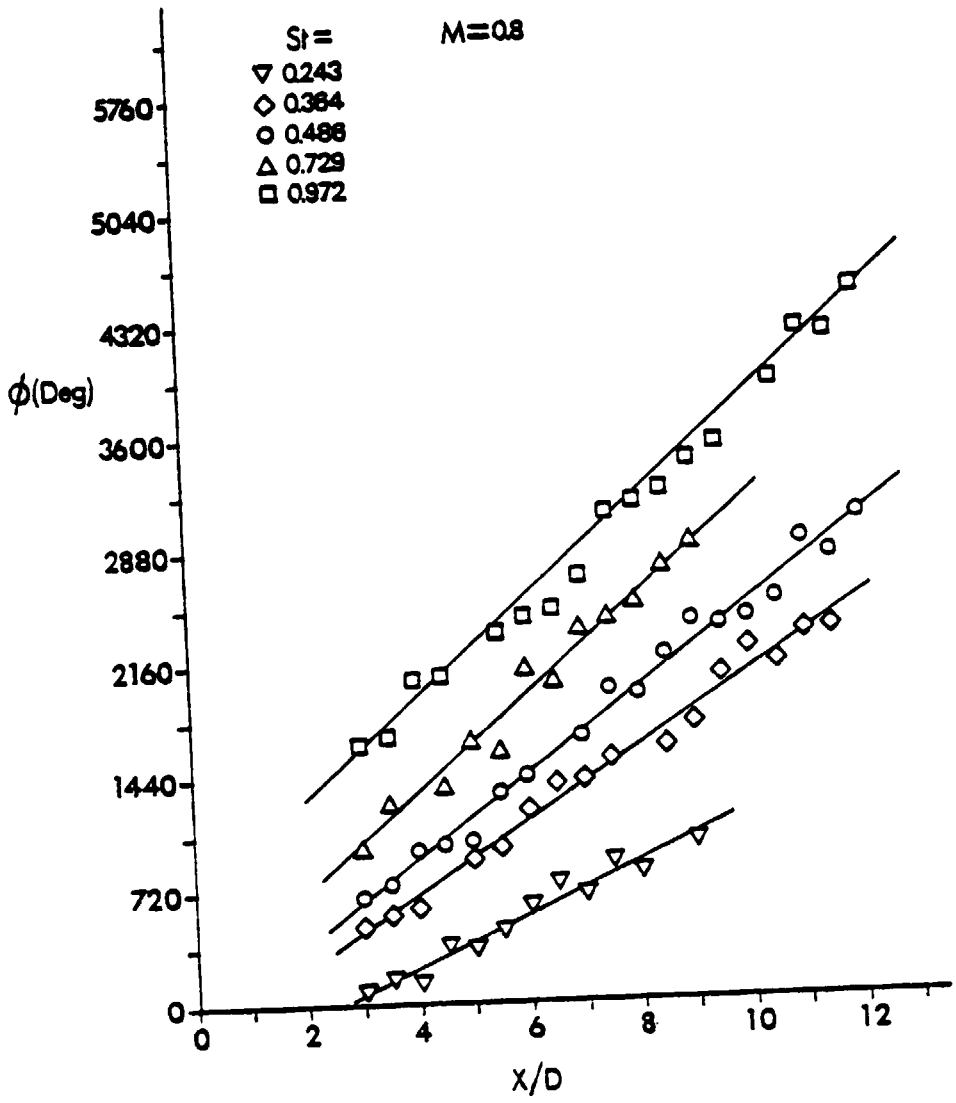

Figure 21. Axial phase distributions, M=0.8

figures show that all frequencies studied were coherent over the same region of the jet. This result was also observable in the data of Armstrong[32]. Since the frequencies studied included harmonics and subharmonics which were present over the same regions of the jet, these data do not support the idea of vortex pairing. This is in contrast to the data of Kibens[27] for low speed, incompressible jets where there were only slight regions of overlap between the fundamental frequency and its subharmonic.

The second technique used for measuring coherent structures consisted of replacing the stationary probe by some type of artificial excitation device. The purpose of this excitation device was to input a disturbance with known frequency, amplitude, and phase into the jet and observe how the jet responded. The advantage of this technique was that the stationary probe was eliminated and hence, the disturbances created by this probe were also eliminated. This advantage would be especially important if one wished to measure the coherence of the noise radiated, since the noise produced by the stationary probe would not be present. The main disadvantage of this technique was that if one wanted to determine the structure that was naturally occurring in the jet, great care had to be excercised so that the excitation did not appreciably alter the jet from its natural condition. Moore[20] and

Morrison[13] have shown that it is possible to change the nature of a jet by using excessive levels of artificial excitation for both subsonic and supersonic jets.

Crow and Champagne[19], Chan[4-6], Morrison and McLaughlin[15], Stromberg et. al.[17], Trout and McLaughlin[34], and Morrison and Wattanachayakul[33] have all used artificial excitation devices in order to measure the axial wave number of the coherent structure in subsonic and supersonic jets. Crow and Champagne, and Chan used acoustical excitation devices in subsonic ($M < 0.3$) jets. Morrison, Stromberg, and Trout all used a glow discharge device to excite high speed, compressible jets ($0.9 < M < 2.5$). Morrison and Wattanachayakul, as well as this current study, used a spark excitaion device to excite the flow. Figure 22 shows the relative phase distributions obtained for the artificially excited $M=0.6$ jet as a function of axial location. This current investigation and a study conducted by Wattanachayakul[35] showed that the spark excitation device yielded axial wave numbers that were the same as those measured with two probes in an unexcited jet. Wattanachayakul also demonstrated the reliability of this measurement technique over three different days. The axial wave lengths he obtained from three different measurements were within the 95% confidence interval of the curve fit.

Figure 23 illustrates the axial wave number-frequency relationship for both natural and artificially excited jets

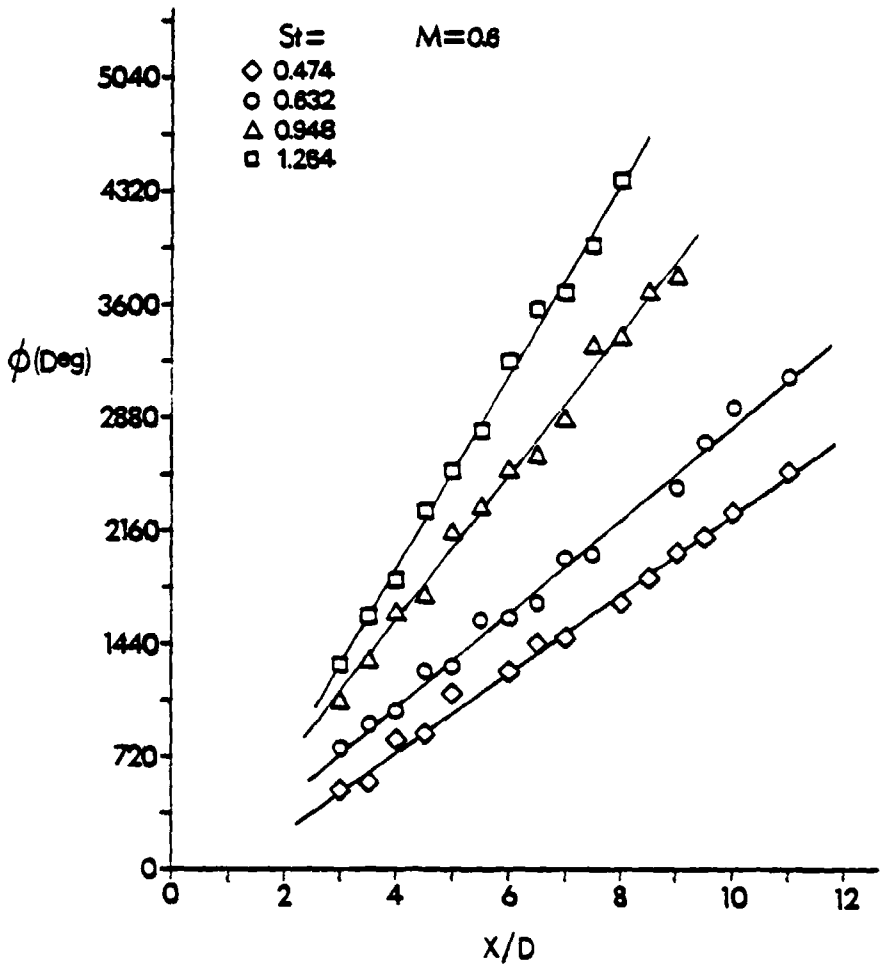

Figure 22. Axial phase distributions for the excited jet, M=0.6

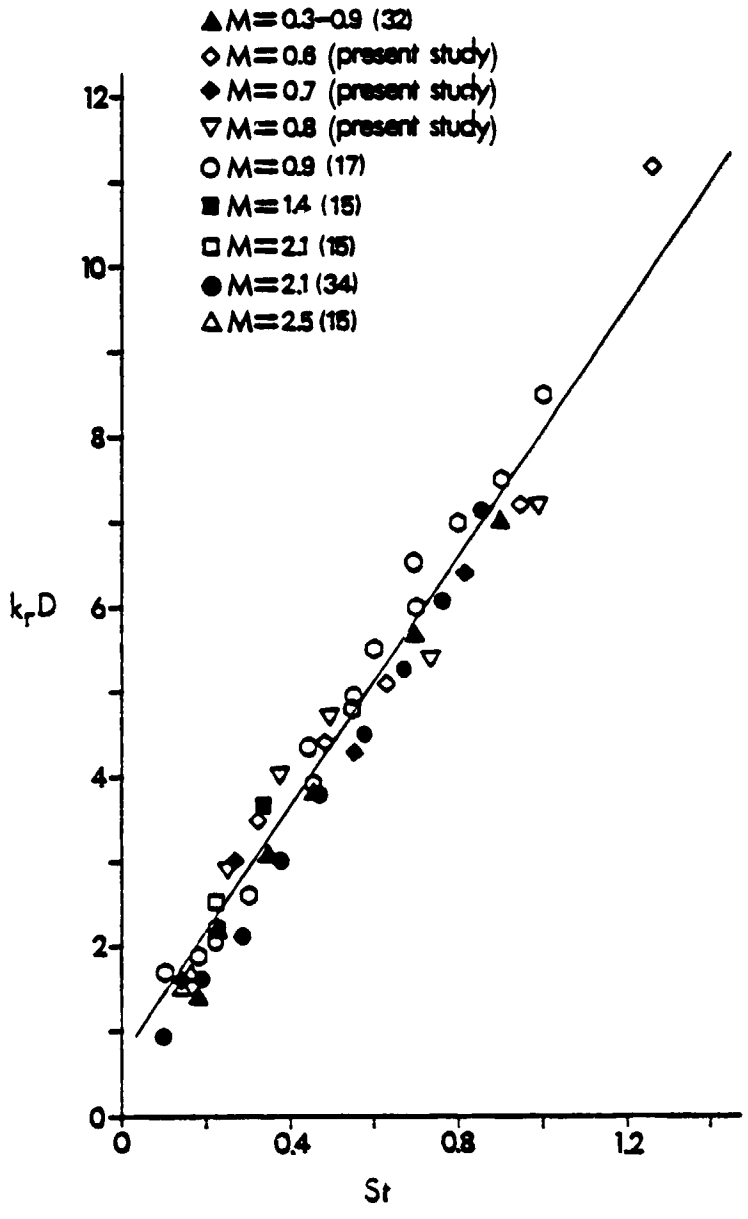

Figure 23. Axial wave number variation with Strouhal number, M > 0.3

with Mach numbers greater than 0.3. The same relationship between the axial wave number and frequency was found for all of these jets. For these jets, the Reynolds numbers ranged from 3,700 to over 500,000, the Mach numbers ranged from 0.3 to 2.5, and some of the shear layers were laminar and others were turbulent with various thicknesses (Table II). Therefore, in these compressible jets, the importance of initial shear layer thickness, whether the shear layer is initially laminar or turbulent, Mach number, or Reynolds number did not matter. A linear curve fit of all the data using a least squares method shows that wave number-frequency relationship can be expressed by:

$$krD = 0.7735 + 7.226*St$$

This expression can be rearranged further to produce an equation relating the axial disturbance velocity (phase velocity, C_{ph}) and frequency. Realizing that $C_{ph}=\lambda f$, $St=fD/U_o$, and $\lambda=2\pi/k_r$, the following expression can be obtained:

$$C_{ph}/U_o = (2*\pi*St)/(0.7735+7.226*St)$$

A plot of this relationship along with data obtained by other investigators can be seen in Figure 24. This figure reveals that above a Strouhal number of about 0.4 the phase velocity (C_{ph}) remains fairly constant at 75% of the jet exit velocity. Below St=0.4, the phase velocity decreases with decreasing frequency. This phase velocity variation at low frequencies was also noted by Troutt and

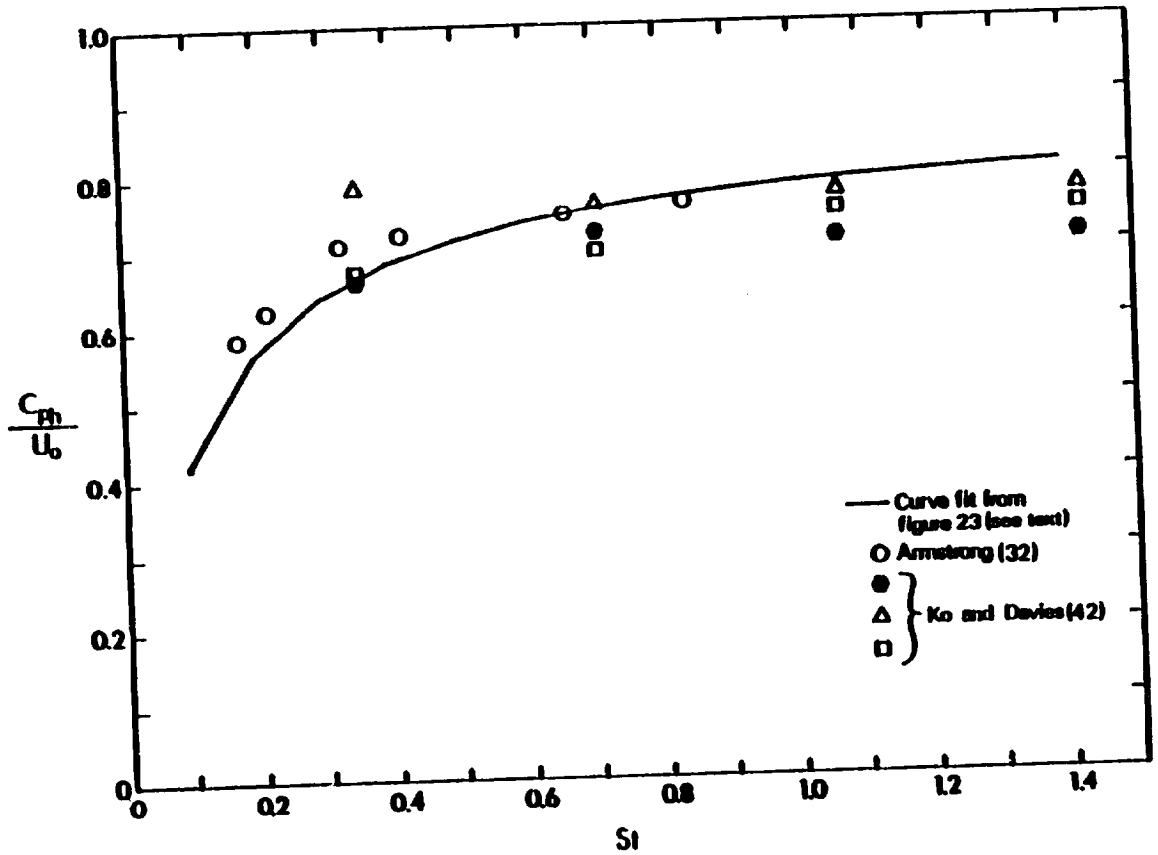

Figure 24. Phase velocity as a function of Strouhal number

McLaughlin[34].

Figure 25 contains the remaining wave number-frequency data where the Mach number was less than 0.3. The works of Crow and Champagne, and Chan compare favorably for the n=0 mode with a curve fit where the wave number-frequency relationship follows the form:

$$krD = -0.7435 + 11.714*St$$

Comparing the slope of this line to the previous curve fit shows that there is a definite difference between the two Mach number ranges. Also, there is a difference between the n=0 mode and the n=1 and 2 modes shown. It remains to be determined whether this is a Mach number effect or if there was an excessive level of excitation used at those low Mach numbers.

It is worth noting that in the present investigation it was possible to watch the cross correlation develop as the Saicor analyzer computed the correlation. During this time, one could observe that the coherent structure at a given frequency was not present in the flow at all times but appeared in "wave packets". It was not determined if several "wave packets" existed in the jet simultaneously or if the jet jumped from one frequency to another (i.e. only one "wave packet" at a given position at one time). Either way, the different frequency "wave packets" in the jet caused a broadening of the flow fluctuation spectra.

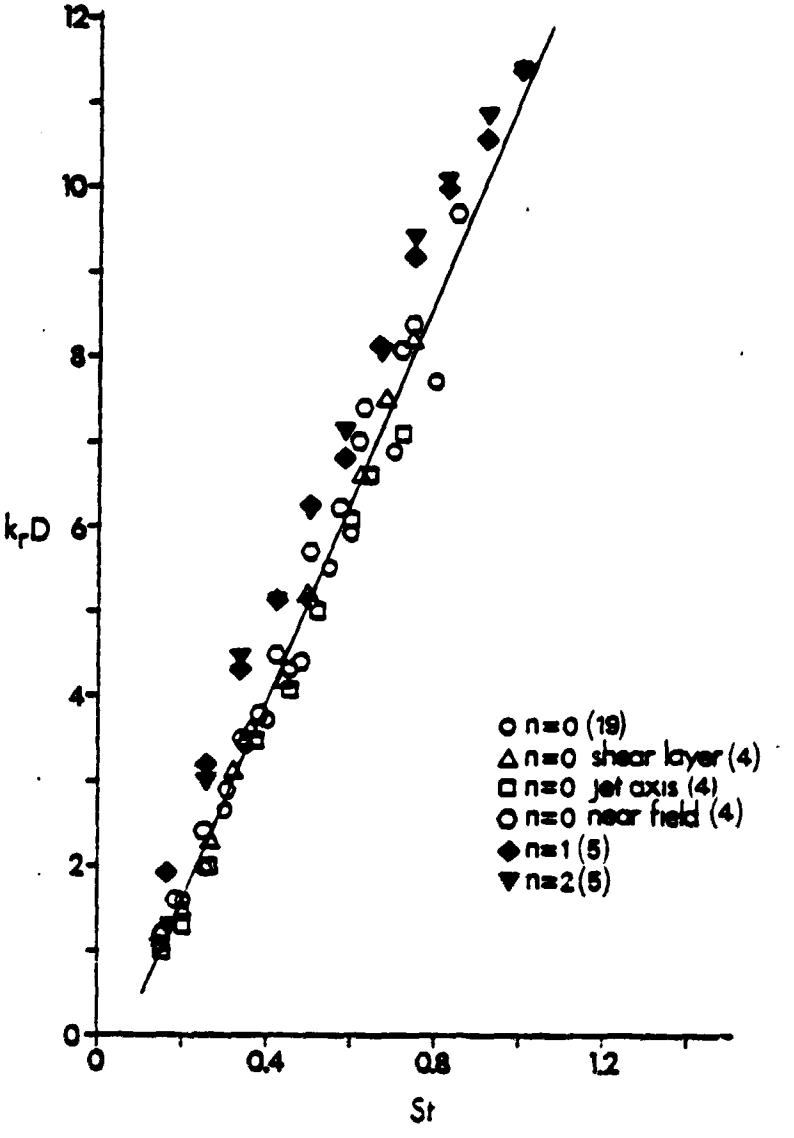

Figure 25. Axial wave number variation with Strouhal number, M < 0.3

Azimuthal Modal Decomposition

A possible explanation for the difference between the incompressible and compressible jets was that perhaps the jets contained different modes which resulted in the different wave number-frequency relationships. The incompressible jets were excited with acoustical drivers in the plenum of the facility. This technique preferentially excited the n=0, axisymmetric mode. However, Chan[5] also used an acoustic driver excitation device which consisted of six acoustic drivers located around the azimuth of the jet which could excite the n=1 and n=2 modes. These two higher modes, which were included in Figure 25, maintained approximately the same wave number-frequency relationship as did the axisymmetric mode n = 0.

The compressible jets studied by Armstrong[32] contained the first three modes at each frequency (n=0, 1 and 2). The jets studied by Morrison and McLaughlin[15] contained a superposition of n= +1 and -1 modes. Stromberg, et. al.[17] observed one frequency which was axisymmetric and another that was antisymmetric. The present study determined that several modes were present at each frequency studied. Therefore, the modes present in the compressible jets did not seem to alter the axial wave number-frequency relationship.

In the current study, the azimuthal phase distribution

for the different frequencies studied at M=0.6 were measured using the same techniques outlined for the axial wave length measurements except the movable probe was traversed in the azimuthal direction. Initially, two probes were tried in an unexcited jet (Morrison and Wattanachayakul[33]) but it was found that only the n=0 mode was measurable. If one considers that higher modes occur simultaneously along with an n=0 mode, a possible explanation exists. The first two modes (n=1 and -1) could combine and cause the jet to flap. The orientation of this flapping in any one azimuthal plane may vary during the time measurements are being made and hence cancel out the effect of the flapping. This would result in only the n=0 mode being measured. In order to overcome this problem and to be able to measure higher modes (n=-3, -2, -1, 0, 1, 2, and 3) the flow fluctuations must be simultaneously measured at six azimuthal locations. Instead of using that many probes, artificial excitation was used in this study to stabilize the jet modes into one plane of oscillation.

Representative of the data obtained, Figure 26 shows the azimuthal phase distribution for St=0.47 measured at x/D=3 and x/D=7 in the Mach number 0.6 jet. This spectral component contains several modes. In order to represent the data, the phase distribution was curve fit using a technique developed by Troutt and McLaughlin[34]. This technique involved superimposing mode numbers according to

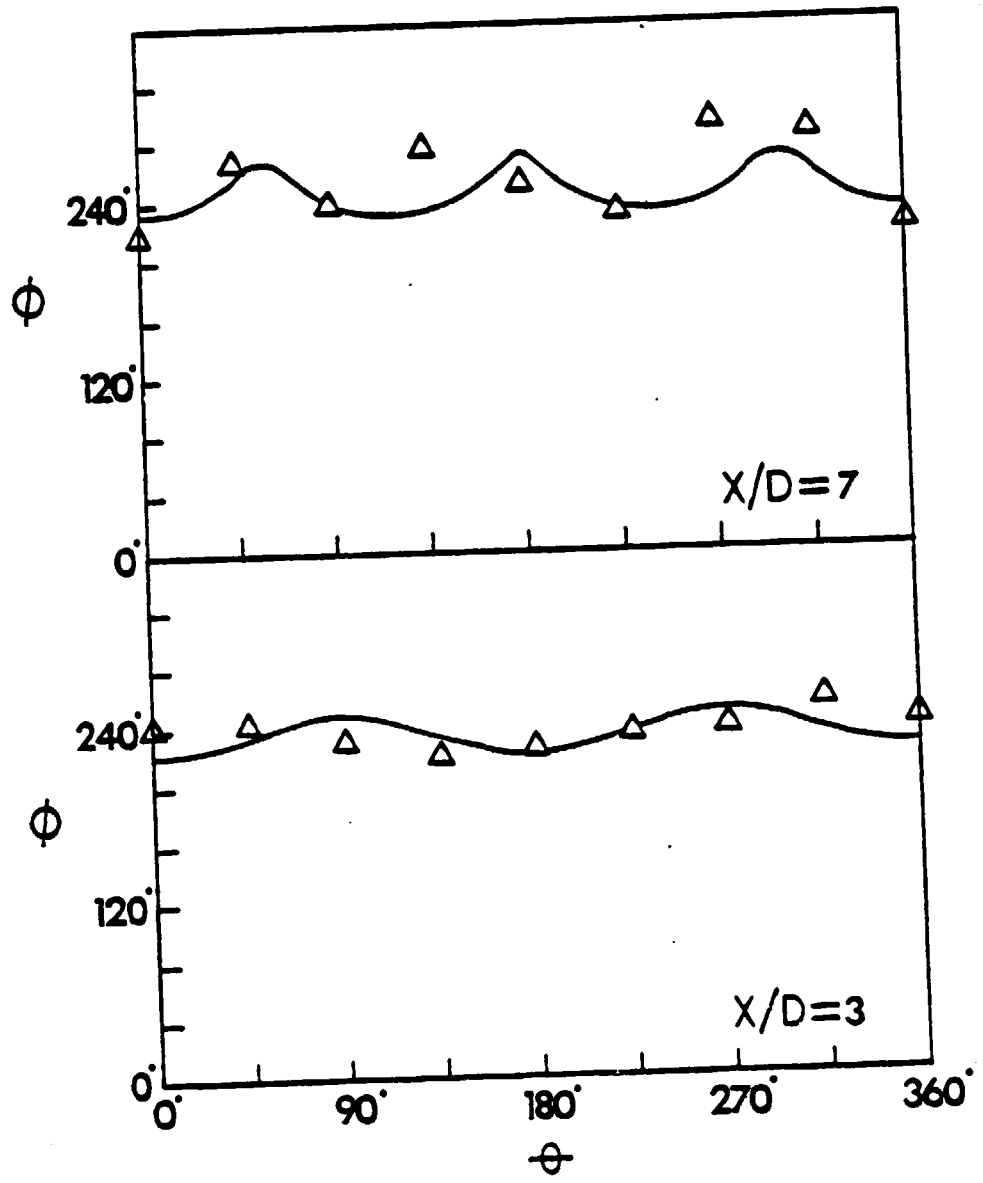

Figure 26. Azimuthal phase distribution, M=0.6, St=0.474

the equation:

$$q_n = \Sigma A_n * \exp(i(n\Theta - wt + \alpha_n))$$

where A_n = amplitude of mode "n"

Θ = azimuthal angle

w = frequency

t = time

α_n = phase difference between modes

To obtain a curve fit, the frequency is held constant and various values of amplitude (A_n) and the phase difference between modes (α_n) are selected for each of the seven modes considered. This is repeated until the curve fit obtained agrees with the measured phase (ϕ) vs. azimuthal angle (Θ) data.

Table III contains the modal decompositions for the spectral components studied in the Mach number 0.6 jet. The table illustrates that the coherent structure in the jet consisted of many different mode combinations which varied with frequency and downstream location. Typically, as the flow progressed downstream, higher number modes increased in importance. This could be due to a loss in azimuthal coherence, causing variations in the lower mode number distributions which were reflected in the addition of higher number modes in order to obtain a curve fit. This is similar to a smoke ring which begins to take on higher mode numbers as it loses its azimuthal coherence just prior to its breakup.

TABLE III

Mach Number 0.6 Modal Decomposition

St	x/D	n = 0	1	-1	2	-2	3	-3
0.16	3	0.90	0.50	1.00	0.50	-0.60	0.00	0.00
	7	0.22	0.00	0.17	-1.00	-1.00	0.00	0.00
0.32	3	0.71	0.28	0.43	0.43	1.00	0.00	0.00
	7	1.00	0.42	0.20	0.60	0.20	0.00	0.00
0.47	3	0.90	0.00	0.00	1.00	1.00	0.00	0.00
	7	1.00	0.00	0.00	0.00	0.00	0.33	0.33
0.63	3	1.00	0.00	0.00	0.50	-0.50	0.00	0.00
	7	1.00	0.00	0.22	-0.11	-0.22	0.00	0.00
0.95	3	1.00	0.32	0.51	0.34	0.13	0.00	0.00
	7	1.00	0.24	0.24	0.00	0.00	0.24	0.12
1.26	3	1.00	0.17	0.17	0.00	0.00	0.17	0.08
	7	1.00	0.06	0.06	0.00	0.00	0.14	0.14

V. RESULTS OF ACOUSTIC MEASUREMENTS

SPL Contours

Sound pressure level (SPL) contours were made in the "near" ($r/d < 60$, $x/D < 60$) field for the natural M=0.6 jet and can be seen in Figure 27. These contours seem to indicate that for this jet the noise is generated from a location near the end of the potential core. This axial location also corresponds to where the mass velocity fluctuations reached a maximum level. The contours obtained for this jet compare favorably with the measurements made by Stromberg[36] on a M=0.9 jet and also with the measurements Mollo-Christensen[18] made on M=0.8 and M=0.9 jets. The maximum sound pressure level measured in the flow field was 122 db.

SPL Directivity

The sound pressure level as a function of the angle from the jet axis (Φ) was measured for all three of the jets studied. These measurements were made at a constant radius of 36 diameters from the nozzle exit. This data is presented in Figure 28. The noise generated increased with increasing Mach number and in all three cases appeared to reach a maximum at 30° from the jet axis. This is consistent with the findings of Mollo-Christensen et.al.[31] who also found that the noise reached a maximum at 30° for

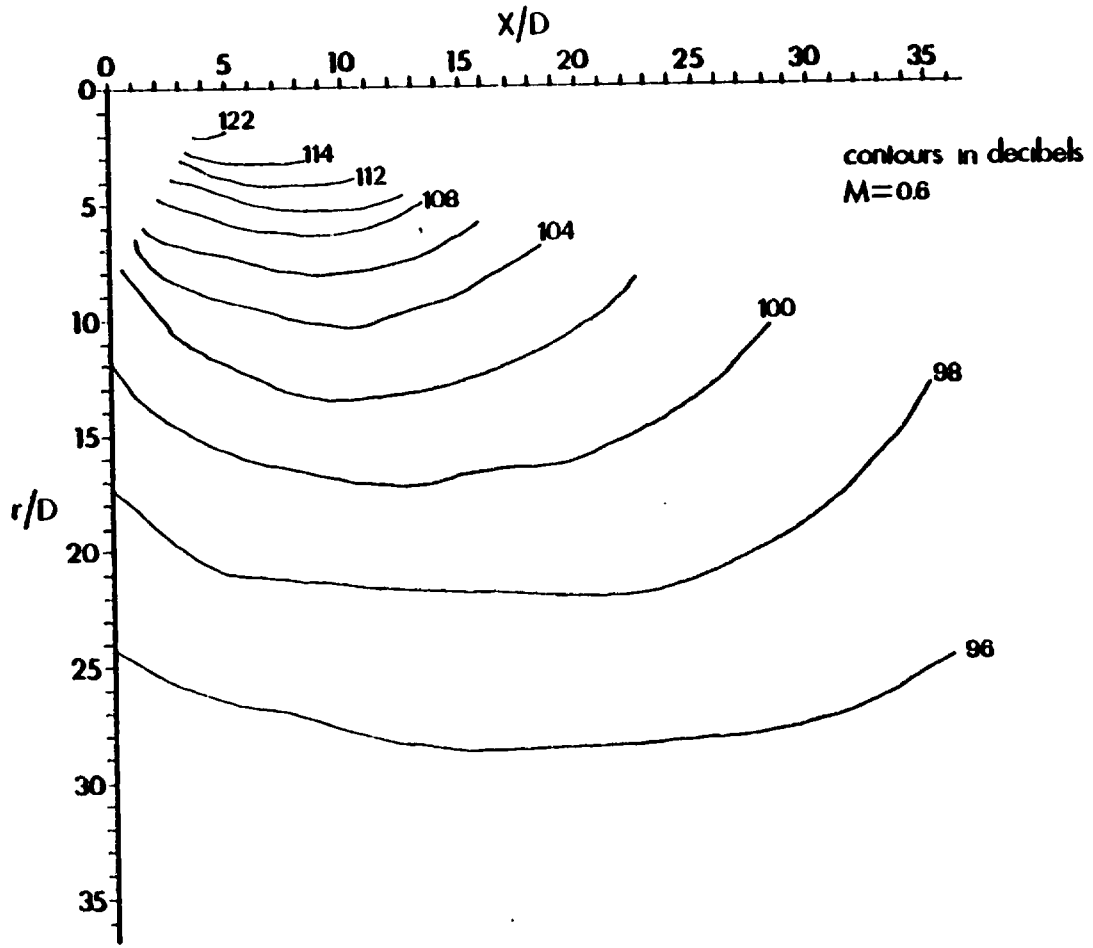

Figure 27. Sound pressure level contours, M=0.6

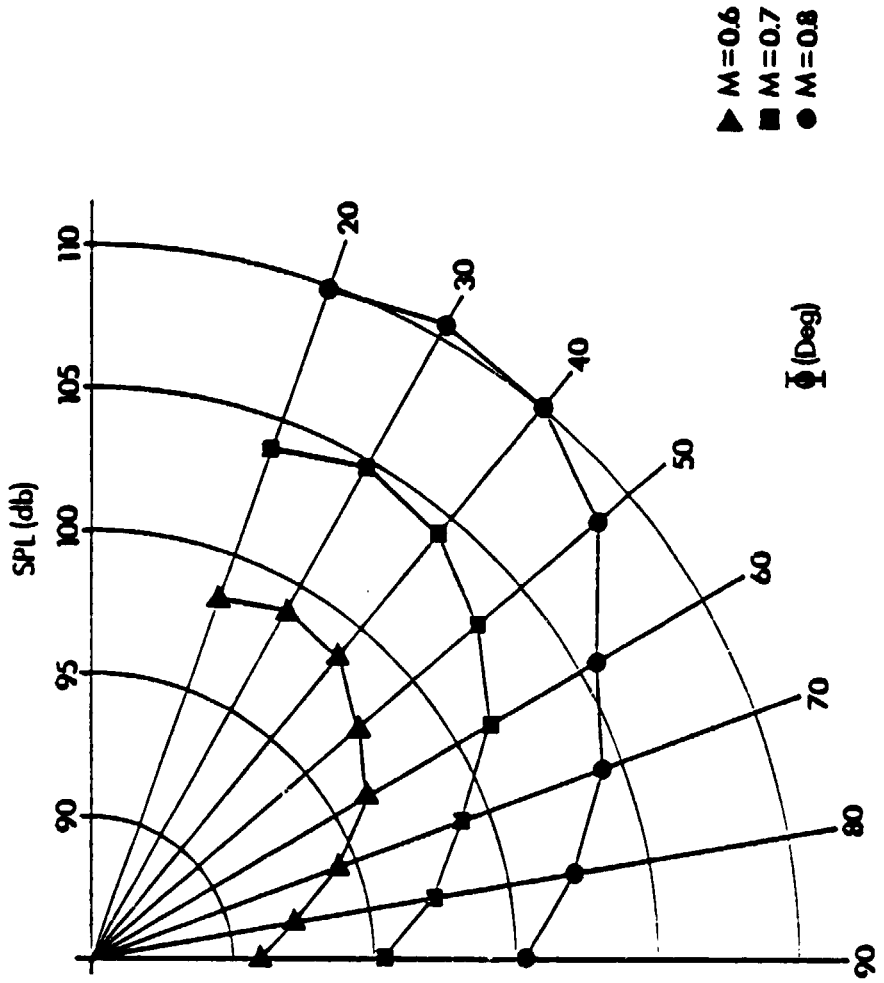

Figure 28. Directivity of full-band sound pressure levels

a high Reynolds number M=0.9 jet.

To determine the effect artificial excitation had on the acoustic field, the SPL as a function of the angle from the jet axis (Φ) measurements were repeated for the excited M=0.6 jet. The microphone signal was 1-20 KHz bandpass filtered while the jet was excited at each of the six selected frequencies. The results of these measurements can be seen in Figure 29. This figure shows that except for the mid-band excitation frequency range ($0.474 < St < 0.632$) the SPL levels follow the trend observed for the M=0.6 jet in Figure 28. When the jet was excited in the mid-band frequency range the sound pressure levels increased. This suggests that the noise production mechanism in the jet is a more effecient noise producer when excited at these mid-band frequencies.

Individual frequencies were studied by 1/10 octave bandpass filtering the microphone signal about the excitation frequency. These individual frequency measurements are shown in Figure 30. Shown in this Figure are the natural jet sound pressure levels along with the excited jet sound pressure levels. In all cases, the excited jet levels are slightly higher than the natural jet levels. The largest differences occurred when the jet was excited at 15 KHz and 20 KHz. These differences are undoubtedly due to the experimental error introduced by the microphone, which had a repeatability factor of ±3db. An

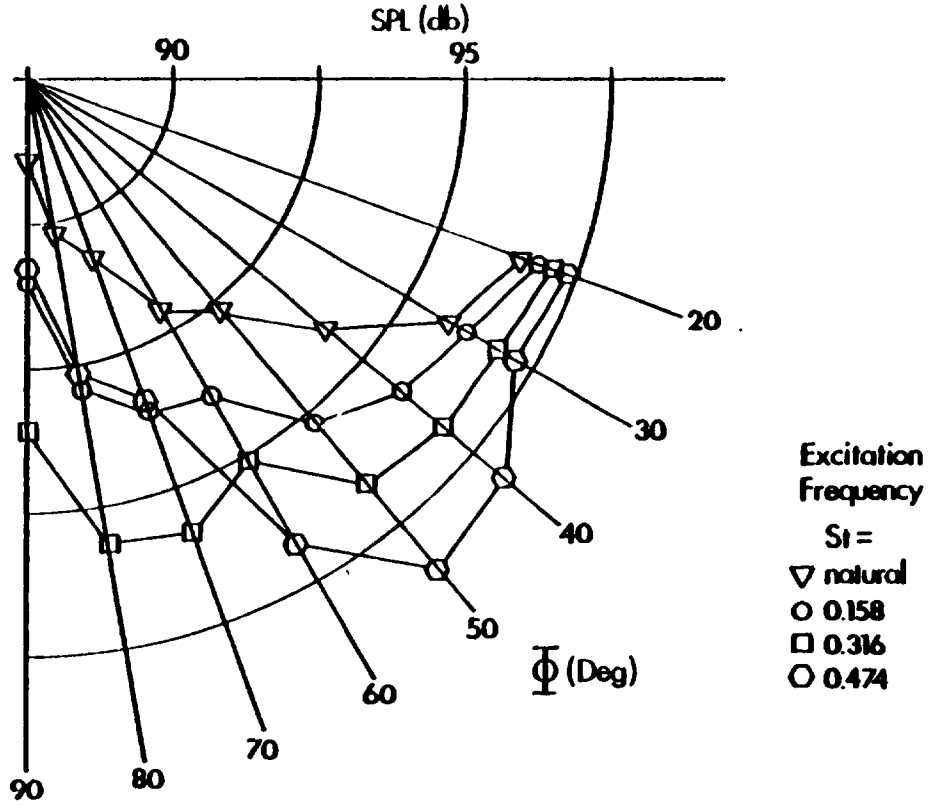

Figure 29. Directivity of full-band sound pressure levels for artificially excited jet, M=0.6

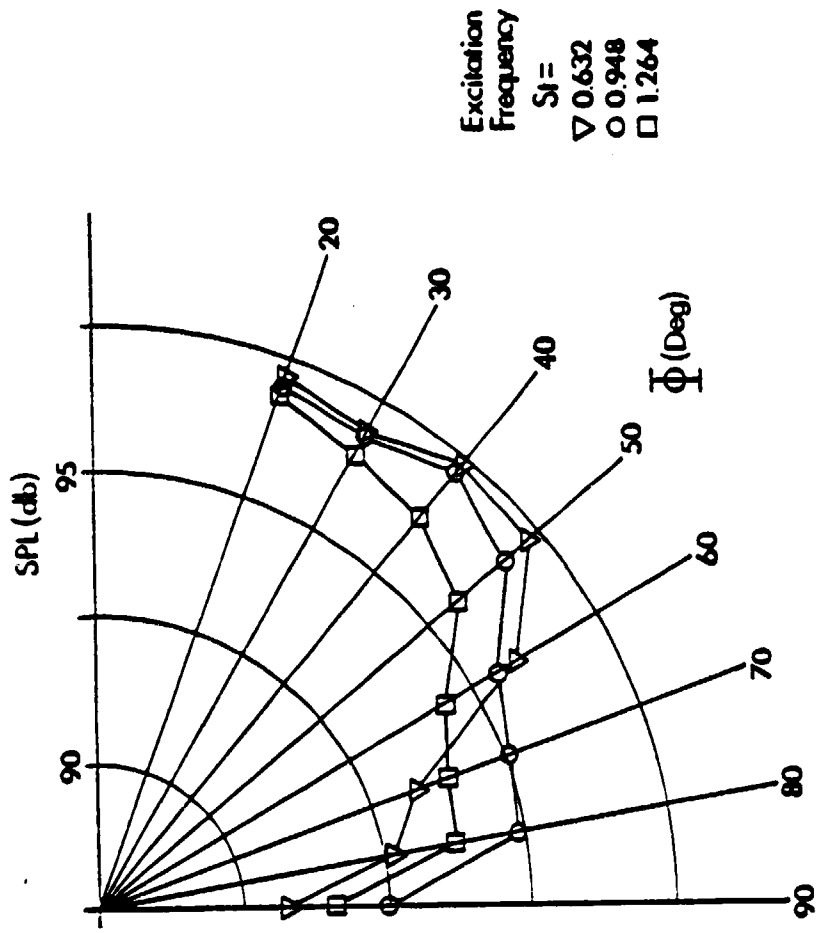

Figure 29. continued

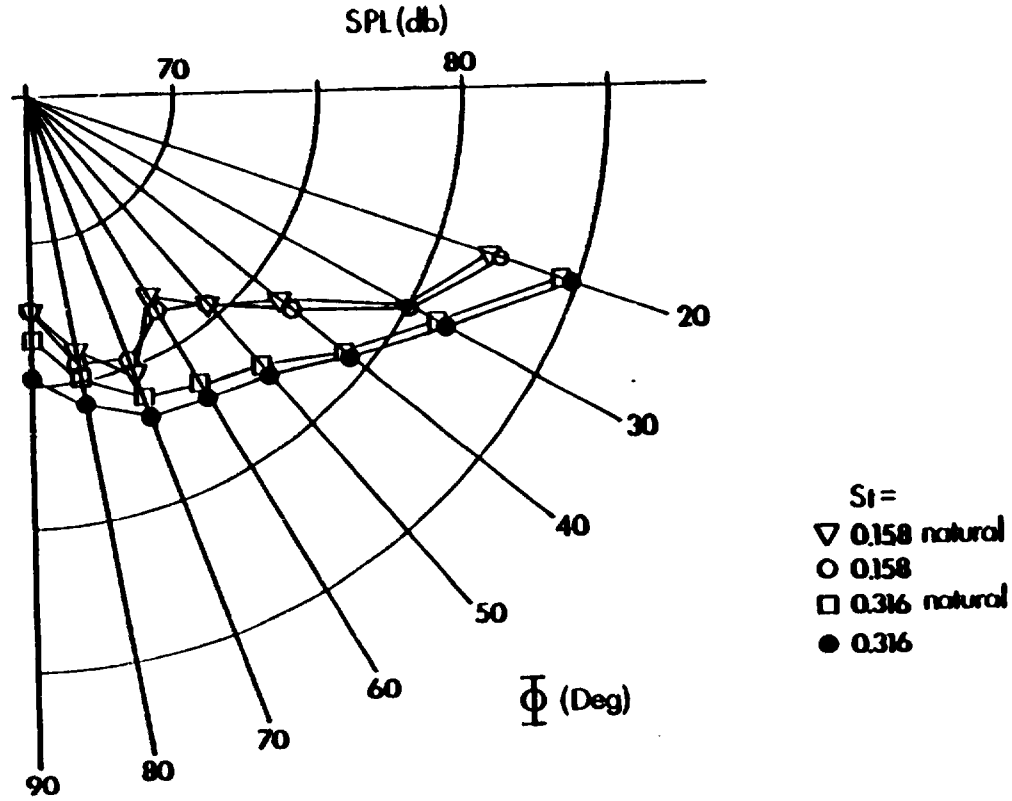

Figure 30. Directivity of individual frequency sound pressure levels for the natural and excited jet, M=0.6

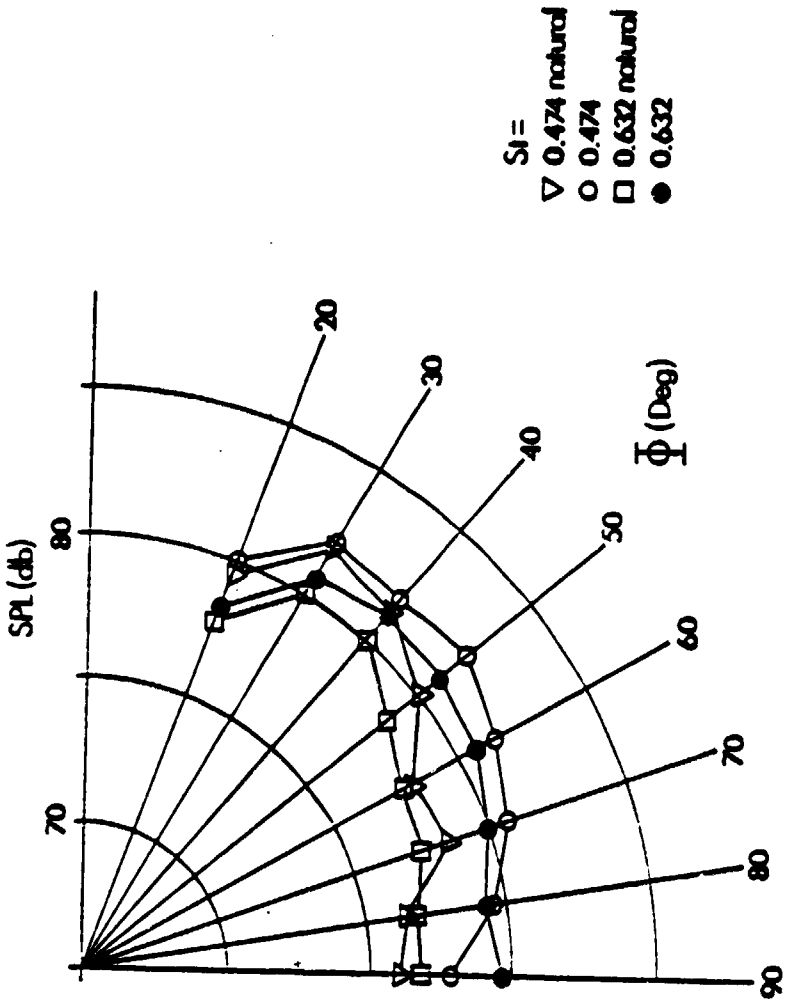

Figure 30. continued

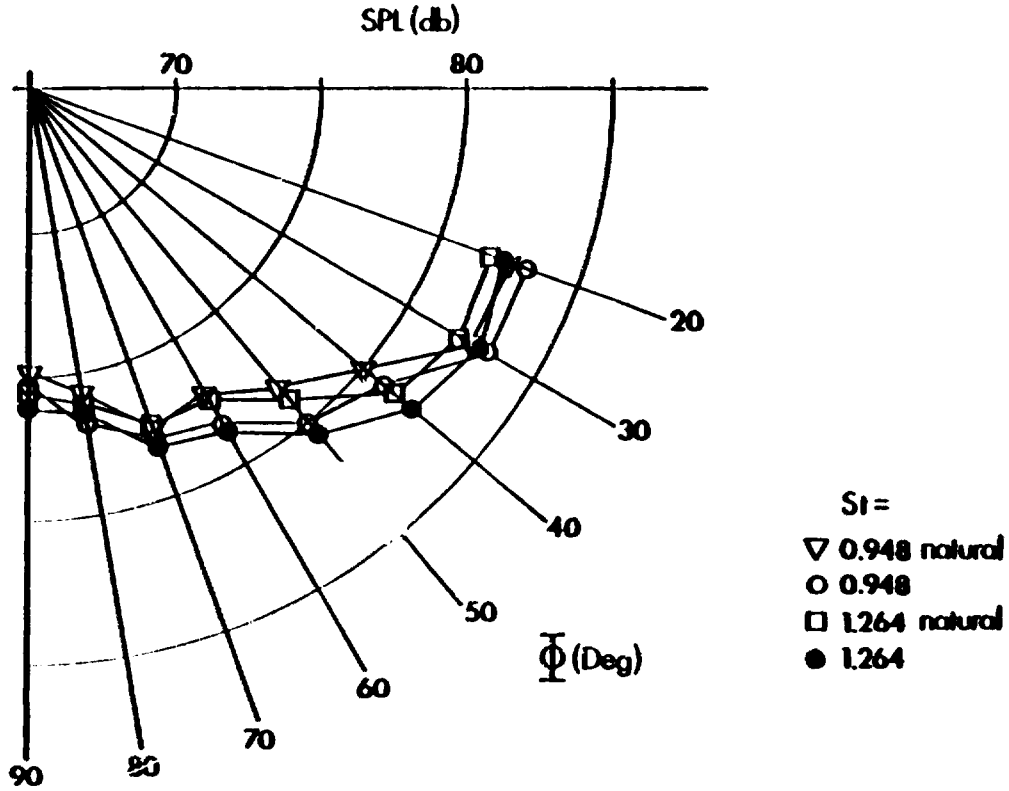

Figure 30. continued

obvious trend observed in this Figure is that the frequencies in the jet shift towards higher values as the angle from the jet axis (Φ) increases. In Figure 29, it was shown that more noise was produced when the jet was excited by mid-band frequencies, but this is not evident in the individual frequency measurements. This indicates that excitation at the mid-band frquencies increased the broad band noise rather than just the noise at that individual frequency.

Spectra were also recorded at various angular locations from the jet centerline for each of the jets and can be seen in Figures 31, 32, and 33. As in the individual frequency directivity plots (Figure 30), these spectra show that as the angle from the jet centerline increased the frequencies shifted towards higher values. (Note that the frequency scale goes up to 50 KHz).

An explanation for this angular dependence of the frequencies in the jet was given by Mollo-Christensen and Narasimha[37]. They postulated that a sound wave travelling in the downstream direction will be moving at the speed of sound with respect to the air in the jet and with a Mach number of M+1 with respect to the outside air. The noise transmission will therefore be at an angle given by:

$$\Phi = \cos^{-1}(1/1+M)$$

Sound waves moving obliquely to the jet axis will be transmitted and reflected by the shear layer. This will

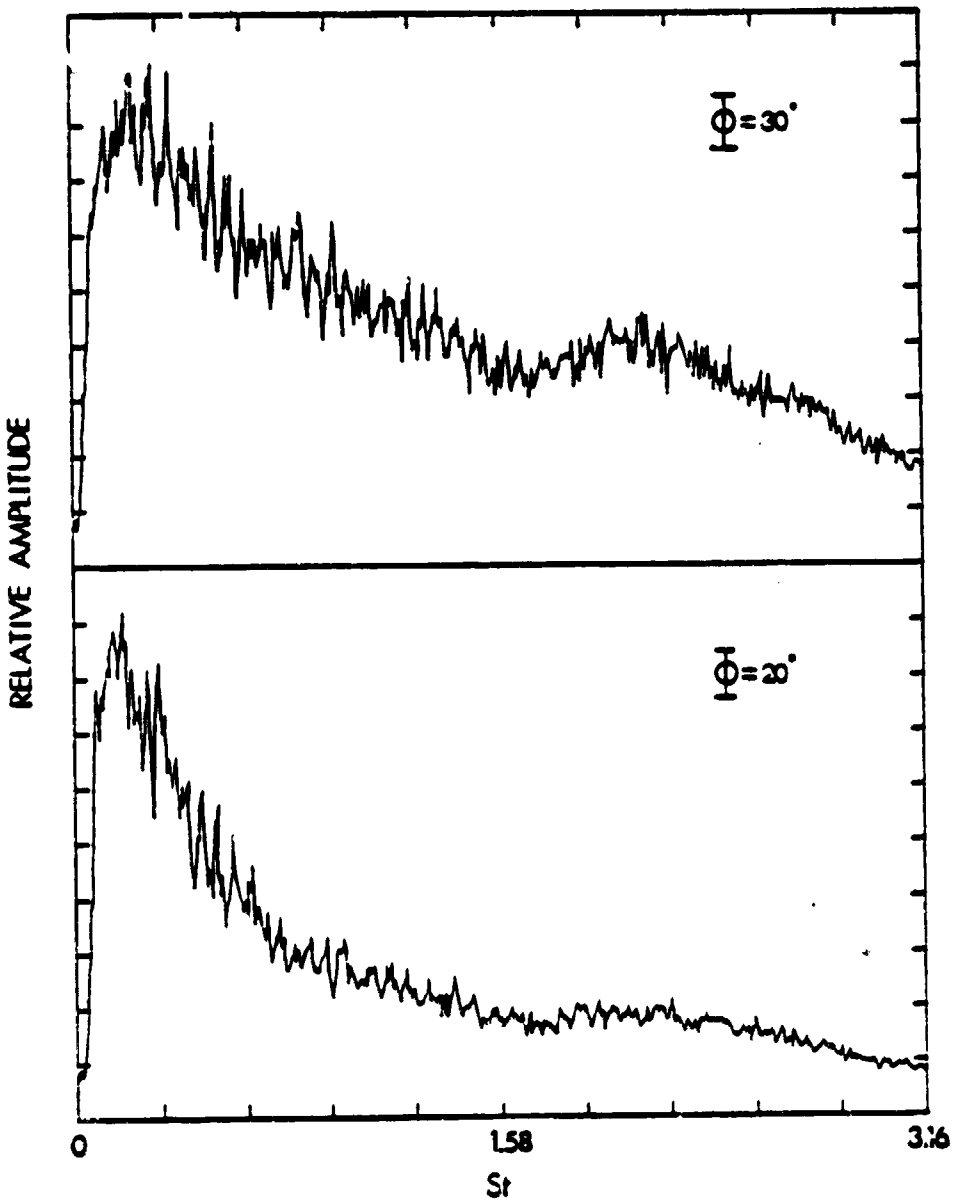

Figure 31. Microphone spectra, M=0.6

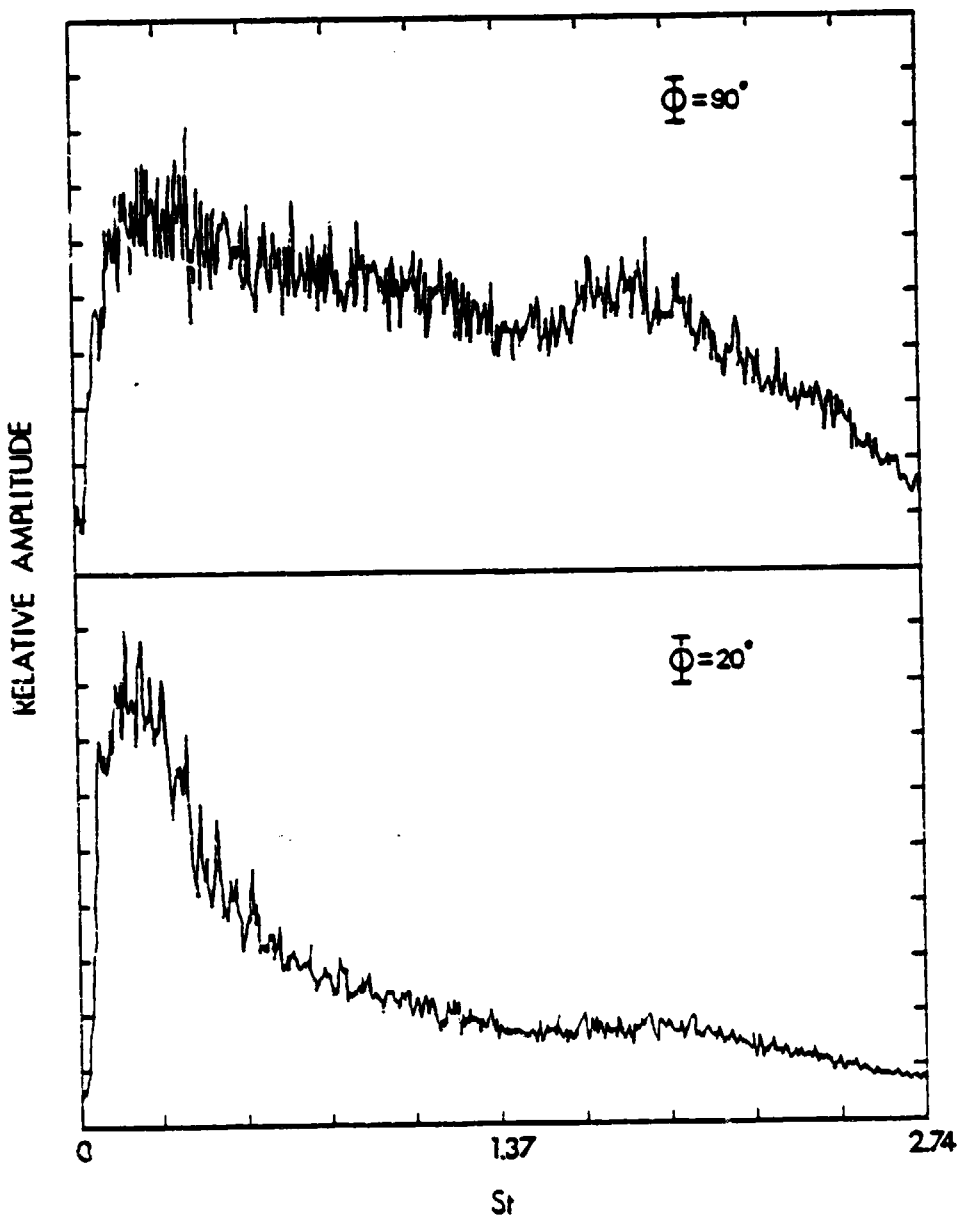

Figure 32. Microphone spectra, M=0.7

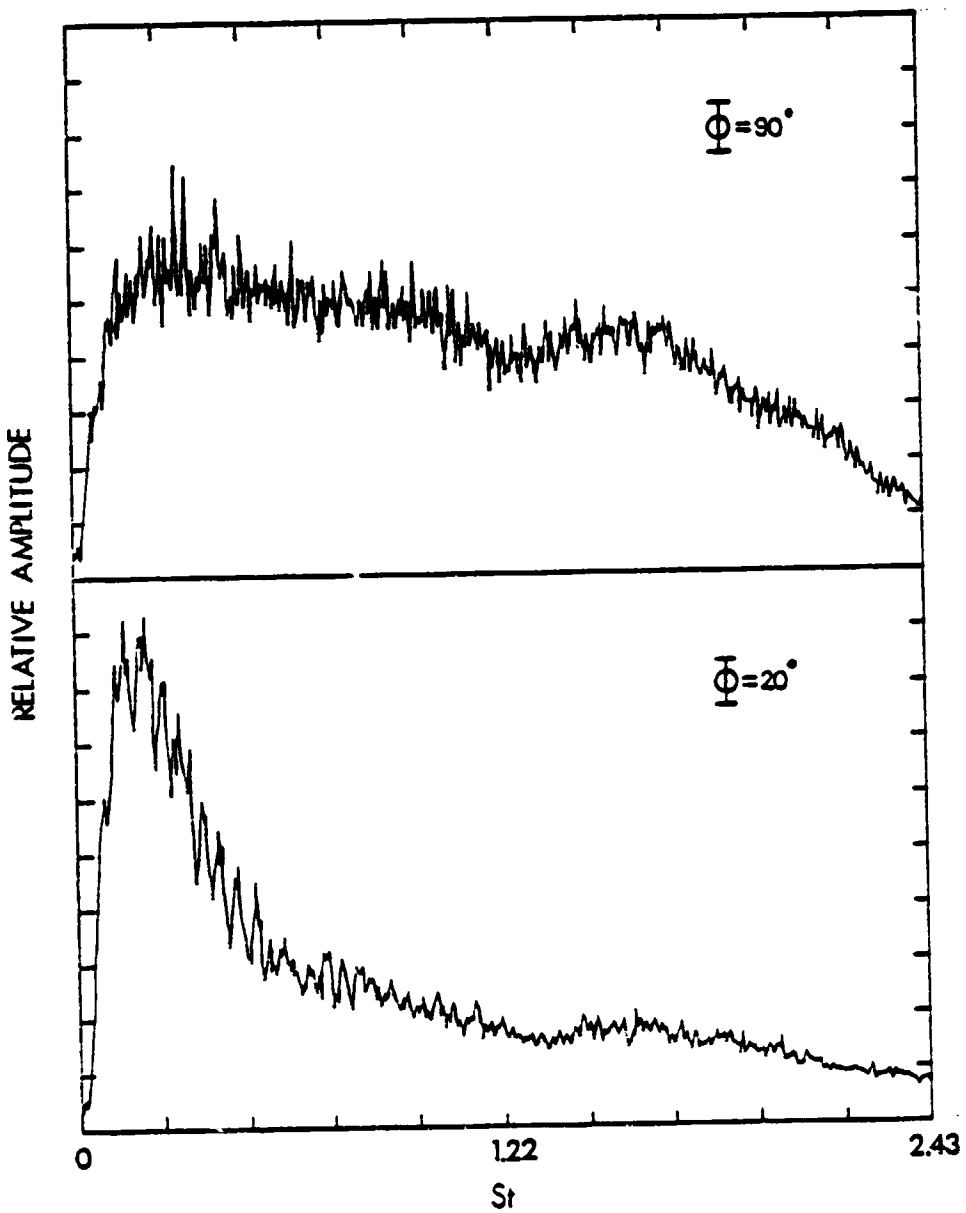

Figure 33. Microphone spectra, M=0.8

cause certain long wavelengths to resonate back and forth across the jet. All waves will be radiated according to the equation stated, but by the time the waves which have been bounced back and forth many times are radiated they have been carried downstream into a region where the Mach number has decreased. Thus if M has decreased the value of Φ will be smaller. This accounts for the low frequency maxima near the jet axis and the the high frequency maxima further away from the jet axis.

In light of the above discussion, it is interesting to note that the axial wave speed (C_{ph}) decreased with decreasing frequency much in the same way that Mollo-Christensen and Narasimha[37] suggested that the convection and refraction carried the lower frequency sound waves into regions of slower mean flow before being emitted to the surroundings. It is possible that there is an interaction between the coherent structure's axial wave speed and the peak sound emission angle (Φ) such that lower wave speeds result in lower angles.

VI. CONCLUSIONS

At Mach numbers less than 0.3, it was shown that the coherent structure was dependent upon the Reynolds number based on the jet diameter, the shear layer thickness, and the turbulence level in the shear layer[28]. For Mach numbers greater than 0.3, the dependence upon Reynolds number and turbulence level did not exist. The coherent structures in the compressible jets possessed the same axial wave number-frequency relationship over a broad range of Mach and Reynolds numbers and were independent of the initial shear layer thickness and turbulence level. Measurements showed that this relationship was valid for jets with several different azimuthal modal compositions.

Spectra obtained for both natural and excited jets revealed that the artifical excitation device used in this study did not alter the frequency content of the jets. It was also shown that axial wave numbers could be obtained using one hot-wire probe and artificial excitation that were the same as those obtained with two hot-wire probes in an unexcited jet. Both of these results are in agreement with the work done by Wattanachayakul[35].

Acoustic measurements revealed that the major noise source in the M=0.6 jet appears to be located near the end of the potential core. This corresponds to the axial location where the flow fluctuations reach a maximum level.

This result was also obtained by other investigators[31,36]. Noise radiated by the jets was found to reach a maximum value around 30° from the jet axis. It was found that the frequency content of this radiated noise was dependent upon the angle from the jet axis. As the angle from the jet axis increased the spectra of the noise shifted to higher frequencies. The noise production mechanism in the jet was found to be more reponsive to mid-band excitation frequencies ($0.474 < St < 0.632$). Excitation at these frequencies caused an increase in full spectrum noise.

REFERENCES

1 Tam, C.K.W., "On the Noise of a Nearly Ideally Expanded Supersonic Jet", Journal of Fluid Mechanics, Vol. 51 (1972), pp. 69-95.

2 Tam, C.K.W., "Directional Acoustic Radiation from a Supersonic Jet Generated by Shear Layer Instability", Journal of Fluid Mechanics, Vol. 46 (1971), pp. 757-768.

3 Tam, C.K.W., "Supersonic Jet Noise Generated by Large-Scale Disturbances", Journal of Sound and Vibration, Vol. 38 (1975), pp. 51-79.

4 Chan, Y.Y., "Spatial Waves in Turbulent Jets", The Physics of Fluids, Vol. 17 (1974), pp. 46-53.

5 Chan, Y.Y., "Noise Generated Wavelike Eddies in a Turbulent Jet", ICAS Paper No. 76-42 (1976).

6 Chan, Y.Y., "Discrete Acoustic Radiation from a High Speed Jet as a Singular Perturbation Problem", Canadian Aeronautics and Space Journal, Vol. 21 (1975), pp. 221-227.

7 Liu, J.T.C., "Developing Large-Scale Wavelike Eddies on the Near Jet Noise Field", Journal of Fluid Mechanics, Vol. 62 (1974), pp. 437-464.

8 Morris, P.J., "The Spatial Viscous Instability of Axisymmetric Jets", Journal of Fluid Mechanics, Vol. 77 (1976), pp. 511-529.

9 Morris, P.J., "Flow Characteristics of a Large-Scale Wavelike Structure in a Supersonic Round Jet", Journal of Sound and Vibration, Vol. 53 (1977), pp. 223-244.

10 Morris, P.J. and Tam, C.K.W., "Near and Far Field Noise from Large-Scale Instabilities of Axisymmetric Jets", AIAA Paper No. 77-1351, 1977.

11 McLaughlin, D.K., Seiner, J.M., and Liu, C.H., "On the Noise Generated by Large-Scale Instabilities in Supersonic Jets", AIAA Paper No. 80-0964, 1980.

12 McLaughlin, D.K., Morrison, G.L., and Troutt, T.R., "Experiments on the Instability Waves in a Supersonic Jet and Their Acoustic Radiation", Journal of Fluid Mechanics, Vol. 69 (1976), pp. 73-95.

13 Morrison, G.L., "Effects of Artificial Excitation Upon a Low Reynolds Number Mach 2.5 Jet", AIAA Paper No. 81-2010, 1981.

14 McLaughlin, D.K., Morrison, G.L., and Troutt, T.R., "Reynolds Number Dependence in Supersonic Jet Noise", AIAA Journal, Vol. 15 (1977), pp. 526-532.

15 Morrison, G.L. and McLaughlin, D.K., "The Instability Process in Low Reynolds Number Supersonic Jets", AIAA Journal, Vol. 18 (1980), pp. 793-800.

16 Morrison, G.L. and McLaughlin, D.K., "The Noise Generated By Instabilities in Low Reynolds Number Supersonic Jets", Journal of Sound and Vibration, Vol. 65 (1979), pp. 177-191.

17 Stromberg, J.L., McLaughlin, D.K., and Troutt, T.R., "Flow Field and Acoustic Properties of a Mach Number 0.9 Jet at a Low Reynolds Number", Journal of Sound and Vibration, Vol. 72 (1980), pp. 159-176.

18 Mollo-Christensen, E., "Jet Noise and Shear Flow Instability Seen from an Experimenter's Viewpoint", Journal of Applied Mechanics, Vol. 34 (1967), pp. 1-7.

19 Crow, S.C. and Champagne, F.H., "Orderly Structure in Jet Turbulence", Journal of Fluid Mechanics, Vol. 48 (1971), pp. 547-591.

20 Moore, C.J., "The Role of Shear Layer Instability Waves in Jet Exhaust Noise", Journal of Fluid Mechanics, Vol. 80 (1977), pp. 321-367.

21 Michalke, A. and Fuchs, H.V., "On Turbulence and Noise of an Axisymmetric Shear Flow", Journal of Fluid Mechanics, Vol. 70 (1975), pp. 179-205.

22 Lau, J.C. and Fisher, M.J., "The Vortex-Street Structure of 'Turbulent' Jets, Part I", Journal of Fluid Mechanics, Vol. 67 (1975), pp. 299-337.

23 Lau, J.C., Fisher, M.J., and Fuchs, H.V., "The Intrinsic Structure of Turbulent Jets", Journal of Sound and Vibration, Vol. 22 (1972), pp. 379-406.

24 Brunn, H.H., "A Time-Domain Analysis of the Large-Scale Flow Structure in a Circular Jet. Part I: Moderate Reynolds Numbers", Journal of Fluid Mechanics, Vol. 83 (1977), pp. 641-671.

25 Kalghati, G.T., "Study of Coherent Structures in Axisymmetric Jets Using an Optical Technique", AIAA Journal, Vol. 18 (1980), pp. 225-226.

26 Maestrello, L. and Fung, Y.T., "Quasi-Periodic Structure of a Turbulent Jet", Journal of Sound and Vibration, Vol. 64 (1979), pp. 107-122.

27 Kibens, V., "Discrete Noise Spectrum Generated by an Acoustically Excited Jet", AIAA Journal, Vol. 18 (1980), pp. 434-441.

28 Kibens, V., "The Limits of Initial Shear-Layer Influence on Jet Development", AIAA Paper No. 81-1960, 1981.

29 Horstman, C.C. and Rose, W.C., "Hot-Wire Anemometry in Transonic Flow", AIAA Journal, Vol. 15 (1977), pp. 395-401.

30 Tester, B.J., Morris, P.J., Lau, J.C., and Tanna, H.K., "The Generation, Radiation and Production of Supersonic Jet Noise - Volume 1", Technical Report AFAPL-TR-78-85, 1978.

31 Mollo-Christensen, E., Koplin, M.A., and Martuccelli, J.R., "Experiments on Jet Flows and Jet Noise Far Field Spectra and Directivity Patterns", Journal of Fluid Mechanics, Vol. 18 (1964), pp. 285-301.

32 Armstrong, R.R., "Influence of Mach Number on Coherent Structure Relevant to Jet Noise", AIAA Journal, Vol. 19 (1981), pp. 677-683.

33 Morrison, G.L. and Wattanachayakul, M., "Large Scale Structures in a Mach Number 0.7 Jet", AIAA Paper No. 81-0059, 1981.

34 Troutt, T.R. and McLaughlin, D.K., "Experiments on the Flow and Acoustic Properties of a Moderate Reynolds Number Supersonic Jet", Accepted for publication in the Journal of Fluid Mechanics.

35 Wattanachayakul, M., "Characterization of the Coherent Structure in a High Speed Subsonic Jet", Unpublished Master of Science Thesis, Texas A&M University, College Staion, Texas, 1980.

36 Stromberg, J.L., "Flowfield and Acoustic Measurements of Low Reynolds Number Jets in the Transonic Range", Unpublished Master of Science Thesis, Oklahoma State University, Stillwater, Oklahoma, 1978.

37 Mollo-Christensen, E. and Narasimha, R., "Sound Emmission at High Subsonic Velocities", Journal of Fluid Mechanics, Vol. 8 (1960), pp. 49-60.

38 Lau, J.C., Morris, P.J., and Fisher, M.J., "Turbulence Measurements in Subsonic Jets Using a Laser Velocimeter", AIAA Paper No. 76-348, 1976.

39 Knott, p., et. al., "Laser Velocimeter Developments for Noise Source Location, Vol. II", Air Force Aero Propulsion Laboratory Report No. TR-(to be assigned), Chapter 3, August 1975.

40 Morris, P.J., "Turbulence Measurements in Subsonic and Supersonic Axisymmetric Jets in a Moving Stream", AIAA Paper No. 76-25, 1976.

41 Nagamatsu, H.T. and Sheer, Jr., R.E., "Subsonic and Supersonic Jets and Supersonic Supressor Characteristics", AIAA Paper No. 73-999, 1973.

42 Ko, N.W.M. and Davies, P.O.A.L., "Some Covariance Measurements in a Subsonic Jet", Journal of Sound and Vibration, Vol. 43 (1975), pp. 347-358.

APPENDIX

Normal Hot-wire Reduction Technique

There are currently two types of hot-wire anemometry in use, namely constant temperature and constant current anemometry. The basic difference between these two types is that during operation, the constant temperature type keeps the temperature of the hot-wire constant and the constant current type keeps the current through the hot-wire constant. The hot-wire anemometry used in this study was of the constant temperature type. Although data reduction techniques are different for the two types, the basic theories are derived from the analysis of the heat transfer energy balance between the hot-wire and the surrounding fluid.

The heat transfer energy balance for hot-wire anemometry operated in a flow field is:

$$I^2Rw = Q + k + c(Tw)' \qquad (1)$$

where I^2Rw = power supplied through the hot-wire

Q = the rate of total convective heat transfer from the hot wire to the surrounding fluid

k = the rate of total conductive heat transfer from the hot-wire to both end supports

$c(Tw)'$ = the rate of energy change of the wire (usually negligible for constant temperature hot-wire anemometry)

According to Horstman and Rose[29], the heat transfer energy equation (1) may be reduced to:

$$\frac{e'}{E} = Au\frac{u'}{u} + A\frac{\rho'}{\rho} - At\frac{T_o'}{T_o} \qquad (2)$$

This means that the instantaneous voltage fluctuation is comprised of fluctuations in velocity, density, and total temperature of the flow.

In high speed subsonic flows, Horstman and Rose have also shown that for local hot-wire Reynolds numbers greater than 20 ($Re_o > 20$) and high hot-wire overheat ratios ($S_{aw} > 0.5$), the velocity sensitivity coefficient (Au) is independent of Mach number and equal to the density sensitivity coefficient (A_ρ). Thus, with $Au = A_\rho = Am$, equation (2) becomes:

$$\frac{e'}{E} = Am\frac{(\rho u)'}{(\rho u)} - At\frac{T_o'}{T_o} \qquad (3)$$

Troutt and McLaughlin[34] and Horstman and Rose have shown that for adiabatic free shear flow, the measured mean total temperature gradients are negligible and one can usually assume that the total temperature fluctuations are also negligible. Equation (3) can then be further reduced yeilding an equation for the mean mass velocity fluctuations ($\tilde{m}$):

$$\tilde{m} = \frac{(\rho u)'}{(\rho u)} = \frac{1}{Am}\frac{e'}{E}$$

The value of Am is different for each hot-wire and is obtained through direct calibration. By producing plots of

mean voltage (E) as a function of mass flow rate (ρU) , Am is computed from:

$$Am = \frac{(\rho U)}{E} \frac{\partial E}{\partial (\rho U)} \qquad T=\text{constant}, \; Rw = \text{constant}$$

Addendum to Kevin Whitaker's Thesis

Crossed Hot-wire Measurements

The bulk of this yearly report is contained in the Master of Science Thesis by Kevin Whitaker. Therefore, the thesis is enclosed and this portion of the document will only address the section of the grant that deals with the crossed hot-wire measurements. The crossed hot-wire measurements were performed using matched crossed hot-wires. The matching of the hot-wires was essential since it allowed us to instantaneously add and subtract the voltages from the hot-wires using operational amplifiers. In this manner, two signals, one proportional to the axial mass velocity fluctuations and the other proportional to the radial velocity fluctuations, were obtained. In addition, these two signals were multiplied together using an analog multiplying circuit in order to obtain a voltage that was proportional to the product of the axial mass velocity fluctuations and the radial velocity fluctuations.

The crossed hot-wire measurements were performed in the Mach number 0.6 jet. Profiles of the axial mass velocity fluctuation, the radial velocity fluctuation and the product of the two for the full specturm are shown in Figure A1. Note, due to a technical oversight these figures are the

mirror image of similar profiles presented in Mr. Whitaker's thesis. Comparing the axial mass velocity fluctuation results to those obtained by Mr. Whitaker using a normal hot-wire we obtain good agreement in amplitude and overall profile shape. However, since the crossed hot-wire was arranged such that the wires were perpendicular to the shear annulus and the normal wire was tangent, we do lose some spatial resolution and have an averaging effect. These measurements show the same asymmetry observed with the normal hot-wire. The radial velocity fluctuations possess the same radial dependence as the axial fluctuations but have a lower amplitude. This is to be expected since the axial fluctuations include not only the axial velociy fluctuations but the density fluctuations as well. The Reynolds stress term also shows the same general radial dependence close to the jet exit but tends to decay faster than the other two quantities. This indicates that the coherence of the turbulence is decaying as the flow moves downstream since the correlation between the axial and radial fluctuation levels is decaying

Radial profiles of the axial and radial fluctuations were measured for the individual frequencies studied. These are presented in Figure A2. The results show the same relationship between the axial and radial fluctuation

profiles as was seen for the full spectrum. These profiles also show that the asymmetry of the flow fluctuations is more pronounced in the mid frequency ranges. The corresponding Reynolds stress profiles are shown in Figure A3. These show that the asymmetry is due primarily to the coherent fluctuations and not to the isotropic turbulence since at St = 0.158, the axial and radial fluctuation profiles which contain both the coherent fluctuations and the isotropic turbulence jet are axisymmetric at this frequency. However, the radial profiles of the Reynolds stress term at this frequency are not symmetric. As the frequency is increased to the range of Strouhal numbers greater than 0.9, the jet becomes axisymmteric.

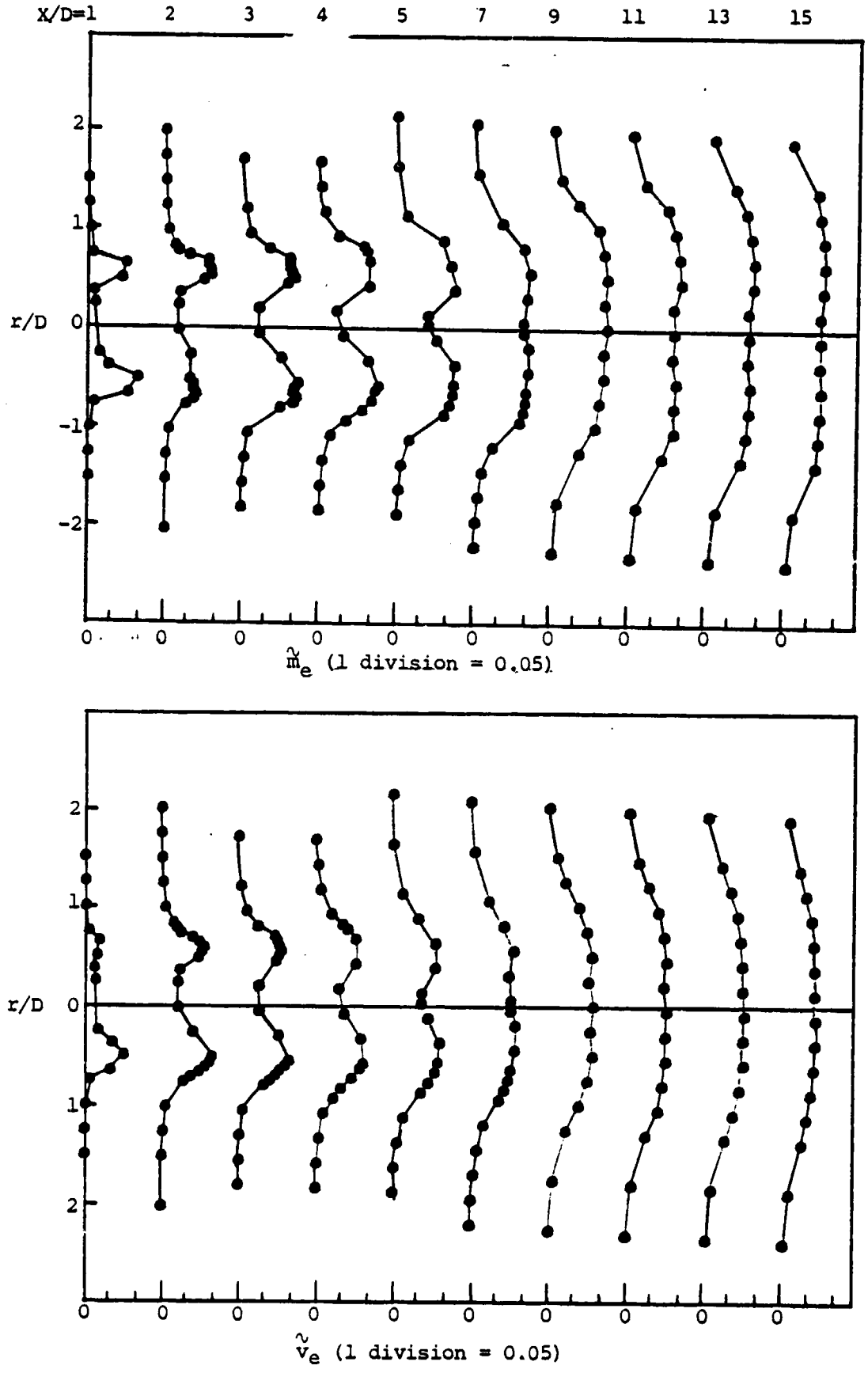

Figure A1. Radial distributions of flow fluctuations full spectrum.

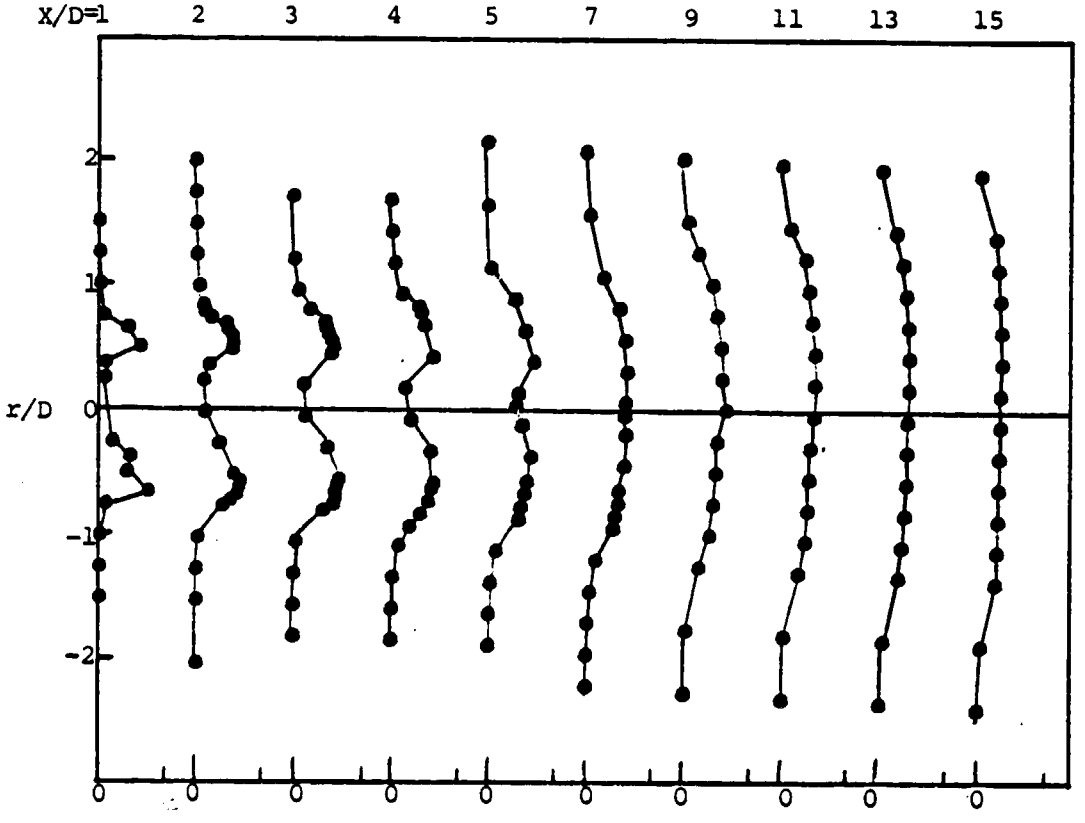

$(\tilde{\rho uv})_e$ (1 division = 0.05)

Figure A1. continued. $V_e = \frac{(v')_{rms}}{\overline{u}_e}$

and $(\tilde{puv})_e = \frac{((\rho u)'v')_{rms}}{(\overline{\rho u})_e \overline{u}_e}$

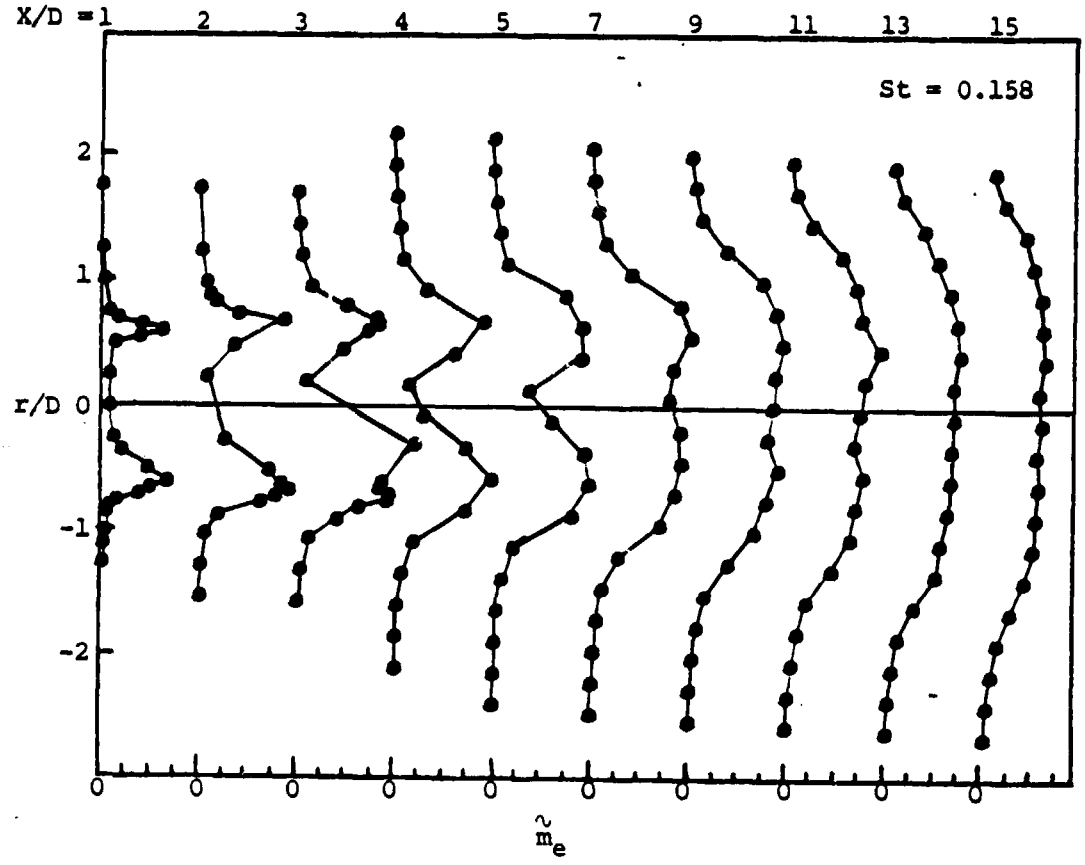

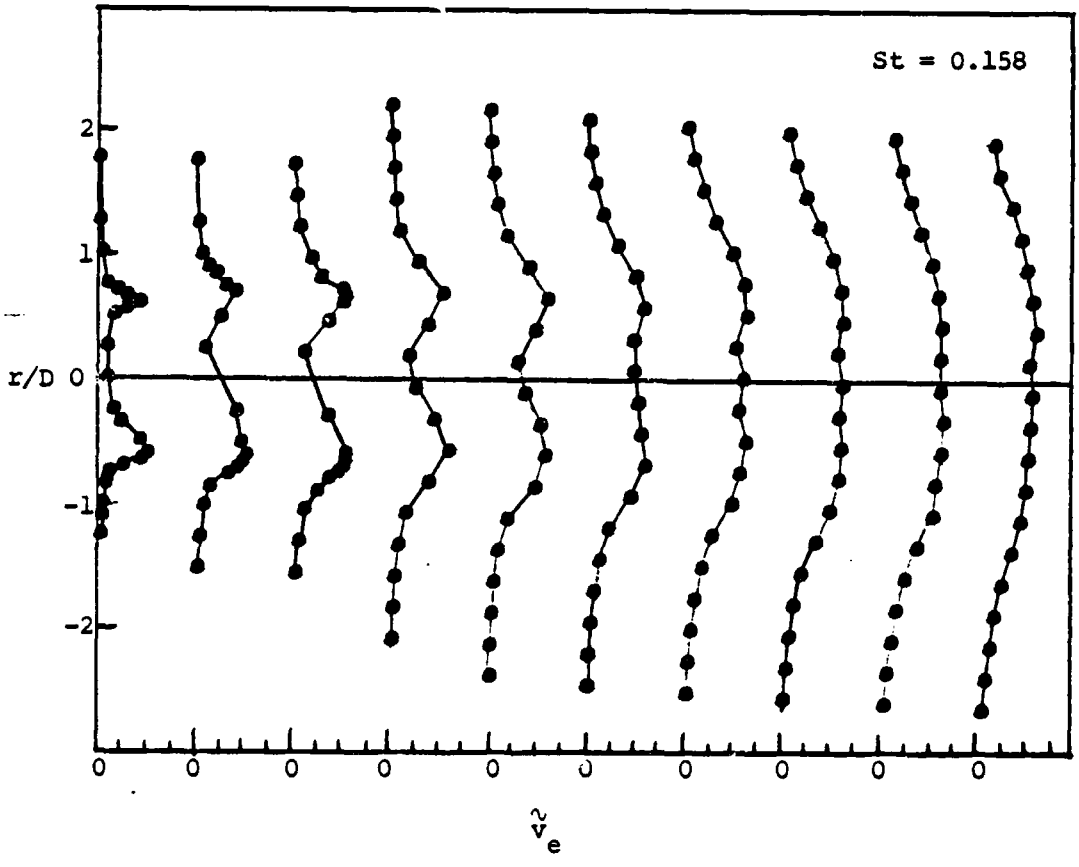

Figure A2. Radial distributions of flow fluctuations.
Horizontal Scale 1 division = 0.005.

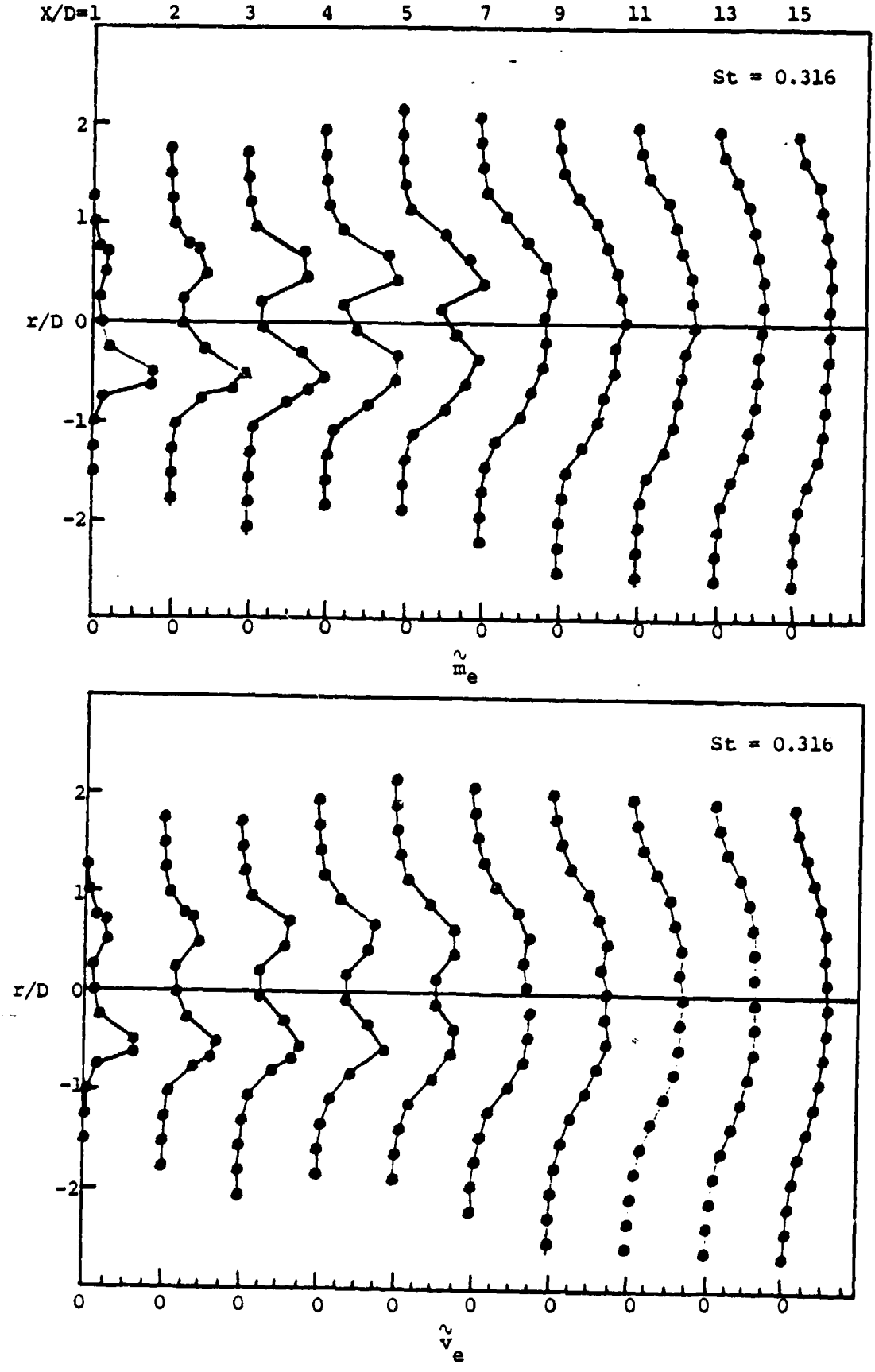

Figure A2 continued.

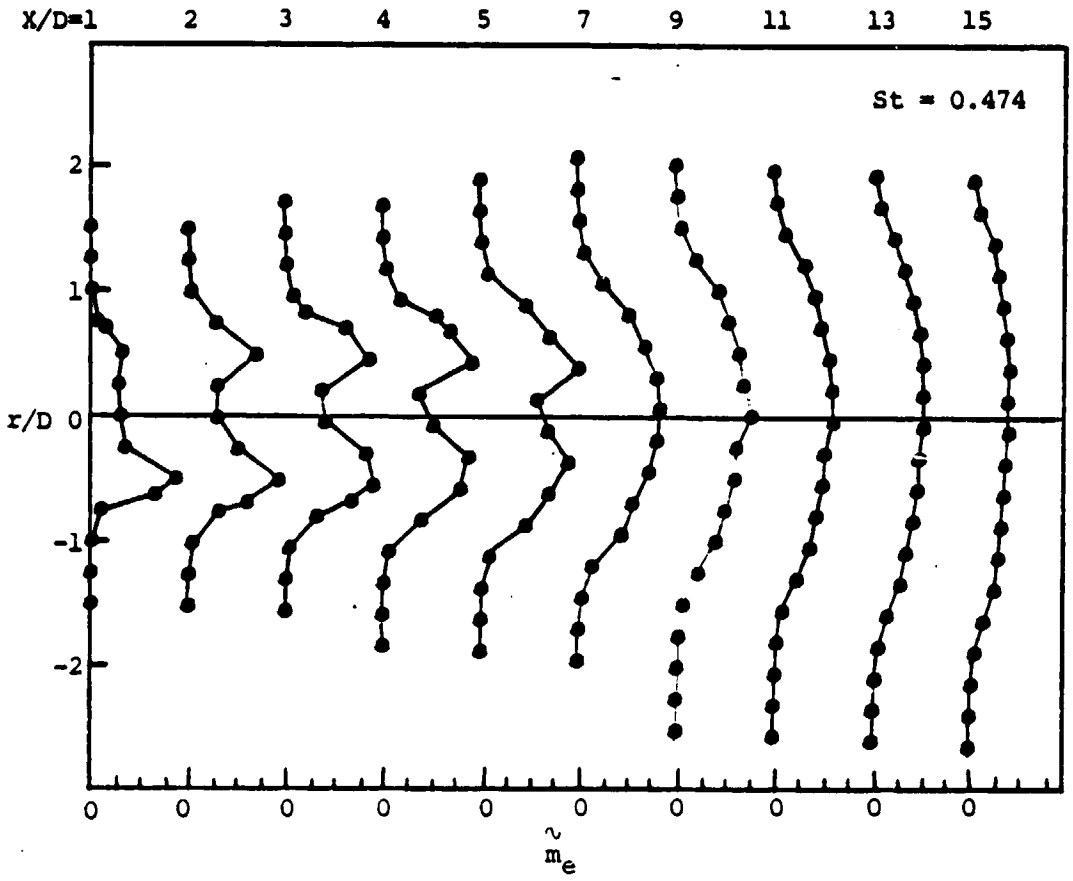

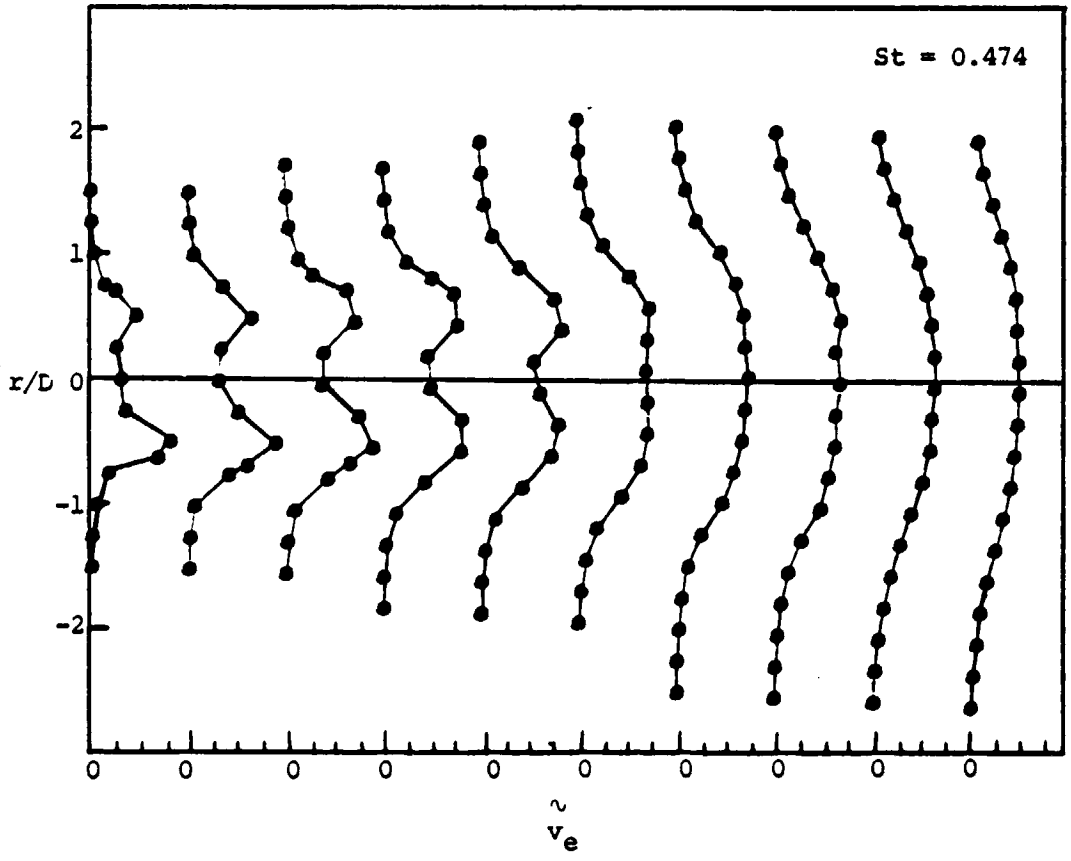

Figure A2 continued.

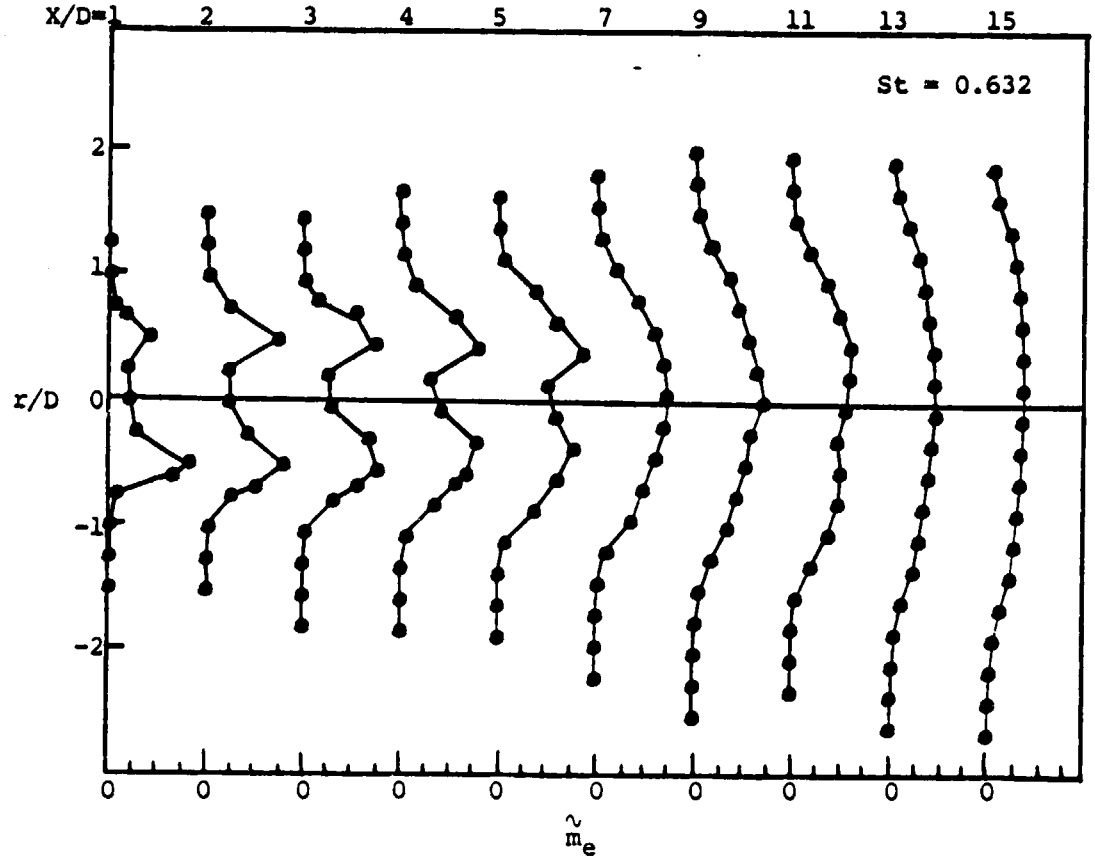

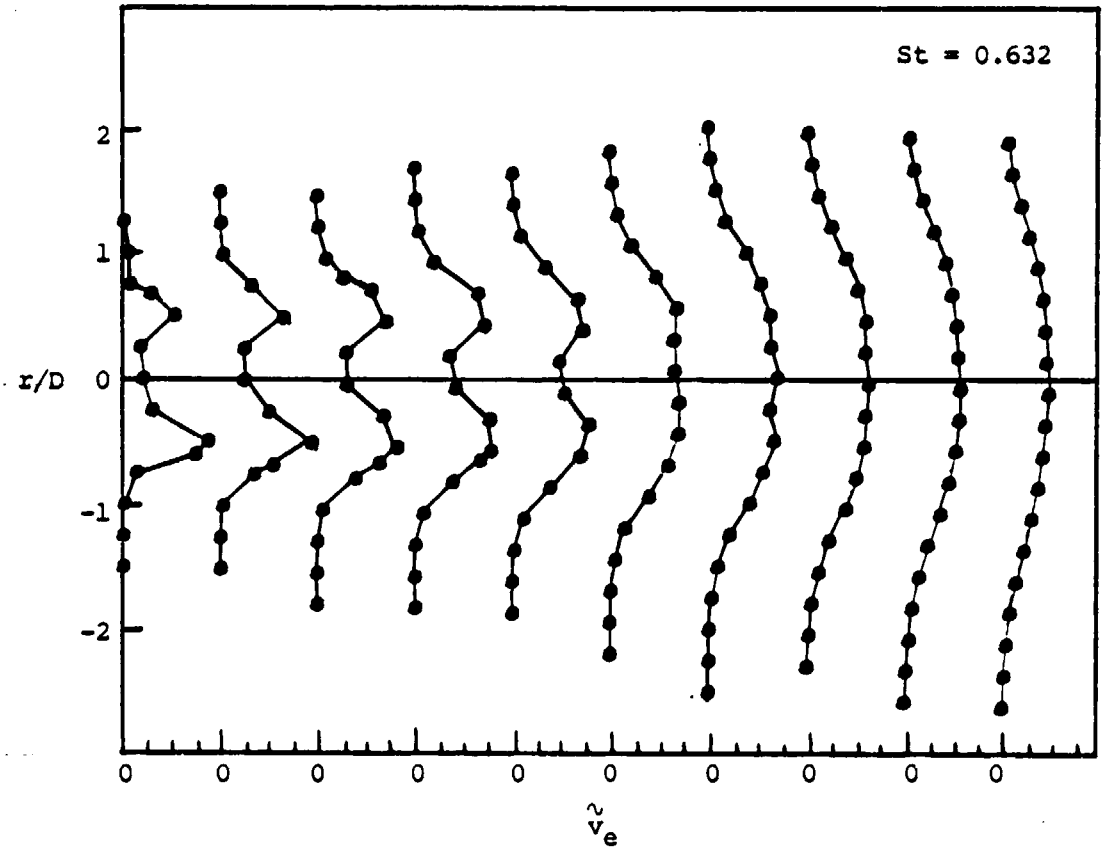

Figure A2. continued.

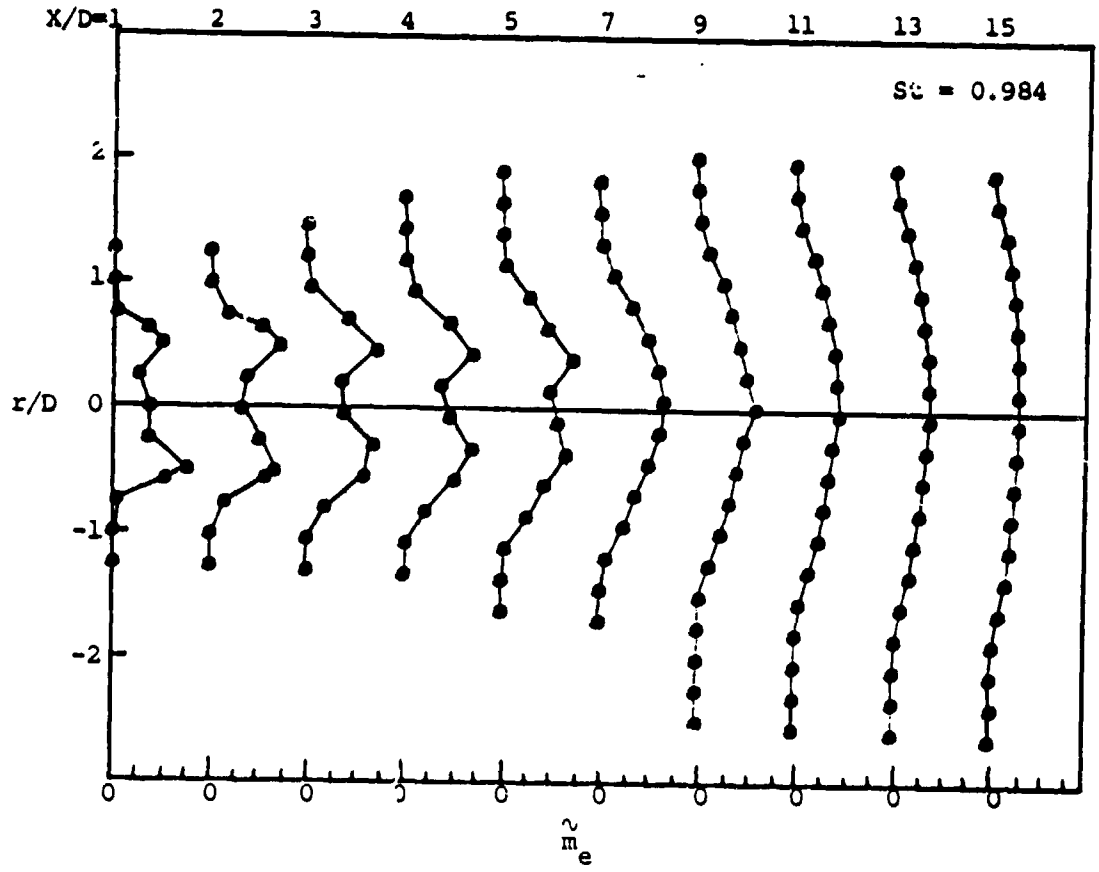

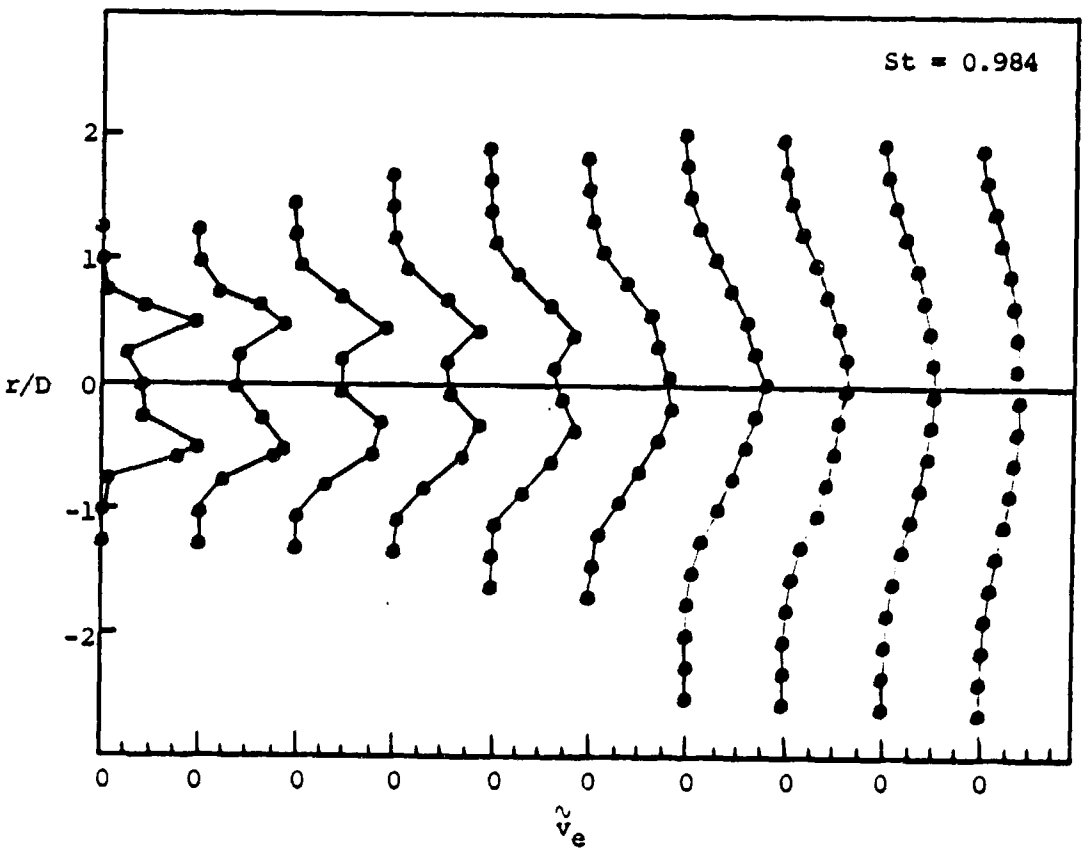

Figure A2. continued.

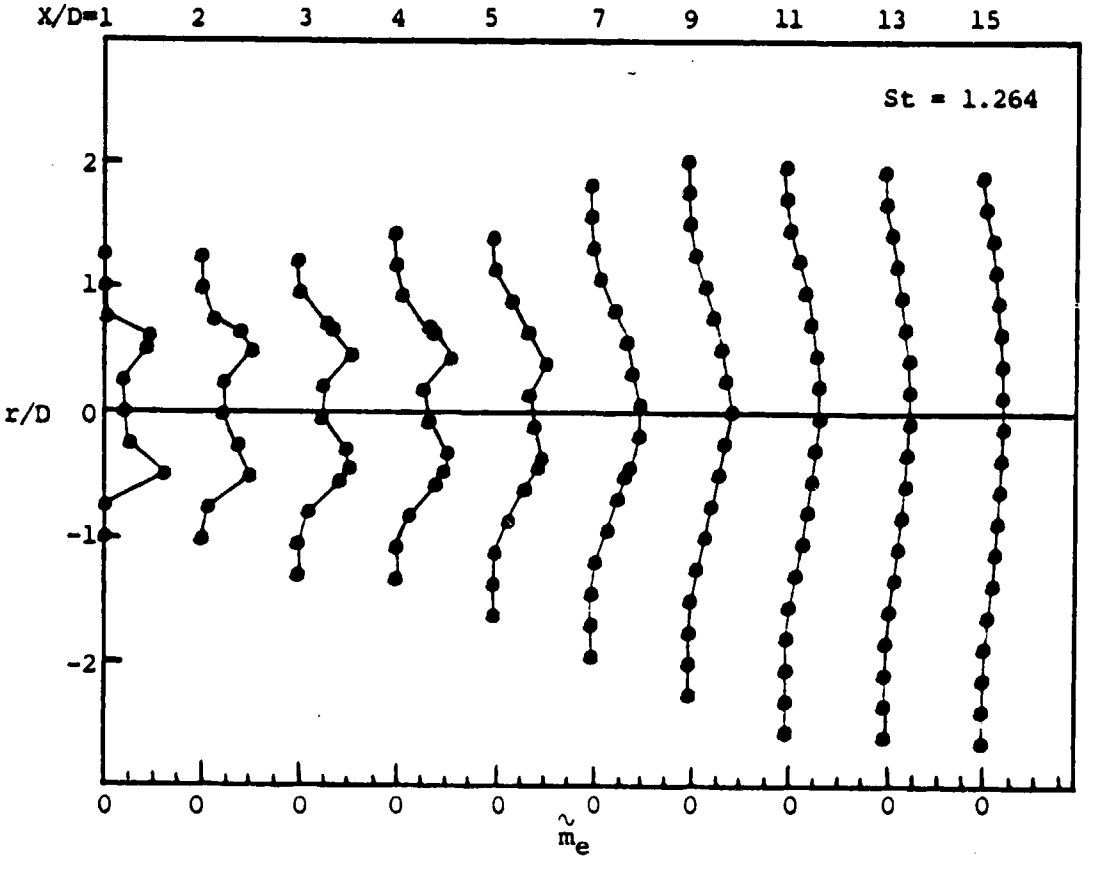

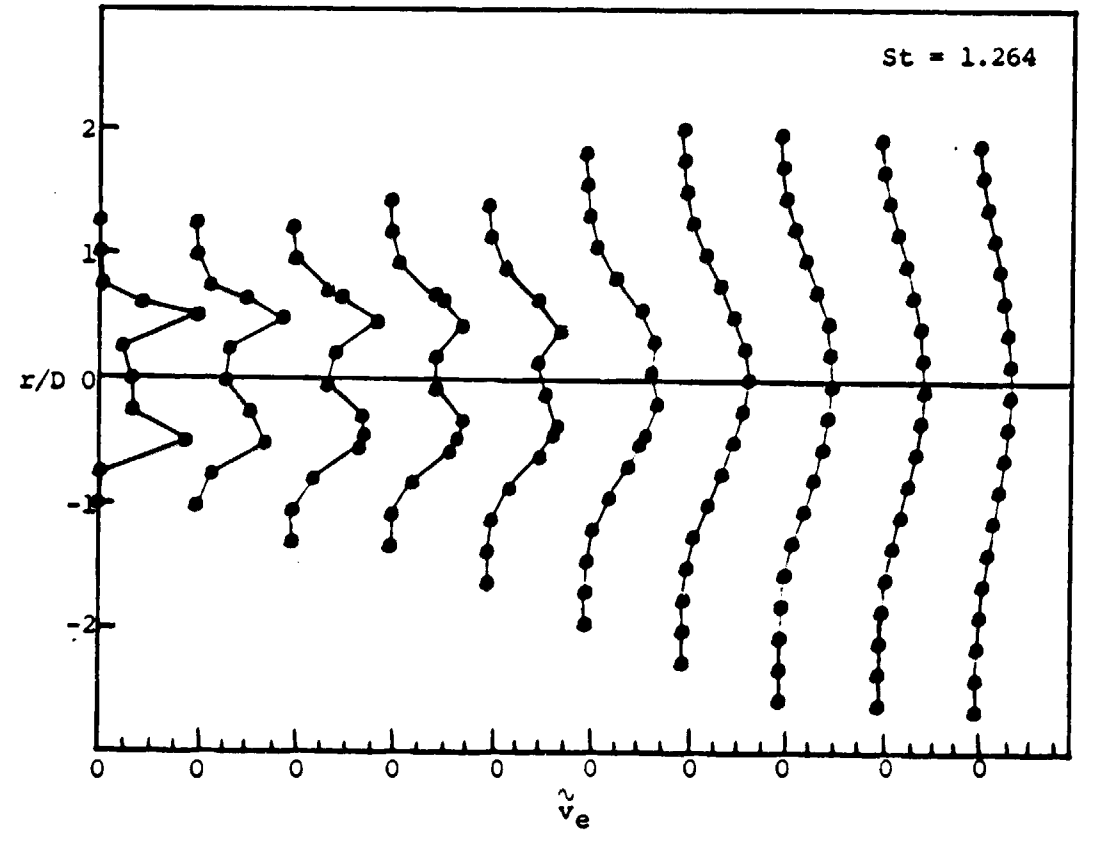

Figure A2. continued.

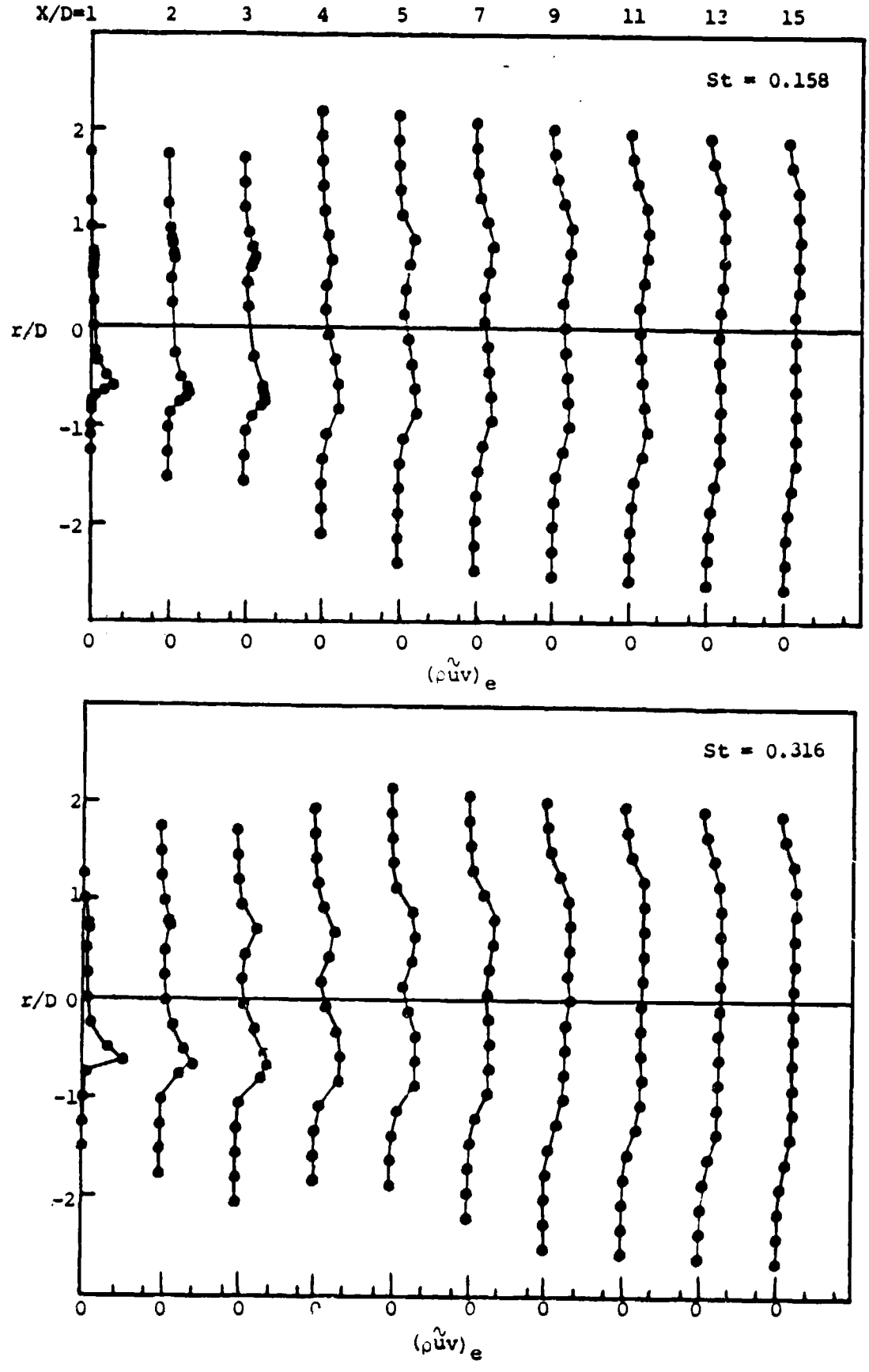

Figure A3. Radial distributions of the axial and radial flow fluctuations correlation (1 division = 0.002).

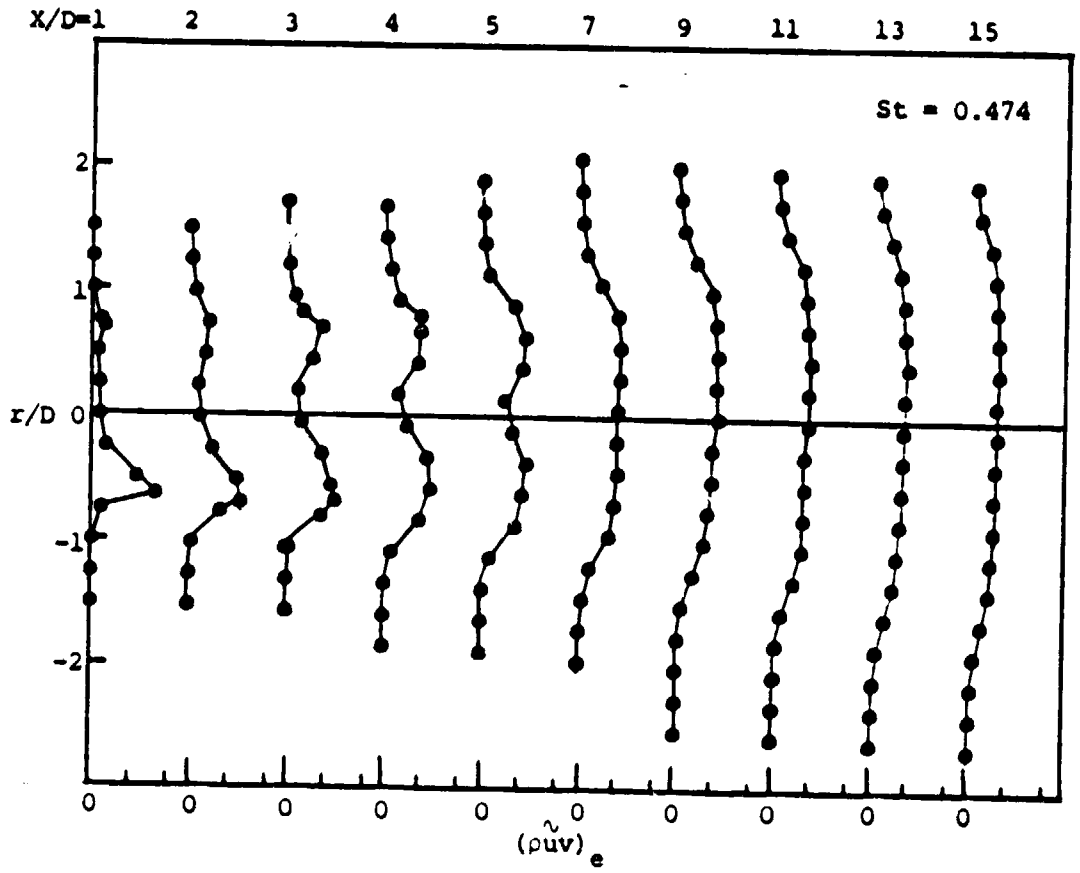

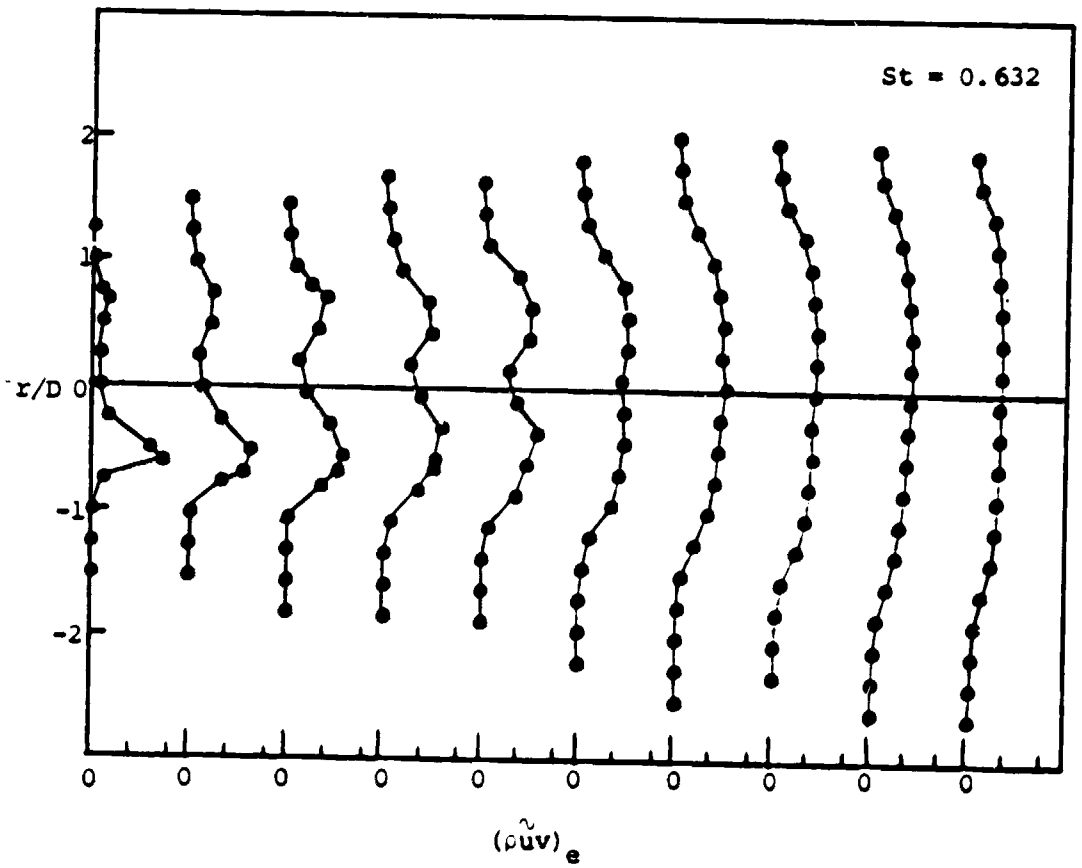

Figure A3. continued.

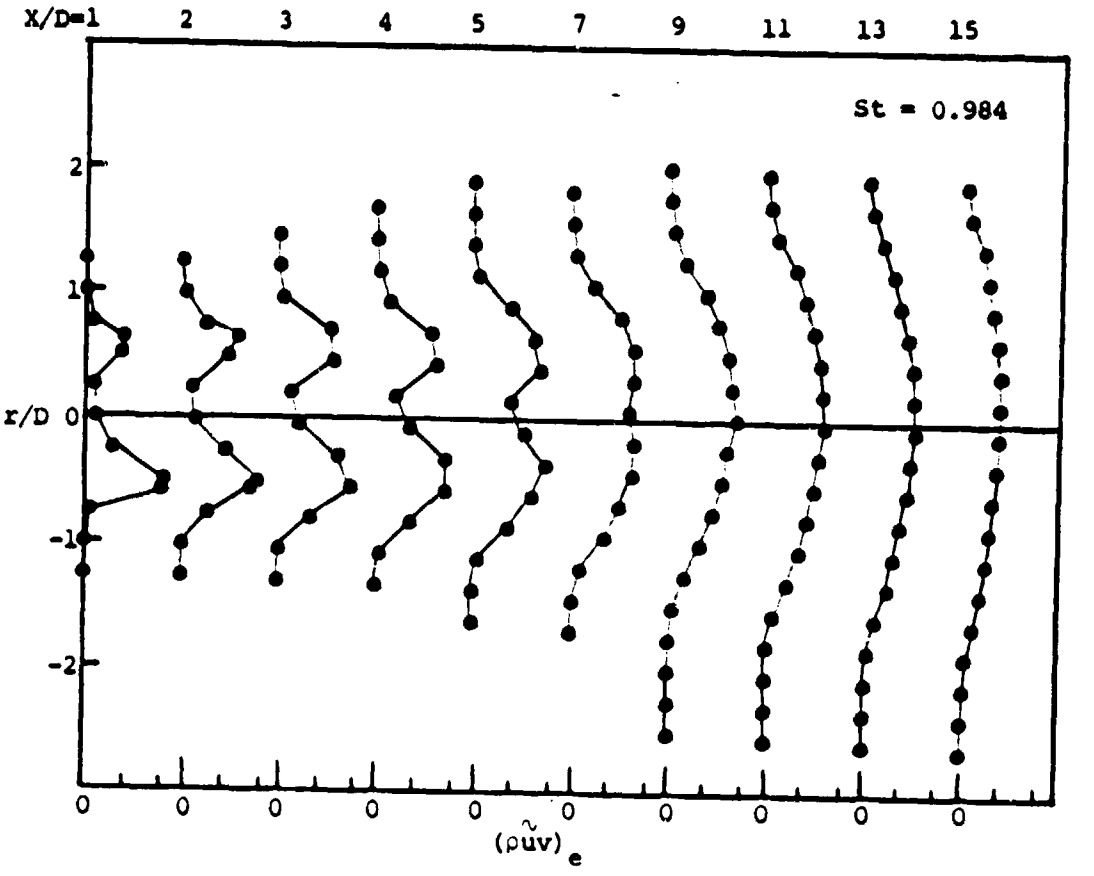

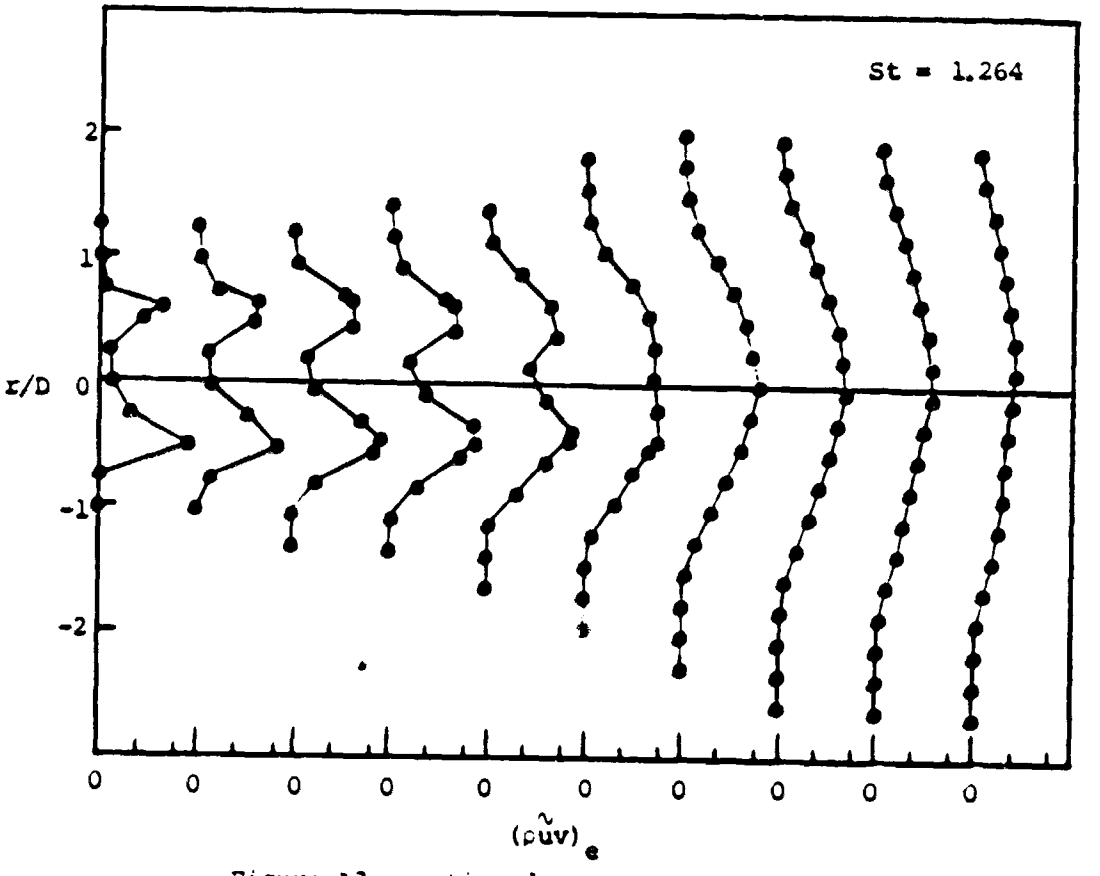

Figure A3. continued.

ORIGINAL PAGE
COLOR PHOTOGRAPH